THE ROLE OF INSULIN-LIKE GROWTH FACTOR BINDING PROTEIN-3 DURING OVAL-CELL MEDIATED LIVER REGENERATION

By

NICOLE CORINNE LUTHER

A DISSERTATION PRESENTED TO THE GRADUATE SCHOOL
OF THE UNIVERSITY OF FLORIDA IN PARTIAL FULFILLMENT
OF THE REQUIREMENTS FOR THE DEGREE OF
DOCTOR OF PHILOSOPHY

UNIVERSITY OF FLORIDA

2009

To my wonderful, loving husband, Emery

ACKNOWLEDGMENTS

I would like to thank my mentor, Dr. Bryon Petersen, for his encouragement and continuing support throughout the course of my work. I would also like to thank the members of my graduate supervisory committee, Dr. Maria Grant, Dr. Chen Liu, Dr. Naohiro Terada and Dr. Phyllis LuValle for their guidance and support. Their assistance and words of encouragement were crucial to the completion of this project.

I would also like to thank my friend and fellow lab mate, Dr. Houda Darwiche, for her continuing support and guidance throughout the years. Words cannot express how grateful I am for her friendship and advice both in and out of the lab. I would also like to express my extreme gratitude to Dr. Seh-Hoon Oh for all of his help throughout the years. I strive to one day have his knowledge and patience. I would also like to thank the past and present members of the Petersen lab, in particular, Dr. Jennifer Williams, for her knowledge, training and friendship. I would also like to thank Dr. Thomas Shupe, Dr. Dana Pintilie, Dr. Liya Grant, Dr. Rafel Witek, and Dr. Youngmi Jung for their knowledge and training throughout this process. I would also like to thank the members of the Sullivan lab, particularly Dr. Leah Villegas, for technical support and for their generous donations of antibodies and materials which helped make this work possible.

Finally, I would not be where I am today without the love and support of my family. I will be forever grateful to my parents, John and Wendy Steiger, for their constant encouragement, guidance and unconditional love. I would also like to thank my sisters Blair and Melanie Steiger for always being there for me and for all they have taught me over the years. Most importantly, I would like to thank my husband Emery who has been by my side through it all. His unwavering love and support has helped bring me to where I am today. I will forever be grateful to him.

TABLE OF CONTENTS

LIST OF TABLES

LIST OF FIGURES

LIST OF ABBREVIATIONS

2AAF	2-acetylaminofluorene
ADH	Alcohol dehydrogenase
AFP	Alpha-fetoprotein
ALB	Albumin
ALS	Acid labile subunit
BSA	Bovine serum albumin
bp	Base pairs
CTGF	Connective tissue growth factor
CYP	Cytochrome P
DMEM	Delbecco’s Modified Eagle Medium
DNA	Deoxyribonucleic acid
ECM	Extracellular matrix
FBS	Fetal bovine serum
FITC	Fluorescein isothiocyanate
GGT	Gamma-glutamyl transpeptidase
GH	Growth hormone
GHR	Growth hormone receptor
HSC	Hematopoetic stem cell
IGF	Insulin-like growth factor
IGFBP	Insulin-like growth factor binding protein
IL	Interleukin
IMDM	Iscove's Modified Dulbecco's Medium
i.p.	Intraperitoneal
LPS	Lipopolysaccharide

MACS	Magnetic activated cell sorting
MMP	Matrix metalloproteinases
NBF	Neutral buffered formalin
NPC	Non-parenchymal cells
NRL	Normal rat liver
OCT	Optimal cutting temperature
PBS	Phosphate buffered saline
PCR	Polymerase chain reaction
PHx	Partial hepatectomy
RNA	Ribonucleic acid
RXR	Retinoid X receptor
siRNA	Short interfering RNA
TGF	Transforming growth factor
TNF	Tumor necrosis factor

Abstract of Dissertation Presented to the Graduate School
of the University of Florida in Partial Fulfillment of the
Requirements for the Degree of Doctor of Philosophy

THE ROLE OF INSULIN-LIKE GROWTH FACTOR BINDING PROTEIN-3 DURING OVAL CELL-MEDIATED LIVER REGENERATION

By

Nicole Corinne Luther

December 2009

Chair: Bryon Petersen
Major: Medical Sciences – Molecular Cell Biology

Insulin-like growth factor binding protein (IGFBP)-3 is one of six characterized binding proteins to insulin-like growth factor (IGF)-I and II, and is primarily produced by the liver. IGFBP-3 has been shown to play a role in cell proliferation and differentiation in a variety of different cell and tissue types, including several different types of cancer. Recently, IGFBP-3 has been identified as a potent chemoattractant for hematopoietic stem cells and endothelial progenitor cells both *in vitro* and *in vivo*. Since hematopoietic stem cells share many common characteristics and cell markers with the hepatic stem cell population known as "oval cells" and because IGFBP-3 is primarily produced in the liver, we hypothesized that IGFBP-3 may act as a chemoattractant for the oval cells during this specific type of liver regeneration. Additionally, IGFBP-3 production has been linked to the TGF-beta superfamily, a pathway known to be induced during oval cell proliferation.

In this study, we set out to determine whether IGFBP-3 plays a role in the proliferation, migration and/or differentiation of the oval cell population during this specific type of liver regeneration. Through the use of the 2AAF/PHx liver regeneration model in the rat, we found that IGFBP-3 is elevated in liver and serum of animals during peak days of oval cell activation. Furthermore, *in vitro* assays found that WB-344 cells, a liver stem cell line similar to oval cells,

were induced to migrate in the presence of IGFBP-3. When expression of IGFBP-3 was knocked down during oval cell activation *in vivo* through the use of IGFBP-3 siRNA, we found oval cell proliferation to be highly upregulated compared to control animals and observed the appearance of numerous atypical ductular structures, which were OV-6 and Ki67 positive. Finally, quantitative real-time PCR analysis of IGFBP-3 siRNA treated livers found that expression of TGF-beta family members, including TGF-betaRII and Smads 2, 3, and 4 were significantly downregulated compared to untreated liver. Therefore, we determined that IGFBP-3 may function as a potent chemoattractant of oval cells during specific types of liver regeneration and may be involved in regulating oval cell proliferation and differentiation *in vivo* via the TGF-beta pathway.

CHAPTER 1
INTRODUCTION

The Liver

Anatomy and Physiology

The largest solid organ of the human body, the adult liver weighs approximately 1400-1600 grams, constituting 2-5% of the adult total body weight. In the adult rat, the liver weighs approximately 7-8 grams, constituting about 5% of the total body weight (1). Structurally, the human and rat liver differ, due to the fact that the human liver is comprised of 4 distinct liver lobules, whereas the adult rat liver is comprised of 5 lobules. The liver possesses a dual blood supply in which blood enters the organ from the portal vein and the hepatic artery. The majority of the incoming blood supplied to the liver is received from the portal vein, which transports nutrient rich blood from the intestinal epithelia of the gastrointestinal tract. While this blood is essentially deprived of oxygen, additional blood supplied to the liver is received by the hepatic artery, which is an oxygen-rich source. The flow of blood from these sources allows for chemicals, nutrients, and toxins to be introduced into the organ where they can be stored or metabolically converted and released back into the bloodstream (1). Additionally, bile, which is produced and secreted by hepatocytes in the liver, is transported in an opposing direction to the flow of blood in the organ via a complex network of excretory biliary ducts. Taken together, the hepatic artery, portal vein and bile duct form network of vessels which is often referred to as the portal triad.

The structure of the liver can be histologically divided into hepatic lobules which are comprised of rows of hepatocytes that are stacked and organized into plates approximately one-cell wide. These plates are arranged into cords that radiate from a central vein and can bifurcate or merge freely with an adjacent cord. Individual hepatic plates can measure 0.3 to 0.5

mm in length from the central vein and contain approximately 20 hepatocytes (2, 3). In the center of each of these lobules are the efferent vessels or what is known as the central hepatic vein. Surrounding each of these hexagonal shaped lobules at the angles are the portal triads, which are comprised of the afferent blood vessels which include the portal vein, hepatic artery, and the bile ducts. In the intercellular space between adjacent hepatocytes, bile canaliculi are formed which connect the portal ends of the hepatic plates with the epithelial cells of the bile ducts or ductules. Separating each hepatic plate are sinuosoid spaces which connect the portal vein to the hepatic vein. This grid-like arrangement of vessels and capillary-like spaces allows for adequate blood flow to reach all of the cells and for removal of blood and metabolites out of the liver (1).

Although the hepatic lobule is described as the histological unit of the liver parenchyma, the liver acinus is defined as the functional unit of the liver (4). The liver acinus is described as being a mass of liver parenchyma that receives a blood supply from the terminal branches of the afferent blood vessels and is drained by a terminal branch of the bile duct. Cells in the liver acinus are arranged into three elliptical zones with no distinct boundaries between these zones. Zone 1 contains hepatocytes which surround the portal triad and is the zone that contains the highest concentration of nutrients and oxygen as blood enters the organ from the afferent vessels. Zone 3 contains hepatocytes that surround the central vein and is the least oxygenated zone. Zone 2 is described as being the intermediate zone between Zones 1 and 3. In this acinar structure, blood flows from Zone 1 to Zone 3, whereas bile flows in the opposing direction from Zone 3 to Zone 1. Hepatocytes, based on their proximal location within the acinus, can vary in their structure and phenotype in order to carry out various metabolic functions within these zones.

Hepatic Cell Types

The liver includes a variety of cell populations which can be classified as being either parenchymal or non-parenchymal in origin. These cell types have been shown to express specific cell markers which aid in their identification and, in some cases, reflect the various functions the cells are capable of performing (5-9). A list of these varying cell surface markers are summarized in Table 1-1. The intricate cell to cell interactions and the organization of these cells within the liver architecture facilitate many of the diverse functions of the liver.

Parenchymal cells

Hepatocytes account for the largest population of cells (60-65%) within the rodent liver, comprising approximately 90% of the total liver weight. Hepatocytes are described as being large, polygonal shaped cells approximately 30-40 μm in diameter. Hepatocytes are a highly metabolically active cell population and therefore contain a vast array of organelles to carry out various functions within the organ. Approximately 15% of the total cell volume within the hepatocyte is occupied by smooth and rough endoplasmic reticulum. In addition to this, hepatocytes contain over 1,000 mitochondria and approximately 50 Golgi complexes per cell (1). Hepatocytes carry out the majority of the metabolic processes of the liver including (but not limited to) the production of bile, synthesis and secretion of plasma proteins such as albumin, and the conversion of toxic ammonia in the circulatory system to urea.

Bile duct epithelial cells, also referred to as cholangiocytes, represent approximately 3-5% of the total liver weight are the second group of cells classified under parenchymal cells of the liver. When bile is produced and secreted by the hepatocytes, it is drained into a network of channels that are lined by these bile duct epithelial cells. These channels begin inside the parenchymal lobule at the canals of Hering and flow into a series of branches that comprise the biliary tree. Although the bile duct epithelial cells represent only a small portion of the total

liver, they are responsible for performing a variety of functions within the liver parenchyma. Bile epithelial cell functions including modification of bile though the secretion of water and bicarbonate, and the absorption of molecules such as glucose and proteins (10).

Non-parenchymal cells

Hepatic stellate cells (formerly referred to in the literature as Ito cells, fat-storing cells, and/or vitamin A storing cells) were first identified in the 1870's by Von Kupffer and later characterized by Ito and Nemoto in 1952. Stellate cells are named for the star-like appearance and are located in the normal liver within the space of Disse and beneath endothelial cells. Stellate cells represent 5-8% of the total cells within the liver and have been shown to play a role in maintaining the extracellular matrix (ECM) of the liver. In addition to this, stellate cells play a role in vitamin A metabolism and store approximately 50-80% of all retinoids found in the body (11). Under normal conditions in the liver, stellate cells are in a quiescent state and become activated in response to liver injury. When activated, stellate cells express markers such as desmin and α-smooth muscle actin and begin to transform into mature, myofibroblast cells. During this time, activated hepatic stellate cells migrate to sites of liver injury or damage where they secrete cytokines and synthesize copious amount of extracellular matrix components such as collagen, proteoglycan and adhesive glycoproteins.

Stellate cells are also capable of degrading interstitial and basement membrane collagens through the production and secretion of proteins such as matrix metalloproteinases (MMPs) (1). Production of these factors are important for the infiltration of certain types of cells involved in regeneration, such as the liver stem cell population known as oval cells. The phenomenon of oval cell-mediated liver regeneration and many of the factors regulating their activation in the liver following injury will be discussed in further detail later on in this chapter.

Kupffer cells, like stellate cells, are star-like in appearance and were first described by Von Kupffer in the 1870's. Kupffer cells are located within the sinusoidal spaces and are found attached to the sinusoidal walls within the liver. Kupffer cells function as specialized macrophages within the liver by removing old and damaged cells in addition to picking up foreign materials such as endotoxins. When activated, Kupffer cells secrete a myriad of cytokines, growth factors and proteases such as TNF-α, interleukin-1 and -6 (IL-1 and IL-6) and reactive oxygen species (12). Several of these factors have been shown to activate the proliferation of hepatocytes and stellate cells and act as chemoattractants for inflammatory cells following injury to the liver. Additionally, during liver injury, Kupffer cells have been shown to produce TGF-β1 which maintains elevated cytokine levels within the liver and activates hepatic stellate cells to begin TGF-β1 production via a paracrine loop (13, 14).

Sinusoidal endothelial cells (SECs) of the liver comprise the sinusoidal wall, also referred to as the endothelium or the endothelial lining. Sinusoidal endothelial cells can be distinguished from other endothelial cells based on the presence of numerous fenestrae. These fenestrae present on the surface of endothelial cells function by filtering fluids and removing solutes and particles that pass from the sinusoidal lumen and the space of Disse (1). Additionally, SECs express several cell membrane receptors which allow them to clear specific proteins from the blood, such as hyaluran and components of the extracellular matrix, via endocytosis. Therefore, SECs act as a sieve by removing macromolecule waste products from the blood, thus preventing them from passing to the parenchymal or stellate cells. In addition to this, SECs have also been shown to play a role in regulating lipoprotein metabolism in the liver.

Functions of the Liver

As previously stated, the liver is the largest parenchymal organ in the body and as such, it is responsible for performing a variety of functions in order to maintain homeostasis. Additionally, because of its large size and intricate vascular network, the liver at any one point in time will contain a significant portion of the total blood volume within the body. Because of this, the liver functions not only by filtering and detoxifying the blood, but also acts as a storage site for excess compounds such as vitamins, minerals and glucose, found in the bloodstream. Some of the other major functions of the liver that will be discussed further in this section include the production of bile and the synthesis of blood proteins such as albumin and clotting factors.

Detoxification of blood

One of the most important functions of the liver is the removal of foreign substances from the bloodstream. This includes the removal of a broad spectrum of microorganisms, such as bacteria and viruses, in addition to various toxins and chemicals, such as drugs and alcohol. Enzymes such as alcohol dehydrogenase (ADH), cytochrome-P (CYP) and uridine glucuronosyltransferase (UGT) aid in the chemical modifications of several compounds and facilitate their removal from the bloodstream. Furthermore, the ability of the liver to convert non-hydrophyllic drugs to a more water-soluble form allows them to be safely excreted by the kidneys.

Bile secretion

Another important function of the liver is the production of bile. Production begins with the hepatocytes which secrete bile acids produced from cholesterol metabolism into the bile caniliculi. Here, the bile acids mix with other components excreted by the epithelial cells such as water, bicarbonate, and phospholipids. Bile is drained from the liver via the common bile duct

and is stored in the gallbladder until needed (15). When food in the gastrointestinal tract enters the duodenum, it stimulates the contraction of the gall bladder to release stored bile into the small intestine. Here, bile functions as a surfactant, emulsifying fats for easier absorption in the small intestine.

Storage of vitamins and nutrients

The liver is responsible for storing excess fat soluble vitamins such as vitamin A, D, E and K and some water soluble vitamins such as vitamin C and B. The liver releases these vitamins into the bloodstream or bile when the body becomes deficient. In addition to this, minerals such as iron, copper, zinc and magnesium are stored in the liver.

The liver is also the largest storage site for glycogen in the body following carbohydrate metabolism. During carbohydrate metabolism, the liver regulates blood glucose levels by converting excess glucose into glycogen which decreases the levels of glucose in the blood. When blood glucose levels become too low, the liver can effectively metabolize glycogen back into glucose, thus increasing blood glucose levels.

Liver Regeneration

Hepatocyte-Driven Regeneration

The liver is a unique organ in that it has the capacity to regenerate itself following physical injury, such as that caused by performing a two-thirds partial hepatectomy (PHx) (16), or chemical damage as a result of exposure to certain types of toxins such as carbon tertrachloride (CCl_4). Under normal conditions, the liver in both humans and rodents is seemingly quiescent, with fewer than 1 in 10,000 hepatocytes undergoing replication at any one point in time. Following injury to the liver, hepatocytes are the main cell responsible for reconstituting the organ.

The process of liver regeneration following partial hepatectomy alone begins with hepatocytes moving from a resting G_0 phase to the G_1 phase of the cell cycle within hours after the surgical removal of the organ. Hepatocyte proliferation begins in the periportal region of the liver and spreads to the centrilobular region. This regeneration requires each hepatocyte to undergo approximately 1.4 rounds of replication to restore the liver to its original size. The early events following partial hepatectomy are largely regulated by cytokines such as TNF-α and IL-6. Production of these cytokines leads to the activation of transcription factors such as NFκB, AP-1 and STAT3, which in turn activate the transcription of growth factors such as HGF and TGF-α. Production of HGF and TGF-α induces significant DNA replication in the hepatocytes which occurs in two separate waves during this process of regeneration. The first wave of DNA synthesis in hepatocytes occurs 24 hours following partial hepatectomy, while the second, smaller wave of DNA synthesis occurs 48 to 72 hours after surgery. Following hepatocyte replication, bile duct epithelial cells are the next cell type to undergo replication in the liver, with peak DNA synthesis occurring 48 hours after surgery. Stellate and Kupffer cell replication follow close behind with sinusoidal epithelial cells being the last group of cells undergoing replication at Days 3-8 post PHx (17).

Although this process is commonly referred to in the literature as "liver regeneration", the correct term for this phenomenon is actually compensatory hyperplasia. Compensatory hyperplasia describes the process of the remaining liver lobules increasing in size, where the end result of this process is not a re-growth of the anatomical form of the liver, but rather a restoration of the organ to its original mass and functional capacity (18). Completion of this process can take approximately 10-14 days in a rodent model whereas in human, completion of the process can take up to 2 months.

Oval Cell-Mediated Liver Regeneration

Oval cell involvement during the process of liver regeneration is a unique and specific phenomenon which only occurs when hepatocyte proliferation is impaired or inhibited (19). In the liver, under normal conditions, very few if any oval cells can be detected within the parenchyma of the organ. This would suggest that oval cells are only activated and present in the liver for specific purposes when hepatocytes are functionally unable to regenerate the liver mass due to chemical insult or injury.

Activation of the oval cell compartment in an animal model can be accomplished through several different procedures including carcinogenesis induced by azo-dyes, choline deficient/ethionine-containing diets (CDE diet) and D-galactosamine or through direct injury to the liver produced by a partial hepatectomy in combination with chemicals such as N-2-acetylaminofluorene (2AAF), dipin or CCl_4 (19-21). For the purposes of this research, to be described in further detail later on in this report, the process of oval cell activation was accomplished through the implantation of a 2AAF pellet, to prevent proliferation of the resident hepatocytes, followed by a 70% partial hepatectomy in a rat model. Administration of 2AAF prior to removal of the liver inhibits the cyclin D1 pathway within the hepatocytes, preventing them from undergoing proliferation. This model is considered the gold standard in oval cell activation and is commonly referred to as the 2AAF/PHx protocol. Oval cells are capable of generating both hepatocytes and bile duct cells, thereby qualifying them as bipotential progenitor cells in adult livers (22).

Morphologically, oval cells are small in size, approximately 10 μm in diameter, with a large, ovoid nucleus and very little surrounding cytoplasm (23). Oval cells can also be identified in histological sections by their basophilic staining in comparison to the surrounding

hepatocytes. During oval cell-mediated liver regeneration, oval cells can be visualized infiltrating the liver parenchyma in and around the periportal regions of the liver lobule (24). Histologically, oval cells are identified in the liver by their expression of specific markers such as OV-6, α-fetoprotein (AFP), and CK19 (24-26). In both the human and rat, oval cells proliferate and differentiate in close proximity to the stellate cells within the liver. Previous studies have also shown that stellate cells and oval cells have a unique relationship where the stellate cells can enhance oval cell growth and differentiation via secretion of growth factors and through direct cell to cell interaction with the oval cells (27).

Multiple signaling pathways and growth factors have been shown to contribute to both early and late events in oval cell activation. These growth factors include α-fibroblast growth factor (αFGF), hepatocyte growth factor (HGF), transforming growth factor (TGF)-α, and TGF-β1 (28, 29). Both stellate cells and oval cells have been shown to produce TGF-α and αFGF within 24 h following surgical resection of the liver, which coincides with an increase in DNA synthesis in both of these cell populations (28). Expression of HGF and TGF-β1 during regeneration has also been linked to stellate cells, although oval cells have also been shown to express low levels of TGF-β1 mRNA when they first enter the liver (30, 31). Additionally, oval cells have been shown to express receptors for all of these growth factors, further supporting a molecular basis for the role of stellate cells influencing the growth of oval cells during this process (30, 32, 33). Interestingly, many of the growth factors which activate oval cell proliferation are similar to those that stimulate hepatocyte replication following partial hepatectomy, despite the fact that oval cells and hepatocytes rarely undergo replication at the same time. One of the major differences between the two types of liver regeneration however, is

the secretion of interferon-γ during oval cell proliferation, which is not expressed during hepatocyte activation (34, 35).

The origin of these hepatic stem cells currently remains a topic of debate. There are many researchers that believe that oval cells are derived from the ductular cells of the canals of Hering, whereas others speculate that they arise from an extrahepatic source such as the bone marrow. Numerous studies conducted in both animal models and humans have suggested that bone marrow cells (BMCs) may give rise to oval cells (25, 36-38). Evidence to support this theory is derived from the observations that oval cells express a variety of hematopoietic stem cell markers such as Thy-1, CD34, c-kit and Flt-3 (39-41).

Oval Cells and Cancer

The stem cell theory of cancer in the liver was first proposed more than 50 years ago, however, the theory is difficult to prove conclusively because it is unclear whether stem cells, such as oval cells, are directly taking part in carcinogenesis or if the presence of these cells in tissue is the result of impaired hepatocyte function and death. When the liver is exposed to a carcinogen or chronic injury, such as that caused by repeated exposure to inflammatory cytokines as a results of viral infection, cell proliferation is required to correct for cell damage and death in order to maintain the integrity and functionality of the organ. This in turn causes any proliferative cell in the liver, including oval cells, to be potentially susceptible to neoplastic transformation.

It has been reported that oval cells may be capable of participating in the formation of certain types of cancer in the liver, including hepatocellular carcinoma (HCC) and cholagiocarcinoma (CCC) (42-44). The possibility of oval cells participating in hepatic cancers was first proposed in 1956 by Farber et al. based on their initial observations of oval cells

undergoing morphological changes during early chemical carcinogenesis (23). The direct involvement of oval cells in HCC carcinogenesis was first demonstrated by Dumble et al., where oval cells that were isolated from p53-null mice formed tumors when transplanted into nude mice (42).

Several studies have also identified cells expressing a progenitor cell phenotype that were present in HCC liver sections. In a study by Wu et al., immunonhistological analysis of HCCs found that 28-50% of HCCs expressed markers of progenitor cells such as CK7 and CK19 and that these cells appeared to express an intermediate phenotype between progenitor and mature hepatocytes (45). In addition to this, they noted that HCCs expressing hepatocyte and biliary cell markers such as albumin, CK7, and CK19 carried a significantly poorer prognosis and higher recurrence after surgical resection and liver transplantation (45). These findings bring up another important problem with the stem cell theory of cancer, being that many believe HCCs are not the results of neoplastic changes in progenitor cells, but rather a regression or "dedifferentiation" of mature hepatocytes (46).

Insulin-Like Growth Factors

Insulin-like growth factors (IGF)-I and II, formerly referred to in the literature as somatomedins, are structurally similar to insulin, hence their name, and have been shown to bind with reduced affinity to the insulin receptor (47, 48). IGF-I and II have been shown to mimic nearly all the functions of insulin in the body and play a role in lipoprotein metabolism (49). Production of IGF-I is primarily regulated by a pituitary hormone known as growth hormone (GH) (50). When GH binds to its receptor, GHR, IGF-I production from the liver is initiated. The liver is the major source of IGF production as well as the primary source for IGF binding proteins that carry IGFs in circulation. IGF-I is an important autocrine, paracrine and endocrine hormone necessary for proper cell growth and survival, and has been shown to play an integral

role in development in nearly every cell of the body (50). In addition to this, the IGF-I receptor is distributed throughout the body with most cells expressing multiple copies of the receptor. Interestingly however, the liver expresses very little IGF-IR compared to other tissues.

IGF-I and II are closely related in both their structure and function as potent mitogenic growth factors although, the two proteins differ in the time points at which they are expressed in the body. For example, in the rat, IGF-II is expressed at high levels in the fetus which diminish shortly after birth, whereas IGF-I expression increases after birth, with continued expression into adulthood. Therefore, IGF-II function appears to be limited to prenatal developmental stages, whereas IGF-I plays an integral role in postnatal growth and further development (47, 51).

Insulin-Like Growth Factor Binding Proteins

Insulin-like growth factor binding proteins (IGFBPs) are a group of highly conserved proteins that function mainly by binding to and regulating the bioavailability of IGF-I and, to a lesser extent, IGF-II (52). Although more than a dozen IGFBPs have been identified, IGFBPs 1-6 remain the most well known and best characterized binding proteins in the current literature. IGFBPs have been shown to either inhibit or facilitate the promitogenic and anti-apoptotic effects of IGF-I and II by several mechanisms. First, by binding to IGFs, IGFBPs can prevent IGFs from interacting with their respective receptors, thus inhibiting cell proliferation. In addition to this, it is believed that IGFBPs can interact directly with the IGF receptors to block the binding of IGFs, which also leads to an overall reduction in cell proliferation. However, by binding to IGFs, IGFBPs have been shown to extend the half-life of these proteins in circulation and prevent their subsequent degradation (53). Proteolytic cleavage of IGFBPs by serine proteases, cathepsins, and matrix metalloproteinases, results in the formation of IGFBP fragments that have reduced or no affinity for the IGFs. Therefore, when IGFBPs are cleaved, IGFs are released, thus enhancing the amount of free IGFs available to the cell and leading to

increased cell proliferation. A schematic diagram of these IGF-dependent mechanisms is depicted in Figure 1-1 and adopted from Firth and Baxter, 2002 (54).

Insulin-Like Growth Factor Binding Protein-3

Insulin-like growth factor binding protein (IGFBP)-3 is perhaps the most important and most studied IGFBP in today's literature. IGFBP-3 is a 40-43 kDa glycoprotein which exists in circulation as a 150 kDa complex along with an 80 kDa acid labile subunit (ALS), and IGF-I (55). Approximately 98% of IGF-I found in the blood is bound by IGFBPs, approximately 80% of which is bound exclusively by IGFBP-3. Under normal conditions in the liver, un-bound IGF-I has a half-life of approximately 30 to 60 minutes in circulation (56). However, the half-life of IGF-I is greatly increased when IGFBP-3 is bound to it, extending the half-life from 30 to 60 minutes to approximately 10 to 20 hours in circulation (57, 58). Like IGF-I, production of IGFBP-3 is dependent on GH and is primarily produced by the liver, although each are synthesized by different cell types. IGF-I has been shown to be produced by hepatocytes, along with IGFBP-1 and 4, whereas IGFBP-3 is produced by non-parenchymal cells, such as Kupffer cells (59-61).

IGFBP-3 was first identified and characterized over 20 years ago by several different groups and in several different animal models (62-65). Early comparison studies by Albiston and Herrington have shown that IGFBP-3 is fairly conserved across species and also found that rat and human IGFBP-3 proteins are approximately 83% homologous (65). At first discovery, IGFBP-3 was believed to function only as a carrier for IGFs in circulation, thus modulating the biological functions of these proteins. However, recent studies supports that IGFBP-3, in addition to performing various IGF-dependent functions, also exerts a variety of IGF-independent functions.

The discovery of IGF-independent functions of IGFBP-3 were first shown in various *in vitro* studies using cells that either lacked the IGF receptor, or in cells that do not produce or respond to endogenous IGF-I or II. In experiments performed by Rajah et al. using a mouse fibroblast cell line lacking the IGF-IR, it was found that apoptosis was significantly increased following exposure to IGFBP-3, both by exogenous administration of the protein or by transfecting cells with an IGFBP-3 plasmid (66). In addition to this, a study by Perks et al., utilizing a breast cancer cell line that does not respond to IGF-I, found that IGFBP-3 enhanced call apoptosis following exposure of these cells to a ceramide analog, C2 (67). More concrete evidence of these IGF-independent functions were later shown through the use of mutated IGFBP-3 analogs that are unable to bind to the IGFs (68, 69). Here, the generation of several key amino acid substitutions in the IGF binding site within the IGFBP-3 protein created a marked reduction (>80-fold) in IGF binding. In these studies, the mutated form of IGFBP-3 was found to promote apoptosis, which was concluded to be a function independent of IGFs due to the inability of IGFBP-3 to bind to these proteins and modulate their activity (68, 69).

Although the exact mechanisms by which IGFBP-3 mediates these IGF-independent functions are not well known, there is recent evidence suggesting that IGFBP-3 may potentiate these functions by nuclear translocation and through the interaction with nuclear receptors such as retinoid X receptor (RXR)-α (70). Binding of the nuclear RXR-α by IGFBP-3 was shown to be required for IGFBP-3 induced apoptosis, a process which was further enhanced with the addition of RXR ligands (70). The presence of IGFBP-3 in the nucleus has been identified in a variety of cell types including several types of cancers (71-73). Additional studies have found that the key residues necessary for nuclear translocation of IGFBP-3 (228-232) are identical to those previously shown to be required for association with proteins present in the extracellular

matrix (ECM) of the cell (74). Interestingly, a study by Bhattacharyya et al. determined that IGFBP-3 could induce apoptosis in a human prostate cancer cell line without being secreted or through translocation into the nucleus of these cells (75). In addition to being a secreted protein, IGFBP-3 contains a nuclear localization signal (NLS) which allows it to be translocated into the nucleus of cells where it has been shown to induce apoptosis independently of IGFs (71, 72, 76, 77). In these experiments, Bhattacharyya et al. generated IGFBP-3 mutants which lacked a signal peptide, preventing the secretion of IGFBP-3 into the extracellular space, and IGFBP-3 protein which had been fused to MDGEA at the C-terminal NLS domain, preventing the protein from being translocated to the nucleus of the cell. Generation of these IGFBP-3 mutants would cause IGFBP-3 protein to remain within the cytoplasm of the cells which produced IGFBP-3, where they could interact with intracellular signaling pathways from the cytosol. Results of this experiment were the first to demonstrate that a nonsecreted form of IGFBP-3 which could not be translocated to the nucleus, could induce apoptosis in pancreatic cancer cells though intracellular mechanism and in an intracrine manner (75).

IGFBP-3 has also been shown to regulate cell growth independently of IGF-I through the interaction with the newly identified TGF-β receptor type V (TGF-βRV), which researchers are calling the putative IGFBP-3 receptor. In studies by Leal et al., it was found that IGFBP-3 could directly bind to TGF-βRV, leading to an inhibitory effect on growth and proliferation of mink lung epithelial cells *in vitro*. These were some of the first studies which could conclusively link IGFBP-3 to the direct activation of the TGF-β pathway (78, 79).

IGFBP-3 and cancer

The role of IGFBP-3 during cancer progression is somewhat complex and often times ambiguous in the literature. As IGFBP-3 has been shown to regulate the bioavailability of IGFs

both *in vitro* and *in vivo*, IGFBP-3 can either enhance or inhibit the mitogenic and antiapoptotic effects of IGFs. This, in turn, can either inhibit or enhance the proliferation of cancer cells. Additionally, several groups have also found that IGFBP-3 can alter cell proliferation and migration through IGF-independent mechanisms.

IGFBP-3, in an IGF-independent manner, has been shown to inhibit proliferation and stimulate apoptosis of breast cancer cell lines *in vitro* (80). Additionally, clinical studies involving IGFBP-3 have shown that high serum levels of the protein are often correlated with a reduced risk of developing cancer in post-menopausal women. These findings are supported by several clinical studies which determined that patients with low serum levels of IGFBP-3 are at an increased risk of developing other types of cancer such as colon, prostate and ovarian cancer (81-83). In addition to this, a study by Gong et al. found that mRNA expression of IGFBP-3, -1 and -4 were significantly down-regulated in patients with human hepatocellular carcinoma (HCC) in comparison to patients with normal or cirrhotic livers (84). Several of these studies also determined a correlation between low IGFBP-3 levels and increased tumor grade and aggressiveness (80, 83). These studies suggest that IGFBP-3 may play an important role in suppressing tumor cell proliferation and may also function as a suppressor of tumor metastatic invasion.

Although the majority of studies have shown IGFBP-3 to inhibit proliferation and promote apoptosis, there have been several reports of tumors and cancer cell lines expressing high levels of IGFBP-3 and that, when IGFBP-3 is lost, the ability of these cells to migrate and proliferate is inhibited. For example, a study by Xi et al. determined that a human metastatic melanoma cell line, WM266-4, expressed a 16-fold increase in IGFBP-3 compared to primary cell lines. Additionally, when IGFBP-3 expression was knocked down though the use of siRNA, the cells

displayed on overall decrease in their invasive and proliferative potential (85). In addition to this study, other groups have also reported increased IGFBP-3 expression in colorectal cancers and renal carcinomas. In a clinical study of patients with renal adenocarcinomas, 17 of the 18 patients displayed elevated levels of IGFBP-3. Additionally, patients with the highest levels of IGFBP-3 mRNA were more likely to present with metastatic tumors localizing to other areas of the body such as the lymph nodes (86). These studies suggest that IGFBP-3 may enhance cancer cell migration *in vivo* and promote the metastatic ability of the cells to invade other organs. Additionally, these results suggest that IGFBP-3 may be an important biomarker for the clinical assessment of highly aggressive tumors in humans.

IGFBP-3 and stem cells

As IGFBP-3 has been shown to regulate cell proliferation and migration, in either an IGF-independent or dependent manner, some groups have investigated the role of IGFBP-3 and its effect on stem cell populations both *in vitro* and *in vivo*. The majority of the research involving stem cells and IGBFP-3 has been conducted on hematopoietic stem cell populations. This is of particular interest to our lab because oval cells have been shown to share several cell surface markers with hematopoietic stem cells including Thy-1, CD-34, c-kit and Flt-3 (36, 37, 87, 88).

In a study by Liu et al., it was found that exogenous administration of IGFBP-3 to primitive hematopoietic cells (CD34+CD38-) enhanced cell proliferation while maintaining the ability of these cells to produce functional progenitors. These finding may have major implications for the expansion of these cell *in vitro* for future use in transplantation studies (89). In addition to this, previous works by Chang et al. and Lofqvist et al. have demonstrated the profound effects that IGFBP-3 has had on inducing the migration of CD34+ stem cells and endothelial progenitor cells to areas of retinal damage in oxygen-induced retinopathy mouse

models. Additonally, Chang et al. was also able to show that IGFBP-3 was capable of inducing the differentiation of these cells into endothelial cells in a dose dependent manner, leading to increased tube formation and vessel repair (90, 91). Another unique finding presented by both groups was the protective effect IGFBP-3 provided in the retina, which resulted in decreased vascular damage during hypoxic injury, increased blood vessel stabilization and increased angiogenesis. Overall, both studies demonstrated that addition of exogenous IGFBP-3, or over-expression of the protein through the use of plasmids, could protect against vascular damage, promote a higher rate of vascular repair, and induce stem cell migration and differentiation in these models.

IGFBPs and Liver Regeneration

Several studies have investigated the role of IGFBPs during liver regeneration induced by chemical injury or following partial hepatectomy alone however; few if any research to date has investigated the role of IGFBPs during oval cell-mediated liver regeneration as a result of 2AAF/PHx. Some of the first studies to implicate a potential role for IGFBPs during liver regeneration were conducted on animal models utilizing partial hepatectomy alone. It was observed in these studies that IGFBP-1 protein and mRNA levels, in the serum and liver respectively, were dramatically increased following resection of the liver lobes in both rat (92, 93) and in mice (94), following partial hepatectomy alone. However, a decrease in IGFBP-1 following liver injury would be expected, due to the fact that IGFBP-1 is primarily produced in the liver by hepatocytes, which are also the primary cell type responsible for liver regeneration following partial hepatectomy alone. However, additional studies have suggested that IGFBP-1, which has been shown to be elevated during fetal liver development, also plays a key role in the regenerative process of the adult liver as well (95). In a study by Leu et al, it was determined that IGFBP-1 also plays an important role in protecting hepatocytes from Fas-mediated apoptosis

during liver regeneration. In these studies, it was also found that animals lacking IGFBP-1 displayed an increase in hepatocellular injury and apoptosis following exposure to CCl_4 (96).

Additional studies have also shown that IGFBP-4, another IGFBP primarily produced by hepatocytes, could potentially be involved in liver regeneration following partial hepatectomy alone (97). A study by Demori et al. found that IGFBP-4 levels in the liver and serum increased significantly within 6 to 12 hours following partial hepatectomy alone in the rat. In contrast, a study by Phillips et al. found that serum levels of IGFBP-3 and IGF-1 significantly decreased in PHx experiments (98). Ultimately however, they concluded that this decrease was most likely the result of significant tissue loss, as the production of both of these proteins primarily occurs within the liver and the result of decreased nutrient intake by the animals following surgery.

Another study which supports the potential role for these proteins during liver regeneration was found in experiments performed by Caro et al. Here, they found that following liver injury, expression of the IGF-IR is significantly upregulated, whereas in the normal liver, very few cells express the receptor for IGF-I (99). This suggests an integral role for IGFBPs following liver injury which may be mediated by IGF-dependent mechanisms.

Transforming Growth Factor-β Signaling Pathway

The transforming growth factor (TGF)-β superfamily consists of a large number of structurally related, secreted and dimeric proteins which includes three distinct classes of proteins: the TGF-βs themselves, activins and bone morphorgenic proteins (BMPs). All of the proteins of the TGF-β superfamily function by binding to transmembrane, enzyme-linked receptors with a serine/threonine kinase domain located on the intracellular portion of the receptor. These serine/threonine kinase receptors can be further classified as being type I or type II receptors (100).

TGF-β is a potent inhibitor of cell cycle progression for most epithelial and endothelial cell, as well as for hematopoietic cells. Studies have identified three TGF-β ligands that are present in all mammals which include TGF-β1, TGF-β2, and TGF-β3. TGF-β1 is the major form present in adults, whereas expression of TGF-β2 and TGF-β3 occurs primarily in the developmental stages. All TGF-β ligands signal through a heteromeric complex of type I and type II TGF-β receptors. Generally, activation of the TGF-β pathway occurs when a TGF-β ligand binds to the TGF-β type II receptor, which results in the recruitment and activation of a type I receptor. Activation of the type I receptor leads to the phosphorylation of intracellular signaling intermediates of the TGF-β pathway known as Smads (100). Activated TGF-β receptors phosphorylate Smad2 and Smad3, causing the Smads to dissociate from the receptor and bind to Smad4, the common mediator. The phosphorylated Smad complex then moves into the nucleus where it is incorporated into transcriptional complexes, binds to DNA, and activates a target set of genes for transcription.

TGF-β and Liver Regeneration

TGF-β plays a significant role in the regulation of cell growth and proliferation, both in normal liver and in many hepatic diseases. In the normal liver, TGF-β regulates two important primary hepatocyte functions which include growth inhibition and induction of apoptosis (101-104). Normal liver usually contains very little expression of TGF-β however, following injury, TGF-β is upregulated, most predominantly by nonparenchymal cells such as stellate cells and Kupffer cells (105).

Within the liver, activation of the TGF-β pathway has been shown to inhibit the proliferation of hepatocytes during hepatocyte driven liver regeneration yet enhance the proliferation of oval cells during oval cell-mediated liver regeneration (29, 106). This is also

consistent with findings that demonstrate elevated levels of TGF-β1 mRNA during peak days (Days 9-11) of oval cell proliferation following 2AAF/PHx (107). Resent research by Nguyen et al. suggests that this difference in responsiveness to TGF-β between the two cell types is associated with differences in TGF-β sensitivity. The difference in TGF-β sensitivity between hepatocytes and oval cells may be due to the increased expression of Smad6 present in oval cells compared to hepatocytes. Smad6 has been shown to inhibit TGF-β signaling by interacting with the type-I receptor, which in turn inhibits the ability of the receptor to phosphorylate Smad2. Therefore, Smad2 is not activated and does not translocate to the nucleus to initiate transcription of target TGF-β genes. This was confirmed by the lack of phosphorylated Smad2 (phosphor-Smad2) staining found in oval cells compared to hepatocytes in the livers of animals fed a choline deficient, ethionine supplemented (CDE) diet (108). This suggests that an additional component to the TGF-β pathway enabling oval cell proliferation is activated in an environment where hepatocyte proliferation is inhibited.

TGF-β and IGFBP-3

Several signaling pathways are involved in the upregulation of IGFBP-3, which in turn, activate additional downstream signaling pathways which are involved in regulating cellular activities including proliferation, apoptosis, migration and angiogenesis. An overview of some of the pathways involved in IGFBP-3 expression can be seen in Figure 1-2. Members of the TGF-β superfamily have been shown to stimulate IGFBP-3 protein and mRNA production by both IGF-dependent and IGF-independent mechanisms (109). Since this discovery, additional groups have published reports demonstrating that both TGF-β1 and TGF-β2 enhance IGFBP-3 mRNA and protein expression in a variety of cell lines *in vitro* (110, 111). Like IGFBP-3, TGF-β has been shown to either stimulate cell growth or inhibit cell proliferation and promote

apoptosis depending on the condition and cell type (112). In a study by Cohen et al., activation of the TGF-β pathway by administration of TGF-β1 in human smooth muscle airway cells increased IGFBP-3 mRNA and protein expression and led to a two-fold increase in cell proliferation (113). TGF-β has also been shown to increase cell proliferation in studies involving cancer cells. In a study by Kansra et al., IGFBP-3 was found to mediate the TGF-β1 induced proliferation of highly metastatic colon carcinoma cell lines (140). In addition to this, both these studies found that production of IGFBP-3 through activation of the TGF pathway was inhibited through the use of antisense oligomers to IGFBP-3 or through the use of neutralizing IGFBP-3 antibodies, thus further demonstrating a connection between these two pathways.

Although several groups at this time demonstrated a correlation between TGF-β activation and enhanced IGFBP-3 expression, a direct mechanism linking the two pathways remained unknown until studies by Leal et al. and Fanayan et al. shed some light on this phenomenon. Studies by Leal et al. were the first to demonstrate a putative receptor for IGFBP-3 by which the protein mediated its IGF-I-independent functions. In experiments utilizing mink lung epithelial cells, it was discovered that IGFBP-3 binds directly to a newly discovered TGF-β receptor, TGF-βR type V (TGF-βRV). The TGF-βR type V is approximately 400 kDa in size and appears to bind both TGF-β1 and IGFBP-3 with similar affinity. In these studies, it was determined that IGFBP-3 could not only bind to TGF-βRV directly, but that IGFBP-3 could also inhibit the interaction of the ligand TGF-β1 from interacting with the receptor (78, 79). This was one of the first studies to imply that IGFBP-3 may have a direct role in the TGF-β pathway by binding to a specific TGF-β receptor.

In addition to this, studies by Fanayan et al. were the first to show that IGFBP-3 can directly bind to TGF-β type II receptor, which in turn, stimulates the phosphorylation of TGF-β

receptors type I and the signaling intermediates Smad2 and Smad3 in breast cancer cell lines (114). Additionally, activation of this pathway by IGFBP-3 binding was shown to inhibit the proliferation of these cancer cell *in vitro* (114, 115). Results of these studies were further confirmed by Kuemmerle et al. who found that IGFBP-3 displaced TGF-β1 binding to TGF-βRII and TGF-βRV in a concentration dependent manner and inhibited growth of smooth muscle cells *in vitro* (116).

In addition to studies reporting that IGFBP-3 can bind directly to TGF-β receptors, a study by Gui et al. determined that IGFBP-3 may be able to bind directly to the latent form of TGF-β *in vitro*, thus further suggesting a direct interaction between IGFBP-3 and the TGF-β pathway (117). Results of this study found that IGFBP-3 was able to bind directly to LTBP-1, a component of the large latent TGF-β complex. LTBPs are structural components of the extracellular matrix which bind and sequester TGF-β to the ECM and allow for TGF-β to interact with the plasma membrane (118). Interestingly, several groups have found that the interaction of the large latent complex with the plasma membrane is dependent on the mannose-6-phosphate/IGF-II receptor (119, 120). Gui et al. determined that the interaction between IGFBP-3 and LTBP-1 could occur when IGFBP-3 was either unsaturated or saturated with IGF-I protein (117). Therefore, Gui et al. hypothesized that the IGFBP-3/IGF-I complex can bind to the large latent complex TGF-β via an interaction with LTBP-1 and that proteolysis of this complex at the plasma membrane would release both TGF-β and IGF-I (117).

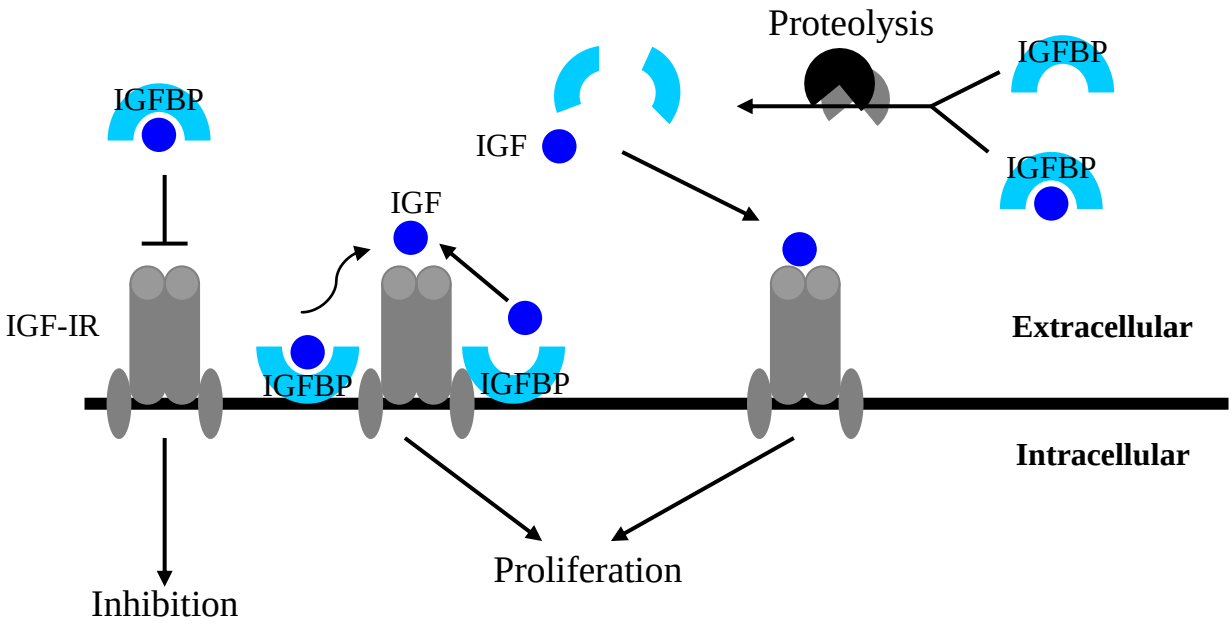

Figure 1-1. Proposed pathways of IGF-dependent functions and activities of IGFBPs. The mitogenic activity of IGFs, mediated through IGF-IR, is inhibited by being sequestered by soluble IGFBPs. Proteolysis of IGFBPs causes IGFs to be released from the binary complexes, leading to increased IGF activity. Cell-associated IGFBPs have been reported to either potentiate or inhibit the effects of the IGFs. Figure adopted from Firth and Baxter, 2002.

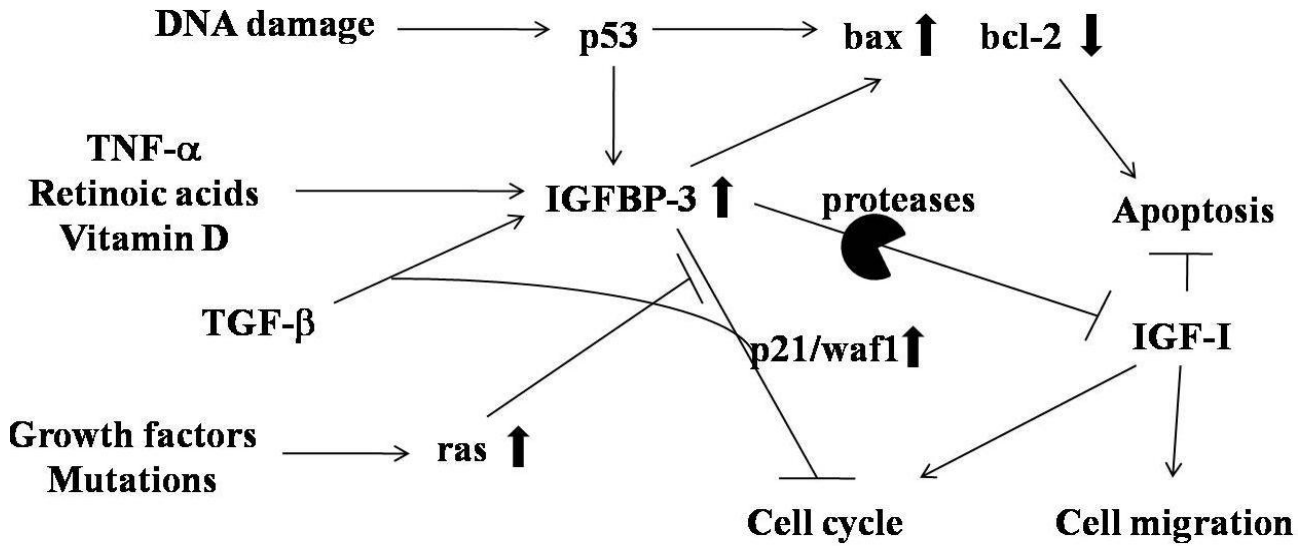

Figure 1-2. Overview of pathways involved in IGFBP-3 action. A variety of proteins and cell signaling factors regulate IGFBP-3 expression.

Table 1-1. Markers used for identifying liver cells.

Markers	Oval cells	Hepatocytes	Bile duct cells	Stellate cells	Endothelial cells
CK7	-	-	+	-	-
CK8	+	+	+	-	-
CK18	+	+	+	-	-
CK19	+	-	+	-	-
ALB	+/-	+	-	-	-
AFP	+	-	-	-	-
GGT	+	-	+	-	-
OV-6	+	-	+	-	-
OV-1	+	-	+	-	-
HES-6	-	+	-	-	-
Desmin	-	-	-	+	-
SE1	-	-	-	-	+

ALB, albumin; AFP, alpha-fetaprotein; CK, cytokeratin; GGT, gamma-glutamyl transpeptidase; HES, hairy and enhancer of split. Legend: + = Expression of marker, - = No expression of marker. Table adopted and compiled from studies by Shiojiri et al. 1991; Marceau et al. 1986, 1990; VanEkyen and Desmet, 1993; Dunsford and Sell, 1989.

CHAPTER 2
STUDY DESIGN AND SPECIFIC AIMS

Oval cell-mediated liver regeneration is a highly complex process that involves the coordination of several signaling factors, chemokines and cytokines to allow for proper maintenance of the liver architecture. When hepatocyte proliferation is inhibited, a hepatic stem cell population, referred to as "oval cells", is activated to aid in liver regeneration. The function of IGFBP-3 during this process of oval cell activation is of particular interest because it is produced in liver and has been shown to induce migration and differentiation of other stem cell populations both *in vitro* and *in vivo*. Additionally, IGFBP-3 production has been linked to the TGF-β superfamily, a pathway known to be induced during oval cell proliferation. In this study, we set out to determine whether IGFBP-3 plays a role in the oval cell proliferation, migration and differentiation during this specific type of regeneration (107, 121).

Insulin-like growth factor binding protein-3 (IGFBP-3) is one of six characterized binding proteins to insulin-like growth factor-I (IGF-I) and is the most abundant IGF binding protein found in circulation (54). IGFBP-3 plays an important role in regulating IGF-I function by binding to approximately 75% of free IGF-I in the serum (55). By binding to IGF-I, IGFBP-3 has been found to regulate the bioavailability of IGF-I as well as prolong its half-life in circulation (122). In addition to this, several groups have identified key functions of IGFBP-3 that appear to be independent of IGF-I.

Recently, IGFBP-3 has been shown to act as a potent inducer of hematopoietic stem cell migration and differentiation both *in vitro* and *in vivo* (91). Due to the fact that IGFBP-3 is produced in the liver and has been shown to activate other stem cell populations *in vivo,* we asked the question of whether or not IGFBP-3 could potentially play a role in regulating the migration, proliferation and/or differentiation of the hepatic oval cells during oval-cell mediated

liver regeneration. Additionally, we asked whether the possible effects of IGFBP-3 during oval cell-mediated liver regeneration involved activation of the TGF-β1 pathway. In order to address these questions, the following specific aims were established:

- **Specific Aim I:** To detect the presence of IGFBP-3 protein and RNA in liver during oval cell-mediated liver regeneration.
- **Specific Aim II:** To determine if IGFBP-3 plays a role in oval cell migration proliferation, and/or differentiation during oval cell-mediated liver regeneration and
- **Specific Aim III:** Determine how oval cell function is altered when expression of IGFBP-3 in the liver is knocked down and to determine a possible signaling pathway that is involved in mediated IGFBP-3 function during this process.

Specific Aim I

Identifying IGFBP-3 expression in the liver during oval cell-mediated regeneration is an essential first step toward determining a potential role for this protein during this phenomenon. By detecting and measuring IGFBP-3 levels during this process, we were able formulate a hypothesis as to how liver regeneration may be affected when expression of IGFBP-3 was altered. Previous studies have shown changes in IGFBP-3 expression during liver regeneration following partial hepatectomy alone (98) however; a role for IGFBP-3 during oval cell based liver regeneration following 2AAF/PHx had not yet been determined.

To detect the presence of IGFBP-3 in the liver, RNA and protein were isolated from whole rat livers obtained from animals that had undergone 2AAF/PHx. RNA and protein isolated from these livers as described in the methods and materials, which were then subjected to RT-PCR and Western blot analysis, respectively. As IGFBP-3 is a secreted protein, serum was isolated

from whole blood taken via venous heart puncture from animals that received 2AAF/PHx and analyzed for IGFBP-3 expression.

Specific Aim II

Many of the underlying factors governing oval cell-mediated liver regeneration *in vivo* have yet to be characterized. As recent research has shown, IGFBP-3 acts as a potent inducer of cell migration, proliferation and differentiation in hematopoietic stem cells and endothelial progenitor cells both *in vitro* and *in vivo* (90, 91). In light of these experiments and the similarity in oval cell and hematopoietic surface markers, we asked whether IGFBP-3 is essential to oval cell migration and proliferation during liver regeneration following 2AAF/PHx.

Many of the activities of the IGFs and IGFBPs are closely linked with the processes of the liver. Although one of the known receptors for IGF-I, IGF-R, has been shown to be expressed by nearly every cell in the body, it is not expressed by hepatocytes in the normal liver. Studies have shown however, that the number of IGF binding sites increases dramatically in these cells during liver regeneration (99). This suggests an integral role for IGF-IGFBP system during the process of liver regeneration which may be essential to oval cell recruitment and proliferation. However, due to the unique nature of IGFBP-3 to both inhibit and promote the proliferative and anti-apoptotic effects of IGF-I, as well as display IGF-I independent activities, it is unclear at the beginning of this study whether or not IGFBP-3 would enhance or inhibit oval cell activation within the 2AAF/PHx model. To begin to address some of these issues, we performed transwell migration and MTT proliferation assays using isolated Thy-1+ oval cells from rat livers during peak time points during our 2AAF/PHx model (Days 9-11) in addition to utilizing a liver stem cell line similar to that of oval cells, the WB-344 cell line. These *in vitro* experiments helped determine what effects IGFBP-3 may have on oval cell activities during liver regeneration.

Specific Aim III

Multiple signaling pathways have been shown to contribute to both early and late events in oval cell activation, which are initiated by several growth factors including α-fibroblast growth factor (αFGF), hepatocyte growth factor (HGF), transforming growth factor (TGF)-α, and transforming growth factor (TGF)-β1 (18, 28). In addition to this, several groups have also shown that activation of the TGF-β pathway induces IGFBP-3 mRNA and protein expression (109). Previous research, in our lab and others, has shown that increasing levels of TGF-β1 seem to correlate with peak days of oval cell proliferation in the 2AAF/PHx model (107, 121). This indicates that the TGF-β pathway is active during this time period and may be initiating the production of cytokines and growth factors which are involved in oval cell proliferation.

Since activation of the TGF-β pathway has been shown to induce IGFBP-3 expression, and studies in our lab have demonstrated TGF-β activation during oval cell proliferation, we have chosen to focus on this particular pathway to determine if TGF-β is inducing IGFBP-3 production and if production of IGFBP-3 is facilitating oval cell proliferation during liver regeneration.

CHAPTER 3
METHODS AND MATERIALS

Experimental Animals

All procedures were performed on Male Fisher-344 rats (Charles River Laboratories Inc., Wilmington, MA) approximately 8 to 10 weeks of age. All animals were maintained on standard laboratory chow and daily cycles of alternating 12 hours of light and dark. Rats were euthanized at the appropriate time points (n=3 per time point) by administration of an overdose (150 mg/kg) of Nembutal sodium solution (OVATION Pharmaceuticals, Inc., Deerfield, IL) via an injection into the peritoneal cavity. This is consistent with the recommendations of the panel on euthanasia of the American Veterinary Medical Association and the Guide for the Use and Care of Laboratory Animals (U.S. Department of Health and Human Services/NIH Publication #86-23). All procedures involving animals were approved by the University of Florida IACUC.

Oval Cell Activation Model

The basic design of the 2AAF/PHx model of oval cell induction was described previously by Petersen et al. (25). Continuous administration of 2AAF in the form of a 28-day time release pellet (Innovative Research Inc., Sarasota, FL) was used to suppress proliferation of mature hepatocytes prior to partial hepatectomy. Briefly, animals were anesthetized with isoflurane prior to the surgical procedures. Upon anesthetization, a 2AAF pellet (70 mg/28 day release, 2.5 mg/day) was implanted in the peritoneal cavity of the animal. One week later, a 70% surgical resection of the liver was performed under general anesthesia as previously described (16).

Isolation of Thy-1+ Oval Cells

Isolation of hepatic oval cells from rat livers during peak days of proliferation (Days 9-11) was accomplished through the use of a two-step collagenase perfusion of the organ. The first step of the perfusion involved the use of a wash solution to remove all blood from the liver,

followed by administration of a collagenase solution to digest the extracellular matrix components of the organ, leaving the structure of the cells intact. The partially digested liver was then passed through a nylon mesh above an autoclaved beaker containing sterile PBS to remove additional cell matrix components. Cells that passed through the nylon mesh were collected in the beaker below and then centrifuged at 500x g to separate the parenchymal fraction of cells from the non-parenchymal cell fraction. Following centrifugation, the Thy-1+ oval cells were further isolated from the nonparenchymal cell fraction via MACS. To accomplish this, the non-parenchymal cell fraction, which contains the oval cell population, was incubated with a FITC-conjugated mouse anti rat Thy-1 antibody for 1 hr. Following primary antibody incubation, the cell fraction was then incubated with anti-FITC magnetic beads for 1 h and then passed through a magnetic column to separate out the Thy-1+ oval cells. The columns were then removed from the magnetic field and washed several times with sterile PBS to remove adhered cells. The cell fraction, now enriched for Thy-1+ oval cells, were then re-suspended in oval cell medium (IMDM, 10% FBS, and 1% insulin) for later use in the various *in vitro* assays.

Models of IGFBP-3 Inhibition in the Rat

In order to determine if IGFBP-3 plays a role during oval cell activation in the rat following 2AAF/PHx, we utilized two different animal models to suppress IGFBP-3 expression in the liver. The first model of IGFBP-3 inhibition was based on a modified protocol adopted from previous studies by Priego et al. and Granado et al. (123, 124). In this study, they demonstrated that administration of LPS through daily intraperitoneal (i.p.) injections at various concentrations ranging from 5 μg/kg to 1 mg/kg could significantly reduce IGFBP-3 mRNA levels in the liver and circulating IGFBP-3 protein levels in the serum (123).

However, in order to determine a more direct "cause and effect" relationship between loss of IGFBP-3 expression and oval cell activation in the liver following 2AAF/PHx, we devised a second model for inhibiting IGFBP-3 expression through the use of multiple siRNA constructs designed against rat IGFBP-3. Schematic diagrams of these models including are depicted in Figures 3-1 and 3-2.

LPS Administration

Male Fisher-344 rats underwent 2AAF/PHx to activate the oval cell population in the liver as previously described in the methods and materials section. One group of animals (Group A) received i.p. injections of LPS (serotype 055:B5; Sigma Chemical, St. Louis, MO) diluted in sterile PBS at a concentration of 5 μg/kg daily, while a second group of animals (Group B) received injections of LPS at a concentration of 5 μg/kg every other day, both starting on Day 0 post-PHx. Animals (n=3 per group) were sacrificed on Day 9 post-PHx and tissue samples collected as previously described in the methods and materials section.

***In vivo* Delivery of IGFBP-3 siRNA**

Silencer *In vivo* Ready Pre-Designed siRNAs (Applied Biosystems, Foster City, CA) against rat IGFBP-3 were used for all siRNA experiments. Three different siRNA constructs to IGFBP-3 (AM16831, #199977, #59620, #47753) were administered to all animals in combination with the 2AAF/PHx protocol to obtain optimal knockdown results. All siRNAs were diluted in sterile PBS, and a total siRNA concentration of 200 μM (100 μM per injection) was administered to rats via a tail vein injection on Day 6 and again on Day 8 post-PHx (n=3). In addition to siRNA, another group of rats (n=3) received 250 ng of IGFBP-3 protein via tail vein injection on Days 6 and again on Day 8 post-PHx. As a control, Silencer Select negative control siRNAs (Applied Biosystems, Foster City, CA) were also administered to rats via tail

vein injections on Day 6 and Day 8 post-PHx at a total siRNA concentration of 200 μM (100 μM per injection). All rats (n=3 per condition) were euthanized at Day 9 post-PHx through injection of an overdose (150 mg/kg) of Nembutal sodium solution (OVATION Pharmaceuticals, Inc., Deerfield, IL) via an injection into the peritoneal cavity. Animals that received siRNA during the 2AAF/PHx protocol and animals that received siRNA in combination with IGFBP-3 during the 2AAF/PHx protocol were then compared to animals at Day 9 post-PHx that did not receive any siRNA or exogenous protein injections.

Tissue Collection

For 2AAF/PHx experiments, animals were sacrificed at standard time points which included Days 0, 3, 7, 9, 11, 13, 17, and 22. For LPS and IGFBP-3 siRNA studies, animals were sacrificed on Day 9 of the 2AAF/PHx protocol. Following euthanasia, tissue from brain, heart, lung, liver, pancreas, spleen, kidney, and intestine was collected for paraffin embedding and frozen tissue sectioning. Additional tissue samples were also taken at this time for isolation of RNA and protein. Blood was also collected from experimental animals at time of sacrifice via a heart puncture. Serum was isolated from the blood samples through the use of blood collection tubes and centrifugation at 12,000 g for 10 min for later use in ELISA studies. Blood serum and samples for protein and RNA were snap frozen in liquid nitrogen and kept at -80ºC until isolation was performed. Tissues for paraffin embedding were fixed overnight in 10% NBF (Richard-Allan Scientific, Kalamazoo, MI). The following day, formalin was exchanged for PBS or 70% ethanol, and the tissue cassettes were then submitted for paraffin embedding by the University of Florida Molecular Pathology Core Facility. Tissue collected for frozen sectioning was immediately placed in cassettes containing Tissue-Tek OCT Compound (Sakura Finetek

U.S.A., Inc., Torrance, CA) and snap frozen in a histobath containing 2-methylbutane. Frozen tissue cassettes were then stored at -80ºC until sectioning.

Immunohistochemistry and Immunofluorescence

Immunohistochemistry and immunofluorescence were performed either on 5 μm paraffin–embedded or OCT frozen sections. For morphology studies, 5 μm paraffin sections were stained with hematoxylin and eosin. The following antibodies were utilized: Ki67 at 1:100 (556003, BD Pharmingen, San Jose, CA), IGFBP-3 at 1:100 (sc-6004, Santa Cruz Biotechnology, Inc., Santa Cruz, CA), and OV-6 at 1:150 (a generous gift from Dr. Stewart Sell, Ordway Research Institute; Albany, NY). Staining was visualized using the appropriate biotinylated secondary antibody with the Vectastain Elite kit and DAB (Vector Laboratories, Burlingame, CA). For IF, Alexa Fluor 488 donkey anti–mouse and Alexa Fluor 568 donkey anti-goat (Invitrogen, Carlsbad, CA, USA) were used as secondary antibodies at 1:1000. Vectastain kit with DAPI (Vector Laboratories, Burlingame, CA) was used for nuclear staining. All slides were visualized using an Olympus B51 microscope and pictures taken on an Olympus U-TVO.5xc camera (Olympus, Melville, NY) with MagnaFire. A complete list of the antibodies and the retrieval methods used for IHC experiments are shown in Table 2-1.

Protein Analysis

Protein Isolation and Quantification

Approximately 50 mg of pooled rat liver tissue was used to obtain protein lysate for various Western blot experiments. The tissues were macerated and then placed in RIPA buffer containing with Protease Inhibitor. The tissue was then pipetted up and down several times with an 18 gauge needle and syringe until thoroughly homogenized. The sample was then vortexed and centrifuged at 10,000 x g at 4°C to separate out the protein and to remove excess lipids and

DNA. The supernatant was then collected in a fresh screw-cap tube. The protein concentration of these samples was then quantified using the Bio-Rad DC Protein Assay (Bio-Rad, Hercules, CA) as per manufacturer's instructions. Samples were then measured in disposable cuvettes through the use of a spectrophotometer set to 750 nm.

Western Blot Analysis

For all Western blot experiments, 25 μg of protein from pooled rat liver or pooled serum samples were utilized. Samples were added to wells of 10% SDS-polyacrylamide precast gels and separated by electrophoresis. The gels were then transferred to Immuno-Blot PVDF membrane (Bio-Rad, Hercules, CA) using standard techniques. Membranes were blocked overnight in a 5% skim milk solution at 4°C. Following this blocking step, membranes were then incubated with their respective primary antibody overnight at 4°C and then incubated with an HRP-conjugated secondary antibody for 1 to 2 h at room temperature. For development of the membrane, ECL plus Western blotting detection kit (Amersham Biosciences, Piscataway, NJ) was utilized. Antibodies used for immunoblotting were as follows: IGFBP-3 at 1:1000 (Santa Cruz #sc-6008) and β-Actin at 1:5000 (Abcam #3280); and horseradish peroxidase (HRP)-conjugated IgG secondary antibodies (Santa Cruz Biotechnology, Santa Cruz, CA).

RNA Analysis

RNA Isolation and Quantification

Approximately 50 mg of pooled rat liver tissue was used to obtain RNA for RT-PCR and qRT-PCR experiments. The tissue was first macerated and then RNABee Reagent was added to the tissue. The solution was then pipetted up and down several times with an 18 gauge needle and syringe until thoroughly homogenized. The homogenized samples were incubated for 5 min at RT to allow for the complete dissociation of the nucleoprotein complexes. Chloroform was

then added to the tubes followed by brief vortexing. The samples were then centrifuged at 12,000 x g for 15 min at 4°C. The upper aqueous phase of the supernatant was transferred to a fresh tube and the RNA was precipitated out through the addition of 70% isopropanol. The samples were incubated for 10 min at RT and then centrifuged at 12,000 x g for 10 min at 4°C. Following centrifugation, the supernatant was removed and the RNA pellet which had formed at the bottom each tube was washed with 75% ethanol. Samples were then vortexed and centrifuged at 7500 x g for 5 min at 4°C. The RNA pellet was then air-dried and then dissolved in RNase-free water. To measure the RNA concentration of each sample, the absorbance was analyzed at OD of 260 and 280 nm in a spectrophotometer. The RNA samples were then stored in fresh screw-cap tubes and stored at -80°C until further use.

RT-PCR

The following primers were used for detection of mRNA in liver tissue obtained from 2AAF/PHx animals. IGFBP-3 Forward Primer: 5' GAAACACCACTGAGTCTGA-GGAGGACC 3' and IGFBP-3 Reverse Primer: 5' GCGACACTGTTTCTTCTTATAGA-ACCCCTTC 3'. These primers generated a 352 bp fragment. The thermocycler conditions used to amplify cDNA products were as follows: 95°C for 4mins, 30 cycles of 95°C for 30sec, 60°C for 30sec, 72°C for 1 min, and 72°C for 7 min for the final elongation step. GAPDH primers were used as a positive control and primer sequences were as follows: Forward Primer 5' TGAGGGAGATGC-TCAGTGTT 3' and Reverse Primer: 5' ATCACTGCCACTCAGAAGAC 3'. Following the PCR reaction, loading dye was added to each sample and then loaded into the wells of a 2% agarose mini-gel containing Ethidium Bromide, along with an appropriate molecular weight ladder. Separation of bands was visualized using a UV light box and final pictures of the gels were taken using the GelDoc XR system (Bio-Rad, Hercules, CA).

Real-Time RT-PCR

Quantitative Real-Time RT-PCR was performed using SA Biosciences TGFβ BMP Signaling Pathway SuperArray pre-designed plates (PARN-035). The list of primers used on these plates can be obtained from the SABiosciences website. RNA isolation was performed as previously described (125). cDNA was generated using the SuperScript III First Strand Synthesis System (Invitrogen, Carlsbad, CA) according to the manufacturer's instructions. The standard conditions used for real-time PCR were as follows: 95°C for 10 minutes followed by 40 cycles of 15s denaturation at 95°C, 30s annealing/elongation at 55°C. SYBR® Green signal was measured at each step, and each sample normalized to β-actin as an internal control. Mean fold gene expression was calculated with SA Biosciences software using the Delta Delta CCT method.

Enzyme-Linked Immunosorbent Assays

Detection of secreted levels of IGFBP-3 in rat serum was performed using a mouse/rat IGFBP-3 ELISA kit (REF E031, Mediagnost Ltd., Reutlingen, Germany) as per manufacturer's instructions. Blood was collected via heart puncture from rats at the time of sacrifice on Day 9 post-PHx. Blood was placed in collection tubes, inverted several times and allowed to sit at room temperature for 20 to 30 minutes. Blood was then centrifuged for 10 minutes at 12,000 rpm at 4°C. The serum layer was then collected and frozen at -80°C until further analysis. ELISA plate readings were obtained using a microplate reader emitting a wavelength of 450 nm (Reference filter ≥590 nm).

Transwell Migration Assays

Cell motility was assessed as previously described by Jung et al. (126). WB-344 cells and isolated Thy-1+ oval cells were seeded at a concentration of $1x10^5$ cells/well onto transwell

membrane filters with a pore size of 5 μm (Corning Incorporated Costar, Corning, NY, USA). Transwell plates were pre-coated with 0.006% collagen in 0.1% acetic acid for 3 h at 37°C. WB-344 cells were fed with DMEM/F12 50:50 media containing 10% FBS and Thy-1+ oval cells fed with IMDM containing 10% FBS and 1% insulin. All cells were allowed to attach overnight at 37°C, 5% CO2. To initiate migration, IGFBP-3 protein (Millipore Corp, Billerica, MA) was added to the lower chambers of the transwell plates at various concentrations (0.1 ng/ml, 1 ng/ml, and 10 ng/ml) in migration buffer (respective cell medium without FBS, containing 0.5% BSA). The assay was allowed to continue at 37°C, 5% CO_2 for 6 h prior to termination. As a negative control, some lower wells contained only migration buffer (without IGFBP-3),or migration buffer with IGFBP-3 at 1 ng/ml added to the upper wells only, or IGFBP-3 added to both the lower and upper wells. Migration assays were performed a minimum of three times to ensure statistical significance.

MTT Proliferation Assay

MTT [3-(4,5-dimethylthiazol-2-yl)-2,5-diphenyltetrazolium bromide; Sigma] proliferation assays were performed as previously described (127). WB-344 cells (1×10^4 cells/well) were seeded in 96-well plates in DMEM/F12 50:50 (with 10% FBS) and were incubated at 37°C, 5% CO_2, overnight. The next day, medium was removed and the cells were cultured in serum free medium (DMEM/F12 50:50 with 0.5% BSA) containing either IGFBP-3 (1 ng/ml) alone, IGF-I (1 ng/ml) alone, or IGFBP-3 with IGF-I (both 1 ng/ml). Plates were then incubated for 24 or 48 h at 37°C, 5% CO_2. At the respective time-point, the MTT assay was terminated and the plates were then analyzed using spectrophotometer at a wavelength of 570 nm.

Statistical Analysis

All results are presented as the means ±s.d, and all data shown were compiled from three separate experiments. Student's t-test was used to analyze the differences between two groups. Values were regarded as significant at * $P < 0.05$ and ** $P < 0.005$. All error bars represent s.d.

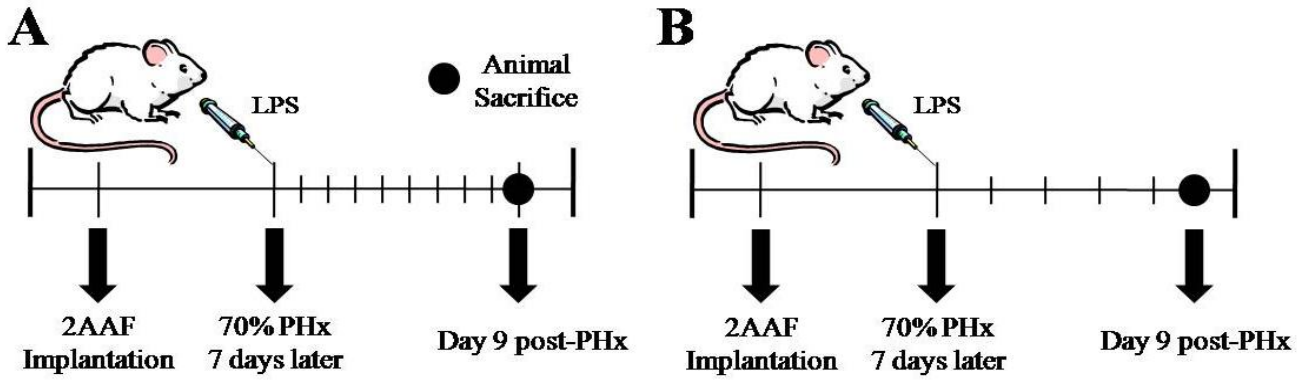

Figure 3-1. Schematic diagram of LPS based animal experiments. As with the standard 2AAF/PHx protocol, animals received a 2AAF pellet, which was implanted into the intraperitoneal cavity, followed by two-thirds partial hepatectomy a week later. A. One group of animals (n=3) received daily i.p. injections of LPS at 5 μg/kg beginning on Day 0 post-PHx and ending on Day 9 before being sacrificed. B. A second group of animals (n=3) received LPS injections every other day beginning on Day 0 post-PHx and ending on Day 8 post-PHx. All animals were sacrificed on Day 9 post-PHx.

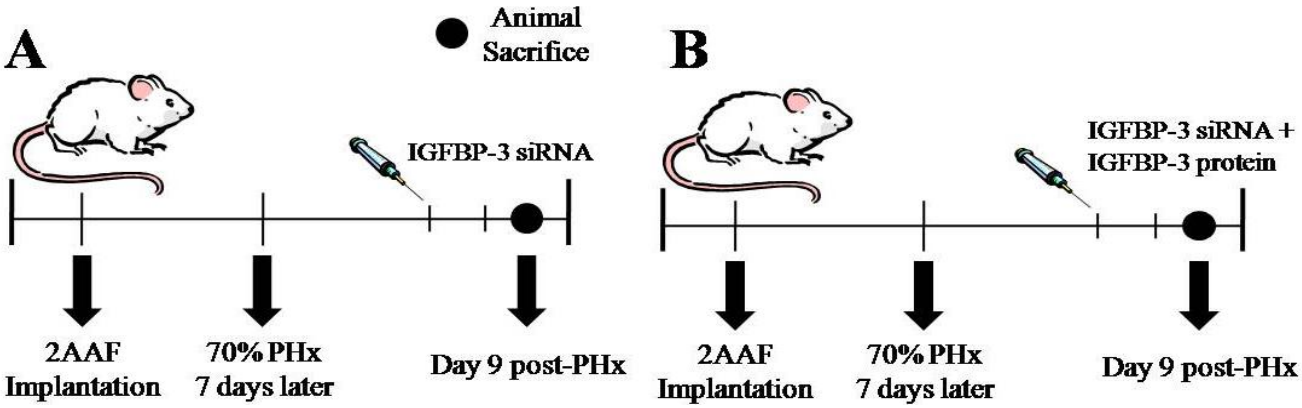

Figure 3-2. Schematic diagram of siRNA based animal studies. As with the standard 2AAF/PHx protocol, animals received a 2AAF pellet, which was implanted into the intraperitoneal cavity, followed by two-thirds partial hepatectomy a week later. A. One group of animals (n=3) received IGFBP-3 siRNA injections via the tail vein on Day 6 and Day 8 post-PHx. B. A second group of animals (n=3) received IGFBP-3 siRNA injections via the tail vein in combination with IGFBP-3 protein on Day 6 and Day 8 post-PHx. All animals were sacrificed on Day 9 post-PHx.

Table 3-1. Antibodies used for immunohistochemistry experiments.

Antibody	Host	Concentration	Section	Retrieval	Company
IGFBP-3	Goat	1:100	Paraffin	Citrate	Santa Cruz
IGFBP-3	Rabbit	1:100	Frozen	None	Santa Cruz
Ki67	Mouse	1:100	Paraffin	Citrate	BD Biosciences
AFP	Mouse	1:150	Paraffin	Trilogy	Dako
OV-6	Rabbit	1:150	Frozen	None	Gift from Dr. S. Sell
Thy-1	Mouse	1:100	Cell cytospin	None	BD Biosciences
CYP3A2	Rabbit	1:100	Paraffin	Citrate	Fitzgerald

CHAPTER 4
ANALYSIS OF IGFBP-3 EXPRESSION DURING OVAL CELL-MEDIATED LIVER REGENERATION IN THE RAT

Introduction

Although IGFBP-3 is primarily produced in the liver under normal conditions by non-parenchymal cells such as Kupffer cells (61), changes in expression of IGFBP-3 during oval cell-mediated liver regeneration have never been examined. As previously stated, several reports have demonstrated either increased or decreased expression of other IGFBPs following partial hepatectomy alone and have shown that IGF-IR is upregulated in response to liver injury (93, 95, 97, 99, 128). In addition to this, oval cells have been previously shown to express IGF-II (29), which suggests a possible role for the IGFBPs during oval cell-mediated liver regeneration, which may be IGF-dependent.

To verify whether or not IGFBP-3 is expressed during oval cell-mediated liver regeneration, rat livers were harvested at standard time points (n=3 animals per time point) from rats that had previously undergone 2AAF/PHx. As a control, livers were also harvested from normal rats that had not been implanted with a 2AAF pellet or undergone a two-thirds partial hepatectomy.

Protein and RNA were then isolated from these liver samples and utilized for Western blot and RT-PCR analysis respectively to determine expression levels of IGFBP-3 during oval cell-mediated liver regeneration. Some liver was also used for paraffin and frozen tissue sectioning and stained for IGFBP-3 to further examine the expression pattern of this protein and to determine if oval cells express IGFBP-3. In addition to this, serum was collected during sacrifice at these time points for ELISA analysis to determine IGFBP-3 levels in the blood during 2AAF/PHx.

Results

Expression of IGFBP-3 in the Liver and Serum During Oval Cell-Mediated Liver Regeneration

RT-PCR analysis of cDNA obtained from whole, pooled liver samples from animals that had undergone 2AAF/PHx determined that IGFBP-3 mRNA is in fact present at all time points during this protocol (Figure 4-1A). In addition to this, Western blot analysis performed on protein isolated from these same liver samples determined that IGFBP-3 protein is also present at all time points during the 2AAF/PHx protocol (Figure 4-1B). In figure 4-1B, expression of IGFBP-3 protein becomes slightly decreased in the days following partial hepatectomy (Days 0-3). In contrast, IGFBP-3 expression increased beginning on Day 9 of the 2AAF/PHx protocol (Figure 4-1C, **P< 0.005). IGFBP-3 protein levels remained elevated in comparison to the normal rat until Day 17, after which IGFBP-3 levels began to decrease and returned to basal levels by Day 22. The increased presence of IGFBP-3 protein at peak days of oval cell proliferation was further confirmed though the analysis of serum harvested from these same animals. ELISA analysis of secreted IGFBP-3 determined thatIGFBP-3 protein levels at Days 9 and 11 post-PHx were significantly higher compared to serum levels of IGFBP-3 normal animals (Figure 4-2, *P< 0.05). By Day 13, serum levels began to decrease and returned to basal levels by Day 22 of the study.

The presence of IGFBP-3 protein in the liver was further confirmed by histological analysis through the use of an IGFBP-3 specific antibody. IGFBP-3 expression in the normal liver appeared to be evenly distributed throughout the tissue, as evidence by positive IGFBP-3 signaling in cells located in between hepatocytes as seen in Figure 4-3, A and B. However, on Day 9 post-PHx, the distribution and intensity of IGFBP-3 protein expression is altered in comparison to normal liver tissue. Highly positive areas of IGFBP-3 staining can be found in

cells surrounding the central vein (Figure 4-3, C and D). In addition to this, there are a few scattered cells around the periportal region of the liver lobule, in close proximity to the infiltrating oval cells, which also stain positive for IGFBP-3 protein expression (Figure 4-3, E and F).

IGFBP-3 is Expressed by Non-Parenchymal Cells During Peak Days of Oval Cell Proliferation in the Regenerating Liver

Due to the fact that IGFBP-3 levels in the liver become elevated during peak days of oval cell proliferation, we set out to determine whether or not IGFBP-3 protein was being produced by the oval cells themselves. Following a two-step collagenase digestion of the liver and simple gravitational enrichment of the isolated liver cells, we obtained the NPC fraction of cells which were then adhered to glass microscope slides and dual-stained for expression of IGFBP-3 and the oval cell marker, Thy-1. Results of this dual immunofluorescent stain indicate a lack of co-localization between Thy-1 and IGFBP-3 (Figure 4-4). This would indicate that the Thy-1+ oval cells do not express IGFBP-3, and that another cell population, most likely the Kupffer cells, is responsible for the increase in IGFBP-3 expression during oval cell-mediated liver regeneration.

Discussion

Through these experiments, we were able to demonstrate that IGFBP-3 protein and mRNA are present in the liver during oval cell-mediated liver regeneration. Additionally, we determined that IGFBP-3 protein expression is increased, both in the liver and as a secreted protein in the serum, during peak days of oval cell proliferation (Days 9-11). Although protein levels of IGFBP-3 in the liver remain elevated until approximately Day 17, IGFBP-3 levels in the serum begin to decrease shortly after Day 11 post-PHx in the rat. This decrease in detected IGBFP-3 levels secreted into the serum may be due to increased levels of matrix

metalloproteinases (MMPs) in the liver, which are believed to facilitate oval cell infiltration into the regenerating liver and have also been found to degrade IGFBP-3. MMPs function by degrading basement membrane protein and play a key role in matrix remodeling during morphogenesis and tissue repair (129). Previous studies by Van et al. have shown that MMP-2 and MMP-9 mRNA levels are elevated in the liver during oval cell-mediated regeneration and correlate with peak days of oval cell proliferation (130). In this study, MMP-2 and MMP-9 mRNA levels were shown to reach maximum levels at Days 9-14 post-PHx and decreased thereafter. In addition to this, in situ hybridization experiments determined that MMP-2 and MMP-9 were predominantly expressed by the oval cell themselves at these time points (130). Interestingly, MMPs such as MMP-2, -7 and -9, have also been shown to cleave IGFBP-3 at specific proteolytic cleavage sites (131, 132). This process is yet another mechanism by which IGFs are released from IGFBP-3 and therefore free to interact with their respective IGF receptor to initiate proliferative and antiapoptotic cell functions (133).

Another possible explanation for the difference in IGFBP-3 protein in the liver and secreted IGFBP-3 at Days 11 and 13 is that IGFBP-3 protein in the liver is binding to cell surface receptors, such as the TGF-βRV, or is translocated into the various liver cells through retinoid X receptors, thus protecting the protein from MMP degradation and maintaining elevated levels of IGFBP-3 in the liver as detected by Western blot analysis. Therefore, as oval cells begin infiltrating the liver and increasing production of MMPs, such as MMP-2 and 9, excess or unbound IGFBP-3 protein in the liver may be cleaved, resulting in decreased levels of whole IGFBP-3 protein that is able to reach the bloodstream in rats at the later time points (Days 13 and 17) following 2AAF/PHx. Additional studies would need to be conducted in order to determine the exact mechanism by which IGFBP-3 levels in the liver help mediate oval cell activation and

to determine if IGFBP-3 protein is somehow protected from degradation during oval cell infiltration into the damaged liver.

IGFBP-3 staining of liver tissue at Day 9 post-PHx demonstrates a unique change in IGFBP-3 protein distribution compared to normal liver tissue. At Day 9 post-PHx, we report an increase in IGFBP-3 expression around the central vein, with a few scattered cells positive for IGFBP-3 around the portal triad region. The unequal distribution of IGFBP-3 protein in the liver suggests that IGFBP-3 may act as a potential chemoattractant of these oval cells across a concentration gradient during oval cell-mediated regeneration. It is well established that oval cells entering the liver at the periportal region begin rapidly proliferating and undergo the process of differentiating into small, basophilic hepatocytes, and eventually mature hepatocytes. Distribution of IGFBP-3 during the peak of oval cell proliferation suggests that oval cells initiate the regenerative process, where IGFBP-3 concentrations are relatively low, and then migrate toward the central vein, where IGFBP-3 concentrations are much higher.

Dual IF staining of non-parenchymal cells demonstrated that IGFBP-3 expression does not co-localize with the Thy-1+ oval cell population, which would indicate that oval cells do not produce IGFBP-3. However, previous reports have demonstrated the that oval cells are capable of responding to several factors secreted by other non-parenchymal cell populations, such as the stellate cells, which secrete factors such as HGF, TGF-α and TGF-β (29). Therefore, it possible that oval cells are activated in response IGFBP-3 protein production from another non-parenchymal cell population during oval cell-mediated liver regeneration. As oval cells have been shown to express IGF-II, it is possible that IGFBFP-3, which can bind both IGF-I and IGF-II, may mediate oval cell migration and proliferation in an IGF-dependent manner during this specific type of liver regeneration.

In addition to the change in IGFBP-3 distribution in the liver during oval cell-mediated liver regeneration, there also appears to be a shift in the types of cells that are positive for IGFBP-3 expression at Day 9 post-PHx in comparison to normal liver. In normal liver, IGFBP-3 is expressed by non-parenchymal cells such as Kupffer cells however; it appears in liver sections at Day 9 post-PHx that several hepatocytes around the central vein and a few scattered around the portal triad are strongly positive for IGFBP-3 expression (Figure 4-3). Although previous reports state that IGFBP-3 mRNA and protein are not produced by hepatocytes in the liver under normal conditions (60, 61), it is possible that hepatocytes may begin to produce IGFBP-3 mRNA and/or protein in response to their inhibited ability to proliferate (as a result of 2AAF administration) or in response to liver injury during oval cell-mediated liver regeneration. However, it is unclear at this point whether hepatocytes are expressing the protein directly or if IGFBP-3 is merely binding to cell surface receptors present on the hepatocytes. Further experiments will need to be conducted in order to determine which of the two possibilities is occurring during oval cell-mediated liver regeneration.

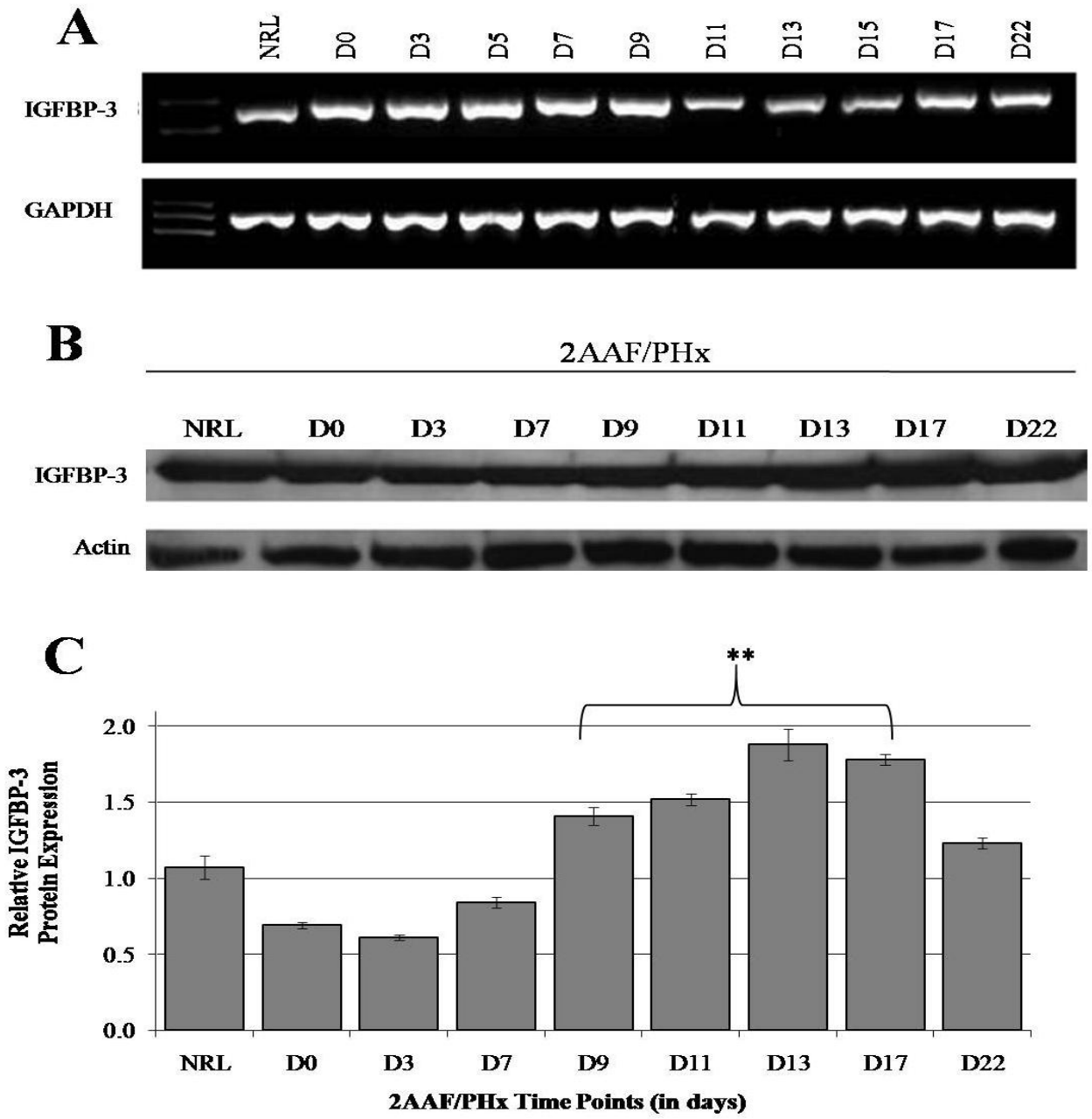

Figure 4-1. Expression of IGFBP-3 mRNA and protein in liver during the 2AAF/PHx time course. A. RT-PCR analysis of normal rat liver (NRL) and liver taken at standard 2AAF/PHx time points verifies IGFBP-3 mRNA expression during oval cell-mediated liver regeneration. B. Western blot analysis performed on protein isolated from liver taken at standard 2AAF/PHx timepoints and probed for IGFBP-3. Protein from NRL was used as a control. IGFBP-3 significantly decreased following PHx (Day 0), and then increased significantly to levels greater than NRL by Day 9. Levels remained elevated until Day 17 and then decreased to baseline levels by Day 22. C. Semi-quantitative analysis of IGFBP-3 protein expression. Data shown were compiled from three independent experiments. Expression was normalized to β-actin and significance calculated compared to control animals. **$P < 0.005$.

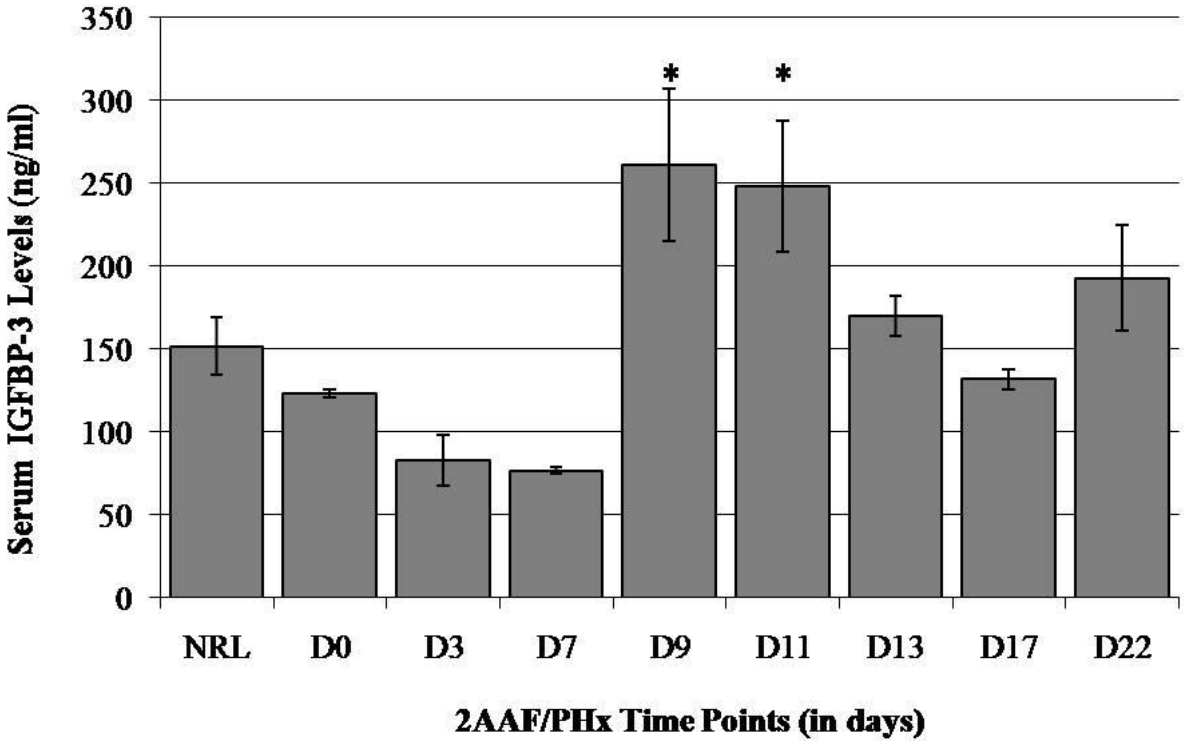

Figure 4-2. Enzyme-linked immunosorbent assay for IGFBP-3 protein expression in rat serum during oval cell-mediated liver regeneration. Serum from untreated rats (NRL) was used as a control. Levels of IGFBP-3 decreased after PHx (Day 0) and continued to decrease until Day 7 post-PHx. At Days 9 and 11, IGFBP-3 levels were significantly increased compared to NRL serum levels. By Day 13, serum levels again decreased and returned to approximately baseline levels by Day 22. * $P < 0.05$

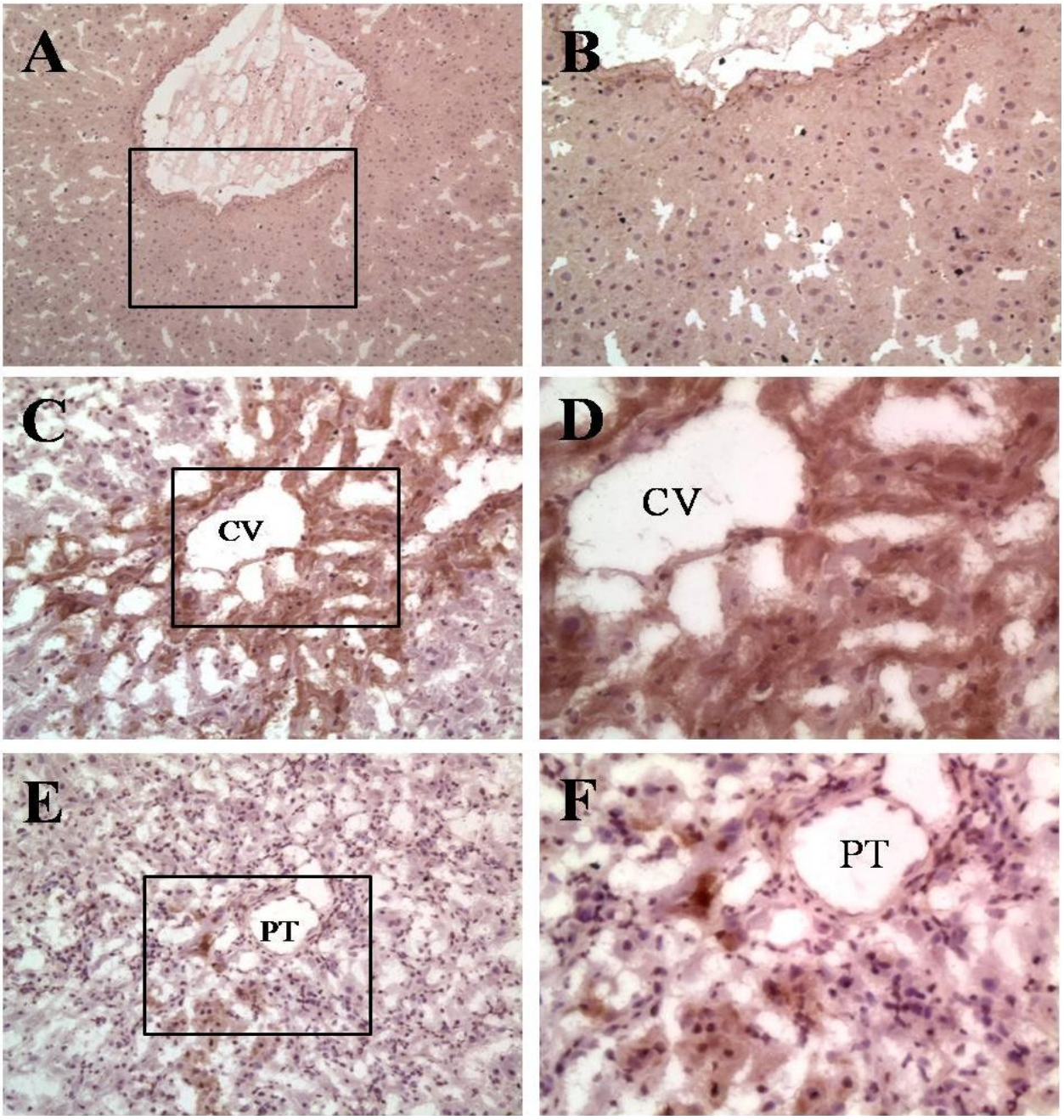

Figure 4-3. Changes in IGFBP-3 protein distribution during hepatic regeneration. A-F. IHC analysis of IGFBP-3 expression in the normal rat liver (A and B) and at Day 9 post-PHx (C-F). In the normal liver, IGFBP-3 expression is distributed throughout the tissue, with areas of strong signal in the interstitial space between adjacent hepatocytes (A and B). Following 2AAF/PHx, there is an increase in IGFBP-3 expression at Day 9 around the central vein (C and D). IGFBP-3 expression can also be found around the portal triad region in Day 9 post-PHx tissue, where oval cell infiltration into the regenerating liver is taking place (E and F). Oval cells do not appear to be positive for IGFBP-3 expression. Portal triad (PT), Central vein (CV). A, C, E, 10x; B, D, F, 20x.

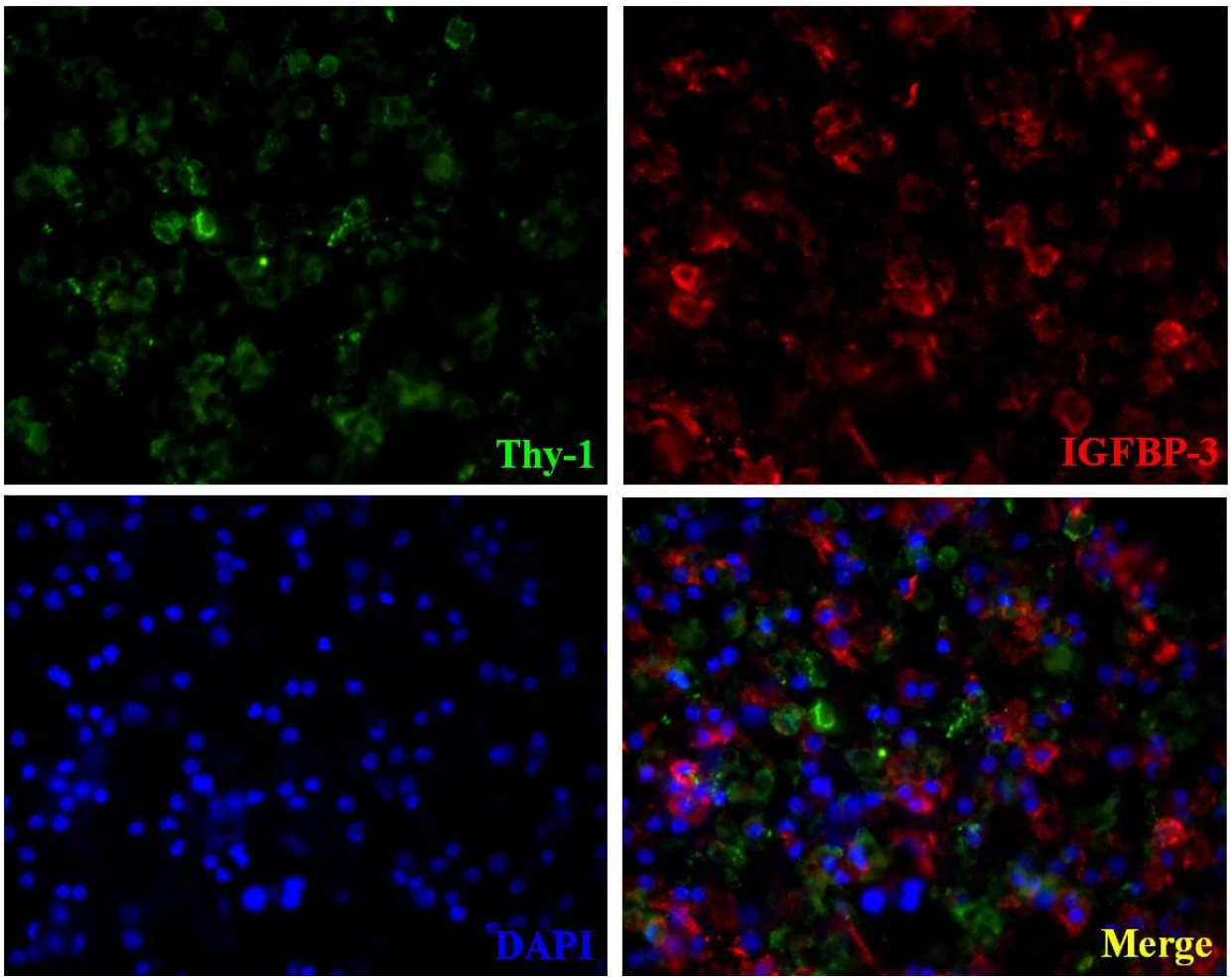

Figure 4-4. IGFBP-3 is not expressed by Thy-1+ oval cells at Day 9 post-PHx in the rat. Dual immunofluorescent stain of a cytospins using cells obtained from the NPC fraction of the liver following a two-step collagenase digestion of the organ. NPCs were stained with antibodies specific for Thy-1 and IGFBP-3 expression. Merged image indicates that Thy-1+ oval cells do not expression IGFBP-3. 20x magnification.

CHAPTER 5
IGFBP-3 INDUCES OVAL CELL AND WB-344 CELL MIGRATION AND INHIBITS IGF-I INDUCED PROLIFERATION *IN VITRO*

Introduction

To determine whether IGFBP-3 could act as a potential chemoattractant and induce oval cell migration, we established transwell migration assays utilizing Thy-1+ isolated oval cells at Day 9 post-PHx and WB-344 rat liver epithelial cells, a cell line that displays liver stem cell properties. WB-344 cells are cells that have been isolated from the liver of an adult male Fischer-344 rat. The phenotypic property of these cells in culture resembles the bipotential nature of the hepatic stem cell population known as oval cells and are therefore used as model for the studying the *in vitro* properties of these oval cells (134, 135). In addition to promoting cell migration, several groups have reported the effects of IGFBP-3 on either promoting or inhibiting the proliferative ability of cells both *in vitro* and *in vivo* (115, 136, 137). To determine what effect IGFBP-3 has on oval cell proliferation, we established several MTT proliferation assays again using WB-344 stem-like cell line. Because IGFBP-3 has been shown to mediate many of its effects either independently or dependently on the presence of IGF-I, we included IGF-I at equal concentrations to IGFBP-3.

Results

Oval Cell and WB-344 Cell Migration Assays

In the presence of IGFBP-3, there was a significant increase in the number of migrating Thy-1+ oval cells in wells containing IGFBP-3 at 0.1 ng/ml and 1.0 ng/ml, compared to the number of cells induced to migrate in chambers containing media with FBS alone (Figure 5-1). Interestingly, IGFBP-3 at the highest concentration (10 ng/ml) appeared to inhibit oval cell migration in comparison to control wells containing FBS alone. The effect of IGFBP-3 on oval cell migration was further confirmed through the use of WB-344 cells under the same conditions

and concentrations of IGFBP-3. As with the Thy-1+ oval cells, there was a significant increase in the number of migrating WB-344 cells in the presence of IGFBP-3, with relatively similar effects at concentrations of 0.1 ng/ml and 1.0 ng/ml (Figure 5-2). However, unlike oval cell migration, the most significant number of migrating WB-344 cells were detected in chambers containing the highest concentration of IGFBP-3 (10 ng/ml). The reason for this difference between the two cell lines in high concentrations of IGFBP-3 is unclear however; the results of these assays suggest that IGFBP-3 can act as a potent chemoattractant for both WB-344 and Thy-1+ oval cells at relatively low concentrations. Based on results obtained from using the Thy-1+ oval cells, we believe that IGFBP-3, at high concentrations, may negatively regulate the migration of these cells *in vivo*.

WB-344 Cell Proliferation Assays

Following exposure to IGF-I at 1 ng/ml for 24 h, WB-344 cell proliferation was significantly increased compared to cells in BSA alone. Alternatively, WB-344 cells exposed to IGFBP-3 showed little difference in cell proliferation after 24 h (Figure 5-3). However, when cells were exposed to IGF-I in the presence of IGFBP-3, cellular proliferation was significantly suppressed (*$P<0.05$). Following 48 h and 72 h of exposure, no significant changes in proliferation could be detected in any of the experimental conditions.

Discussion

In conclusion, *in vitro* migration assays determined that both isolated oval cell and WB-344 cells are responsive to IGFBP-3 at low concentrations, indicating that IGFBP-3 may act as a potential chemoattractant to oval cells during liver regenerations. The inhibitory effects that high levels of IGFBP-3 displayed on oval cell migration may indicate that there is a fine balance between oval cell migration and IGFBP-3 levels in the liver in order to properly regulate oval cell activity during this process. As Western blot and ELISA analysis has shown, IGFBP-3

protein levels are initially low in the liver and serum in the first few days following partial hepatectomy. This decrease in IGFBP-3, in addition to other factors, may initiate an oval cell response, leading to an increase in oval cell migration into the injured liver. As the process of oval cell-mediated liver regeneration continues, we see an increase in IGFBP-3 protein expression in the serum and liver which correlates with the peak of oval cell proliferation. Here, increased IGFBP-3 levels in the liver and serum may act to inhibit further oval cell migration into the regenerating organ. This theory is supported by the difference in tissue distribution of IGFBP-3 protein that is detected in the liver. At Day 9 post-PHx we see a high amount of IGFBP-3 staining around the central vein, with little IGFBP-3 around the portal triad region where infiltrating oval cells are seen entering the liver. It is possible that IGFBP-3 acts to stimulate oval cell migration in a concentration dependent manner from the portal triad region towards the central vein where IGFBP-3 levels are increased. Once oval cells reach the area of liver surrounding the central vein, they encounter elevated IGFBP-3, possibly signaling them to stop migrating and begin differentiating toward either the hepatocyte or biliary lineage.

In addition to promoting cell migration, IGFBP-3 was found to inhibit cell proliferation in the presence of IGF-I when added at equal concentrations. Because IGFBP-3 has been shown to mediate many of its effects either independently or dependently on the presence of IGF-I, these experiments leads us to believe that IGFBP-3 induced effects on oval cell activation may be IGF-dependent. Based on the known functions of IGFBP-3, this phenomenon suggests that IGFBP-3 may be binding to free IGF-I in the culture medium and sequestering it, which may inhibit IGF-I from promoting cell proliferation *in vitro*. Due to the similarities between oval cells and the WB-344 cell line, these results would suggest that hepatic oval cells may be responsive to IGF-I and that the effects mediated by IGFBP-3, *in vitro* or *in vivo,* may be IGF-I

dependent. Further experiments would need to be performed to determine if oval cells express the receptor for IGF-I, which would further suggest a possible role for IGFBP-3 mediated migration and proliferation which is dependent on the presence of IGF-I.

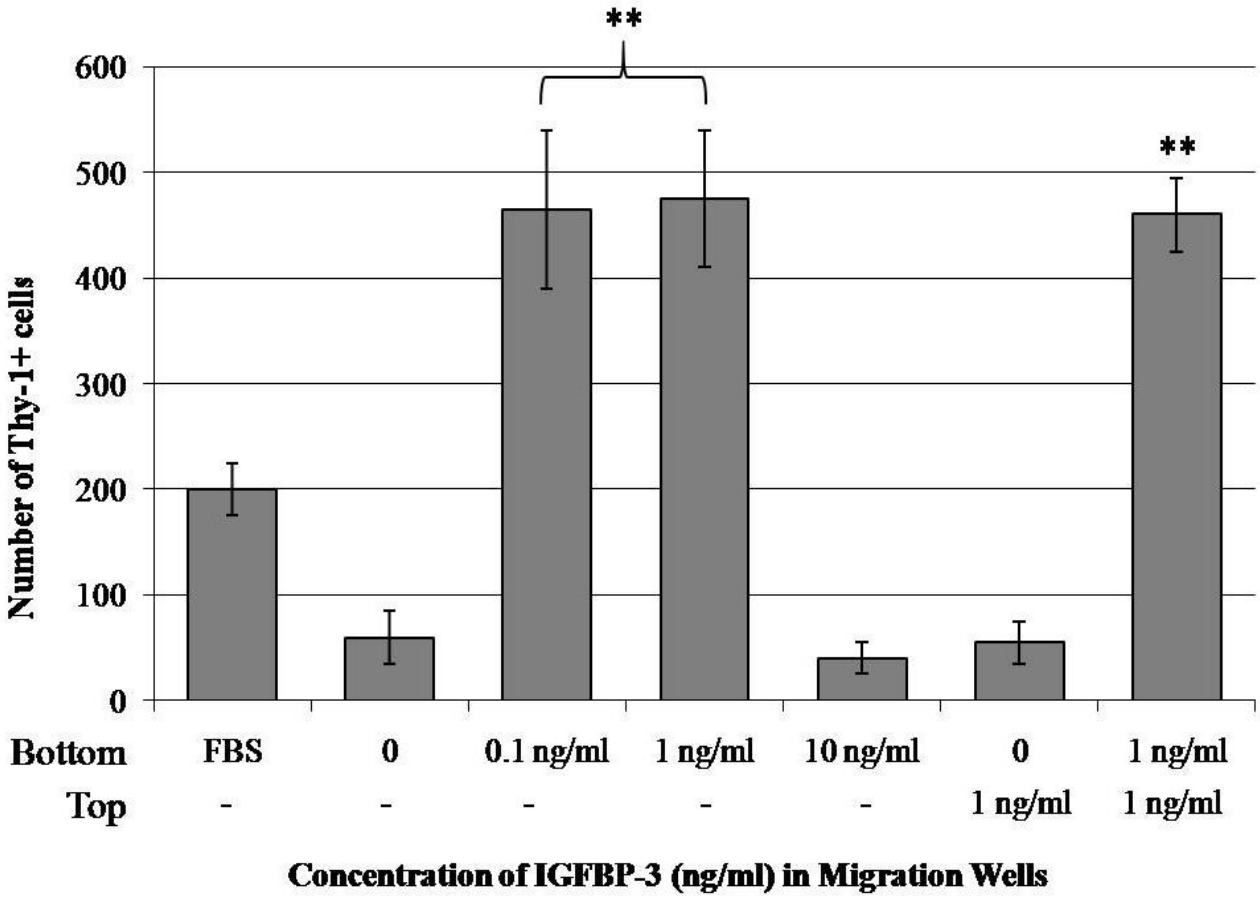

Figure 5-1. IGFBP-3 acts a potent chemoattractant for Thy-1+ oval cells at low concentrations. Analysis of transwell migration assays using Thy-1+ isolated oval cells and various concentrations of IGFBP-3 (0.1, 1, and 10 ng/ml) added to the bottom wells. Oval cell migration increased significantly in the presence of IGFBP-3 with relatively similar effects at 0.1 ng/ml and 1.0 ng/ml. When the highest concentration of IGFBP-3 was used (10 ng/ml), oval cell migration was significantly inhibited. Data shown were compiled from three independent experiments. *$P < 0.05$, **$P<0.005$.

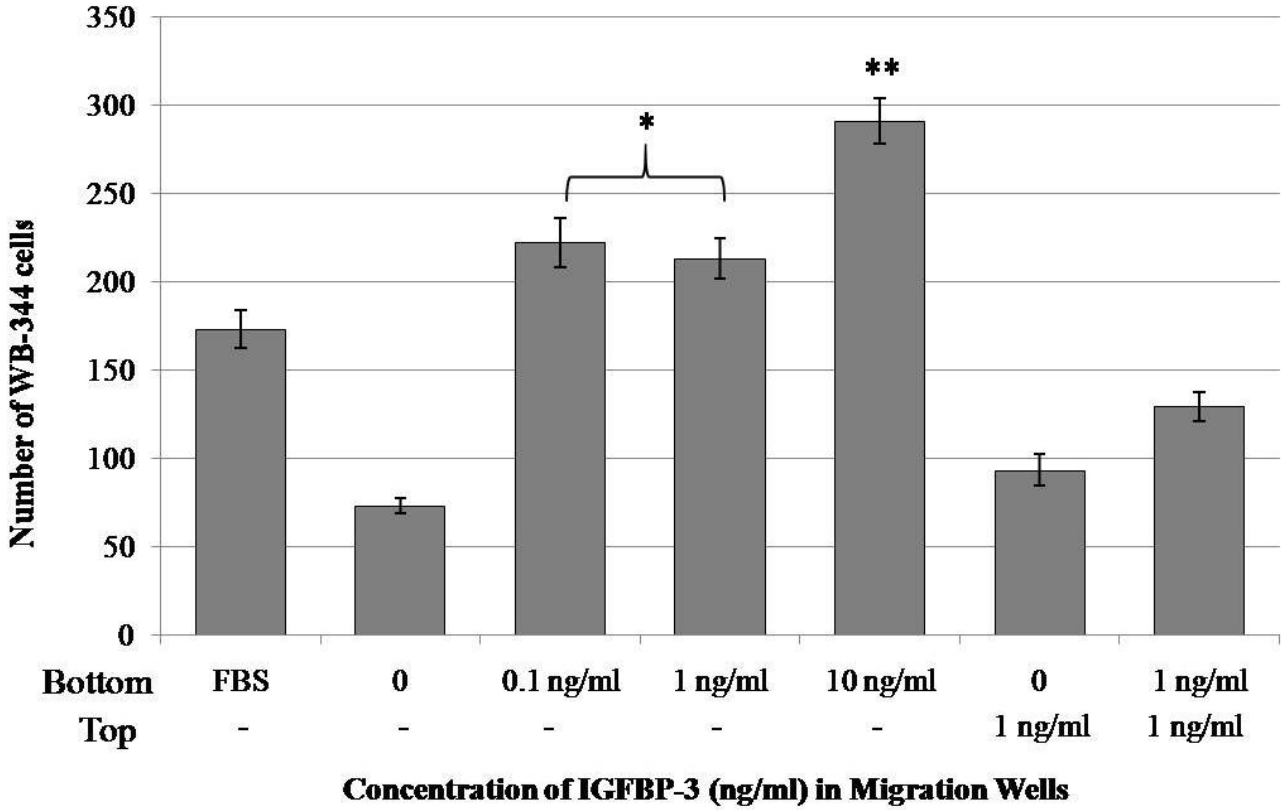

Figure 5-2. IGFBP-3 acts as a potent chemoattractant for the WB-344 oval cell line at various concentrations. Analysis of transwell migration assays using WB-344 cells and various concentrations of IGFBP-3 (0.1, 1, and 10 ng/ml) added to the bottom wells. WB-344 cell migration increased significantly in the presence of IGFBP-3 with relatively similar effects at 0.1 ng/ml and 1.0 ng/ml. The most dramatic increase in cell migration was seen when the highest concentration of IGFBP-3 was used (10 ng/ml). Data shown were compiled from three independent experiments. *P <0.05. **P<0.005.

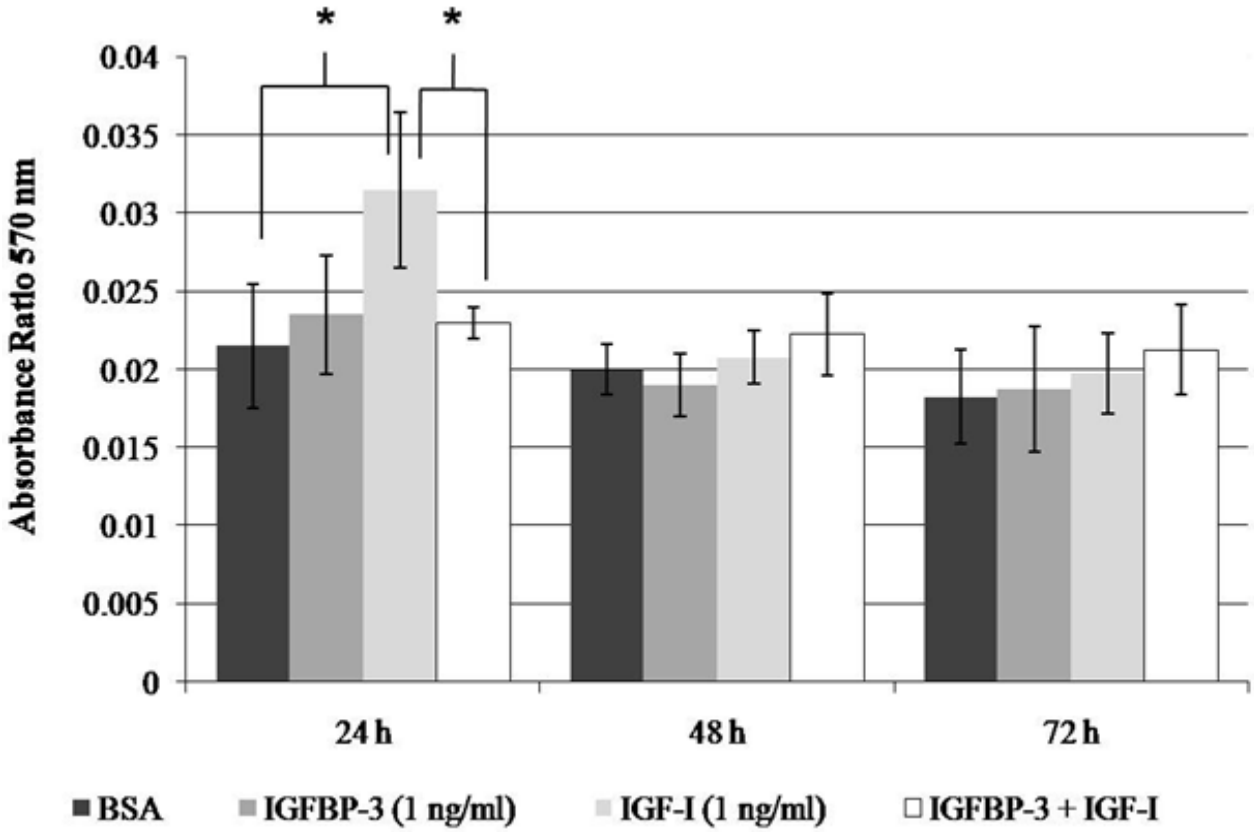

Figure 5-3. IGFBP-3 inhibits IGF-I induced proliferation of WB-344 cells. MTT proliferation assays were performed on WB-344 cells *in vitro*. After 24 h, IGFBP-3 alone had no effect on WB-344 cell proliferation. IGF-I (1 ng/ml) significantly increased WB-344 cell proliferation compared to cells treated with media containing BSA (0.5%) alone. When IGFBP-3 (1 ng/ml) and IGF-I were added together, the proliferative effect of IGF-I was significantly inhibited. Following 48 h and 72 h, all conditions showed relatively the same amount of WB-344 cell proliferation. Data shown were compiled from three independent experiments. *$P < 0.05$.

CHAPTER 6
LPS ADMINISTRATION DURING LIVER REGENERATION INHIBITS IGFBP-3 EXPRESSION AND REDUCES OVAL CELL ACTIVATION *IN VIVO*

Introduction

Endotoxin, also known as lipopolysaccharide (LPS), is a cell wall component that surrounds Gram-negative bacteria such as *E. coli*, which often provokes a strong immune response in both humans and animals. Previous studies have shown that LPS administration to rats is effective at reducing gene expression of IGF-I in the liver, which in turn, greatly reduces the amount of circulating IGF-I present in the serum (138). The inhibitory effect of LPS on the IGF-I axis is also exerted on IGFBP-3. Studies by Priego et al. found that rats treated with very low concentrations of LPS (5 μg/kg) displayed decreased levels of secreted IGFBP-3 protein and mRNA in the liver, with no significant changes in the levels of IGF-I protein and mRNA levels in serum and liver, respectively (123, 139). Decreased protein expression of IGFBP-3 in liver is believed to be the result of increased activation of Kupffer cells in response to LPS treatment.

To determine if LPS induced suppression of IGFBP-3 expression in the liver during oval cell-mediated liver regeneration could significantly alter oval cell activation during this phenomenon, we established two experimental animal models. One group of rats received 2AAF/PHx in combination with either daily injections of LPS (Group A) or 2AAF/PHx in combination with LPS injections every other day (Group B), both beginning on Day 0. Based on the aforementioned studies, we chose to administer the lowest possible dose of LPS necessary to inhibit IGFBP-3 production in the liver without producing any significant changes in IGF-I expression in the liver. At the conclusion of these experiments, analysis of the LPS treated livers from Groups A and B found that there was no significant difference in oval cell activation between the two experimental groups. Therefore, all results shown in this section are

representative of the group of animals that received daily, i.p. LPS injections at a concentration of 5 μg/kg (Group A).

Results

Confirmation of Reduced IGFBP-3 Expression in the Liver Following LPS Administration

RT-PCR analysis of RNA isolated from LPS treated animals demonstrated that IGFBP-3 mRNA is still present in the liver during oval cell-mediated liver regeneration, indicating that LPS does not completely inhibit IGFBP-3 gene transcription in the liver (Figure 6-1A). However, Western blot analysis of LPS treated animals demonstrates a significant reduction in IGFBP-3 protein (~60% decrease) in the livers of these animals in comparison to animals at Day 9 post-PHx alone and normal, untreated animals (Figure 6-1, B and C). A reduction in IGFBP-3 protein was further confirmed through ELISA analysis. Serum harvested from LPS treated animals at Day 9 post-PHx displayed significantly reduced levels of circulating IGFBP-3 protein in comparison to both normal liver and liver from animals at Day 9 post PHx alone (Figure 6-2). These results are support the findings of the aforementioned studies by Priego et al. in which LPS was shown to significantly suppress IGFBP-3 protein expression in liver and serum of treated rats. These findings however, are the first to show that LPS in combination with 2AAF/PHx confers a similar response in IGFBP-3 protein expression.

LPS Administration Results in Decreased Oval Cell Activation Following 2AAF/PHx in the Rat

Once we confirmed that IGFBP-3 protein in rat liver and serum were significantly suppressed in animals treated with LPS following 2AAF/PHx, we then set out to determine what effects this would have on the oval cell response during the peak of cell proliferation during liver regeneration. Hematoxylin and eosin staining of LPS treated livers at Day 9 post-PHx revealed that although small, ovoid cells are present in the liver tissue at this time point, there was a

dramatic decrease in the number of these cells infiltrating in and around the portal triad region in comparison to untreated animals at Day 9 following 2AAF/PHx alone (Figure 6-3). To further confirm that these small, ovoid cells are in fact the oval cell population, we then performed OV-6 staining on these livers. Day 9 post-PHx is a well established time point that is used to mark the peak of oval cell proliferation. At this stage during oval cell-mediated liver regeneration, we would expect to find numerous OV-6 positive oval cells that are actively undergoing proliferation in order to compensate for the loss of liver tissue and inactivation of hepatocyte activity. However, Figure 6-4 clearly shows the dramatic reduction in the number of OV-6 positive cells infiltrating the liver around the portal triad region in the LPS treated livers at Day 9 post-PHx in comparison to untreated animals at Day 9 post-PHx. In addition to the reduction in the oval cell response in these LPS treated livers; we also noted a decrease in the number of cells that were actively undergoing proliferation as evidenced by a lack of Ki67 positive staining in the cells surrounding the periportal region of the liver lobule (Figure 6-5). At Day 9 post-PHx alone, there are several small, ovoid shaped cells around the periportal region which are Ki67 positive whereas the LPS treated livers display few if any cells that are positive for Ki67.

To further confirm that the loss of IGFBP-3 protein expression in the liver correlates with a significant decrease in oval cell activation in the LPS treated livers, we performed a dual immunofluorescent stain for IGFBP-3 and OV-6 expression. Here, at Day 9 post-PHx we again see large number of OV-6 positive cells around the portal triad region of liver, the presence of which is absent in the LPS treated livers at Day 9 (Figure 6-6). In addition to this, we also see a large amount of positive staining for IGFBP-3 protein expression in this region in the untreated livers at Day 9 post-PHx. When these images are merged, we see that there are cells which are highly positive for IGFBP-3 which are directly adjacent (or in close proximity) to the infiltrating

OV-6 positive oval cells in the portal triad region at Day 9 post-PHx alone. In contrast however, very little IGFBP-3 staining is present in the LPS treated livers at Day 9 post-PHx (Figure 6-6, merge).

Due to the fact that LPS acts as a toxin and triggers physiological and endocrinological responses to sepsis within the body, we wanted to determine if any functional changes within the cells of these LPS treated livers could account for the reduced oval cell response in comparison to untreated livers at Day 9 post-PHx. Cytochrome P450 (P450) enzymes are responsible for the metabolism of various drugs, xenobiotics, and endogenous substrates. CYP3A2 is one of the major P450 enzymes in liver microsomes which is found only in male rats, and is the main isoform responsible for the production of reactive oxygen species (ROS) in comparison to other P450 isoforms. Immunohistochemical analysis of CYP3A2 expression in these livers shows a dramatic increase in P450 staining in animals treated with LPS in comparison to untreated animals at Day 9 post-PHx (Figure 6-7).

Discussion

LPS is known to trigger several physiological and endocrinological responses to sepsis within the body including secretion of inflammatory cytokines, and cell apoptosis. Because of this, the direct effects of LPS on oval cell activation during liver regeneration are difficult to determine and decreased oval cell activation following LPS treatment may not necessarily be the result of changes in IGFBP-3 expression. Although LPS administration during oval cell-mediated liver regeneration was found to suppress IGFBP-3 protein levels in serum and in the liver, it is unclear if this decrease alone is a direct factor in the decreased presence of oval cells during liver regeneration, or if reduced oval cell activation is a side effect of LPS induced toxicity in the rat. This notion that administration of LPS during oval cell-mediated liver regeneration induced toxicity within the liver is supported by the finding of increased P450

expression in LPS treated livers in comparison to Day 9 post-PHx alone. Therefore, it would appear that administration of LPS triggers an increase in P450 expression in the liver, which in turn may lead to elevated levels of reactive oxygen species, activation of TNF-α signaling, or activation of other signaling pathways which could account for the decrease in the number of oval cells during liver regeneration.

In light of this, we determined that a direct cause and effect relationship between IGFBP-3 and oval cell activation during 2AAF/PHx needed to be established. We therefore decided to utilize siRNA to directly target and knockdown IGFBP-3 expression during oval cell-mediated liver regeneration.

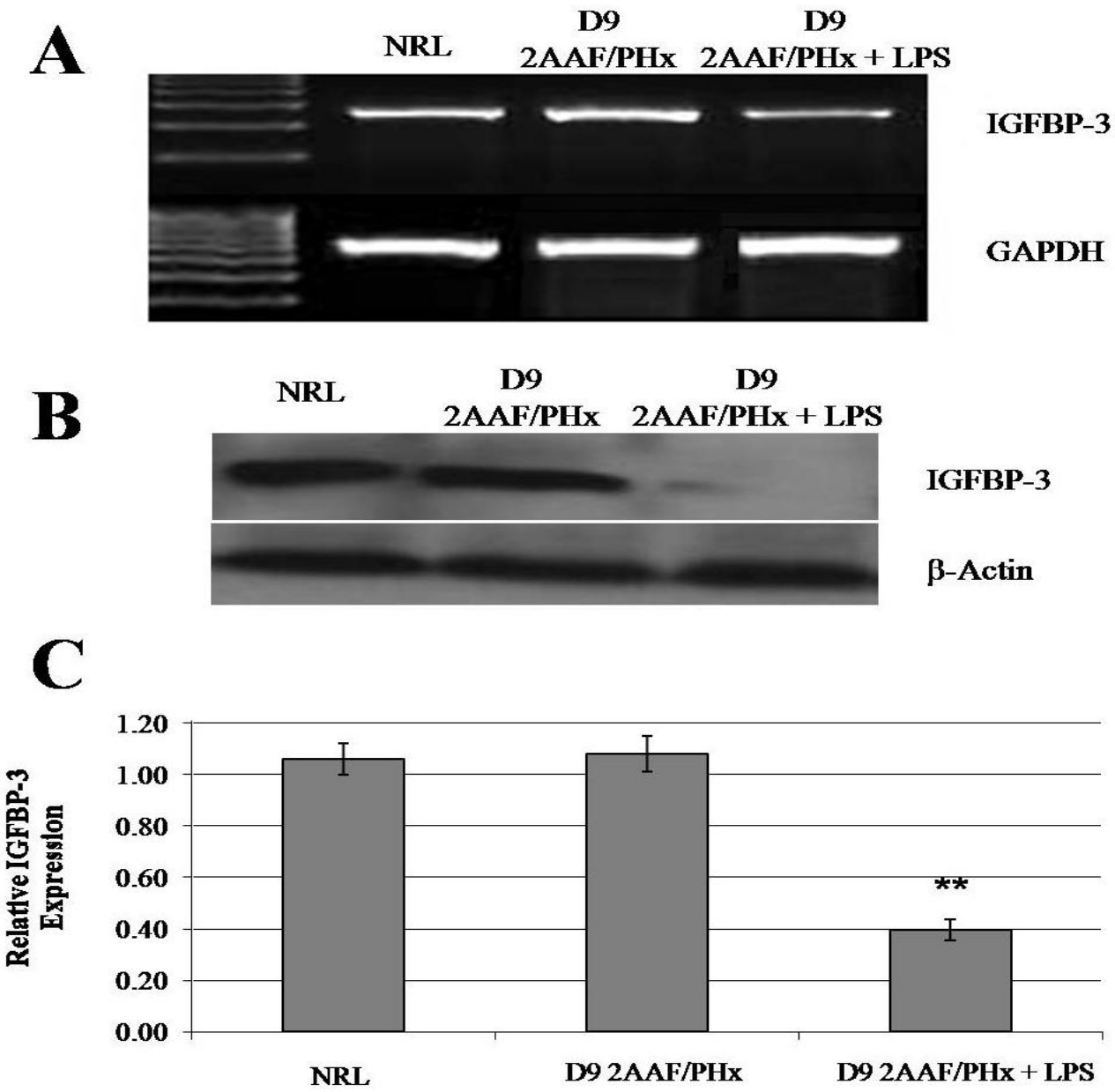

Figure 6-1. LPS inhibits IGFBP-3 protein expression in livers at Day 9 following 2AAF/PHx. A. RT-PCR analysis of RNA isolated from NRL, and livers at Day 9 post-PHx alone or in combination with LPS treatment. IGFBP-3 mRNA is detected in the liver following administration of LPS. B. Western blot analysis determined that IGFBP-3 expression is significantly down regulated in the liver at Day 9 in animals that received LPS compared to livers at Day 9 following 2AAF/PHx alone. C. Semi-quantitative analysis of IGFBP-3 protein expression. Data shown were compiled from three independent experiments. Expression was normalized to β-actin and significance calculated compared to control animals. **P <0.005

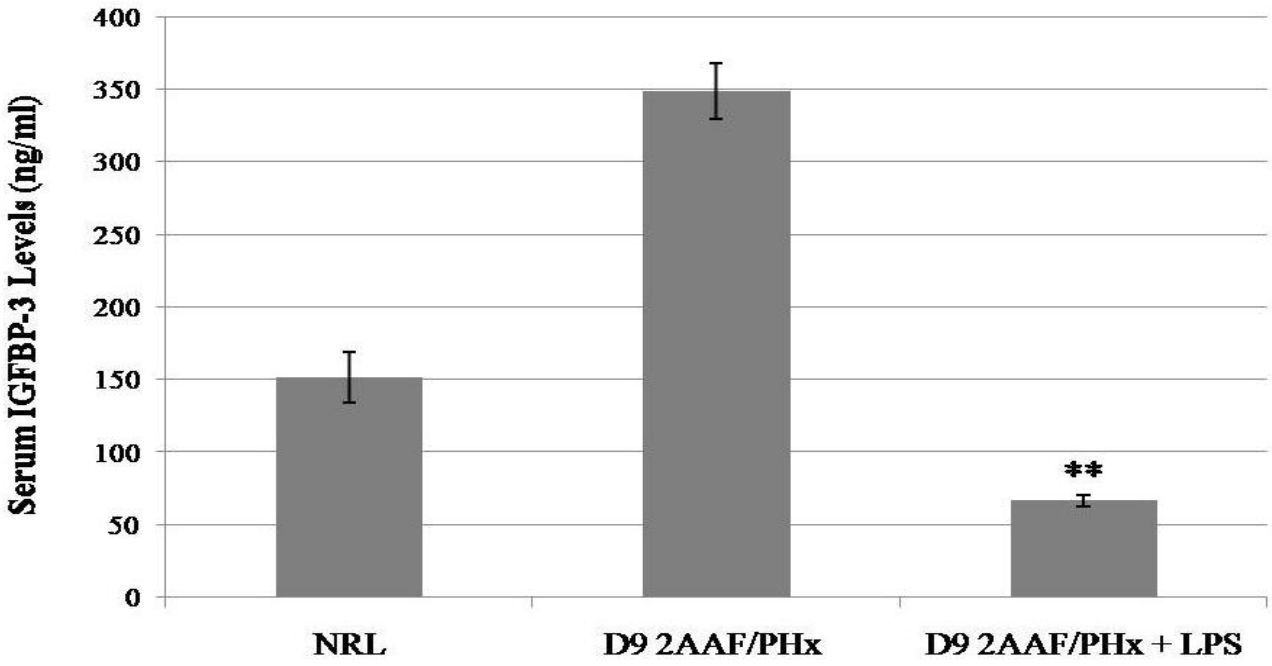

Figure 6-2. LPS administration results in a significant reduction in circulating IGFBP-3 protein in serum at peak oval cell proliferation. Enzyme-linked immunosorbent assay for IGFBP-3 protein expression was performed on rat serum harvested from normal, untreated animals and animals that received 2AAF/PHx alone or in combination with LPS. Animals treated with LPS during the 2AAF/PHx time course show dramatically reduced IGFBP-3 protein levels in serum compared to control animals and animals at Day 9 post-PHx. **P <0.005

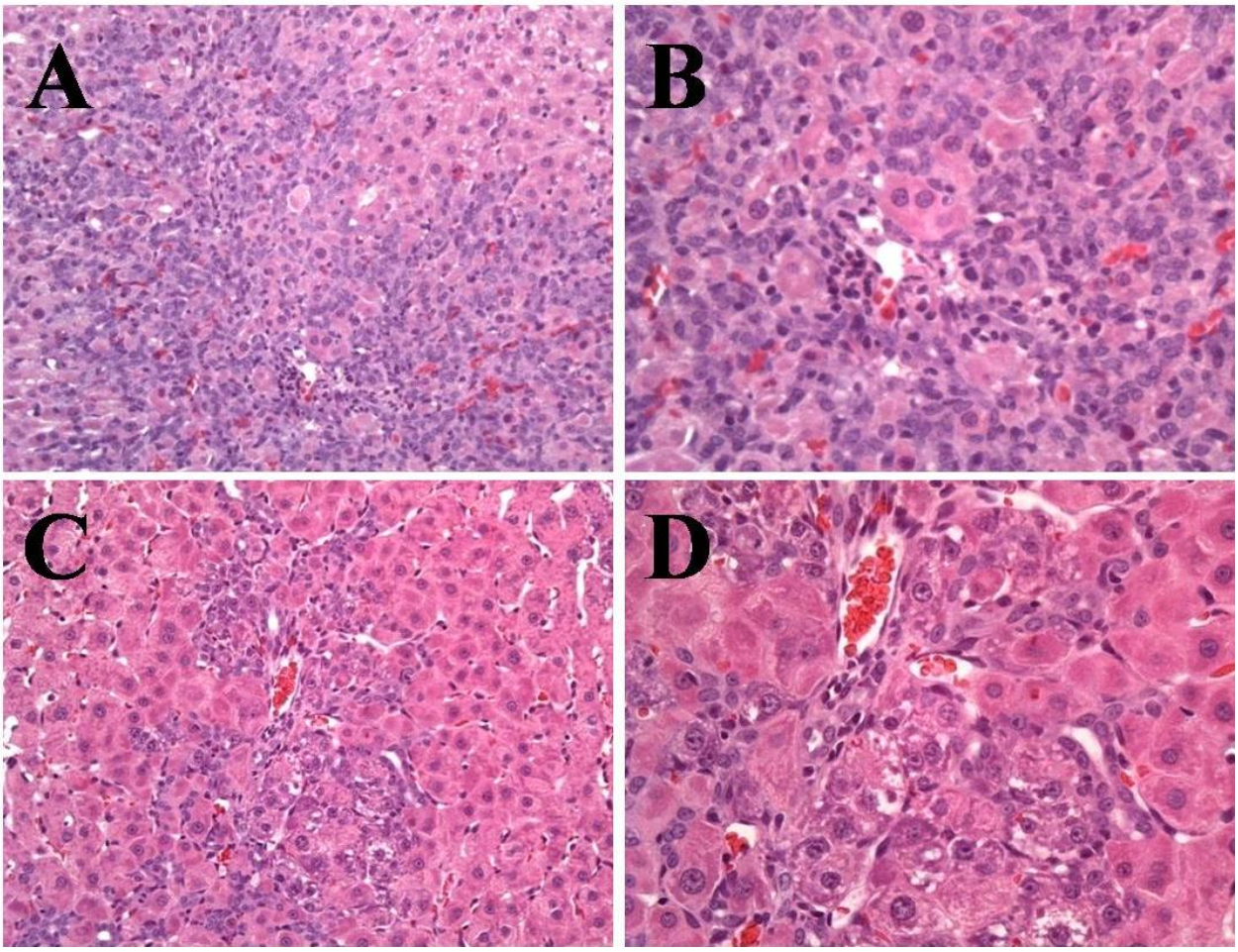

Figure 6-3. LPS administration leads to a reduction in oval cell response at Day 9 post-PHx. Hematoxylin and eosin staining of Day 9 liver tissue from animals that received 2AAF/PHx alone (A-B) and 2AAF/PHx in combination with LPS administration (C-D). Note the reduction of infiltrating oval cells around the portal triad region of the liver in LPS treated animals (C-D) compared to animals at Day 9 following 2AAF/PHx alone (A-B). A and C, 10x, B and D, 20x.

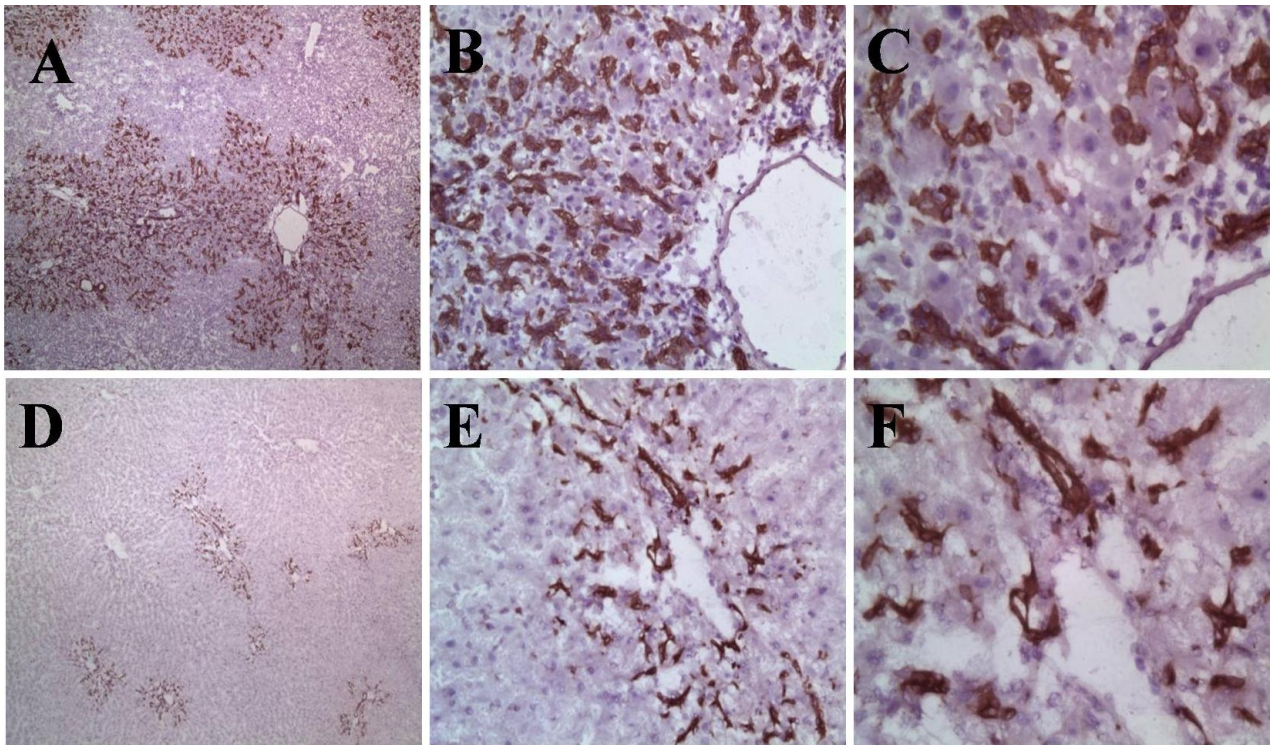

Figure 6-4. LPS administration reduces the number of OV-6 positive oval cells at Day 9 following 2AAF/PHx. A, B, C. OV-6 staining of liver sections at Day 9 following 2AAF/PHx alone. D, E, F. OV-6 staining of LPS treated livers at Day 9 post-PHx. Note the significant reduction in OV-6 positive cells around the portal triad region of the liver in the LPS treated animals compared to 2AAF/PHx alone at Day 9 post PHx. A and D, 5x; B and E, 20x; C and F, 40x.

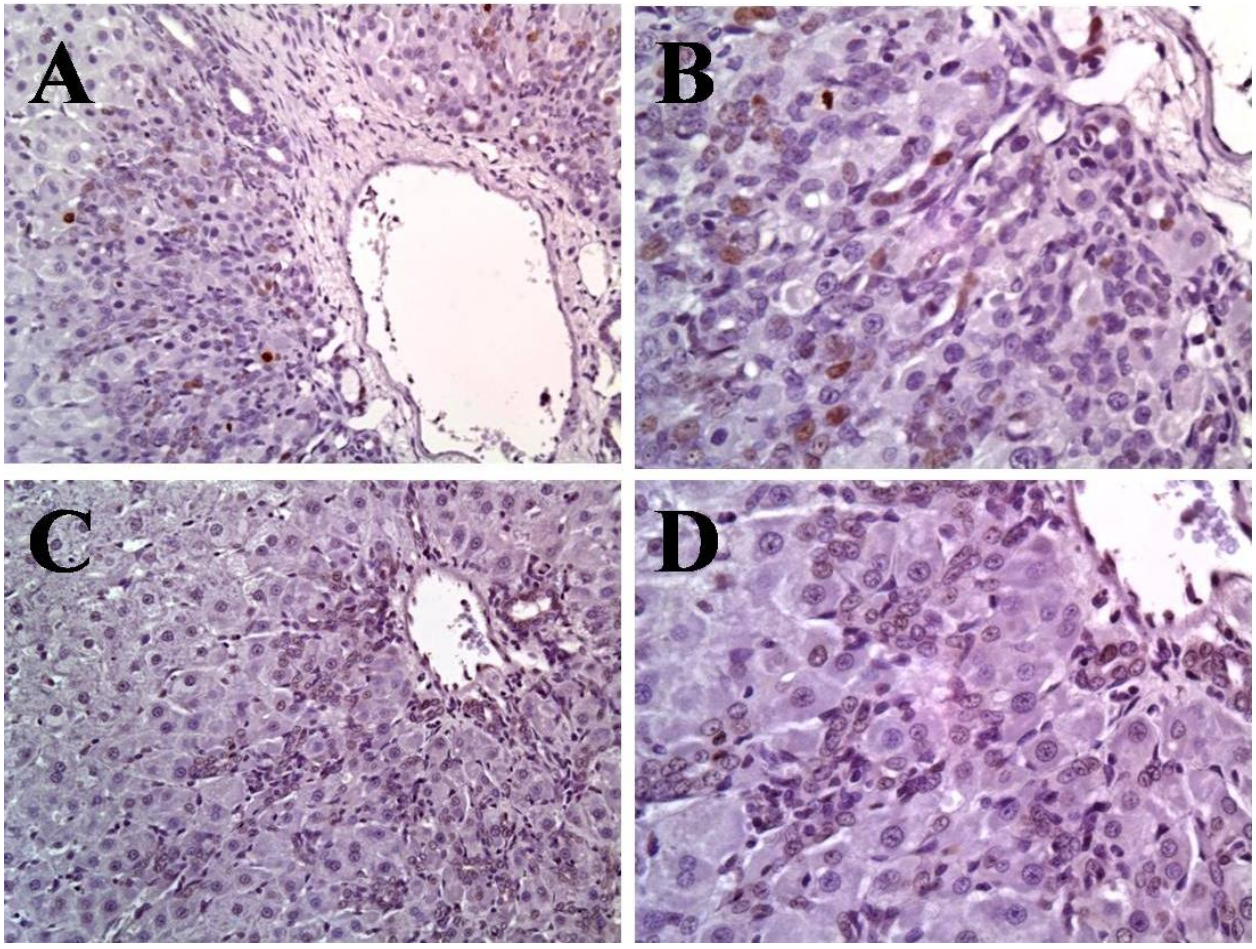

Figure 6-5. LPS administration reduces the number of proliferating cells during oval cell-mediated liver regeneration. A-B. Representative Ki67 stain of liver at Day 9 post-PHx alone. C-D. Ki67 stain of LPS treated liver at Day 9 post-PHx. Note the difference in the number of proliferating, KI67 positive cells around the portal triad region in livers treated with 2AAF/PHx alone compared to LPS treated livers taken at Day 9 post-PHx. A and C, 10x; B and D, 20x.

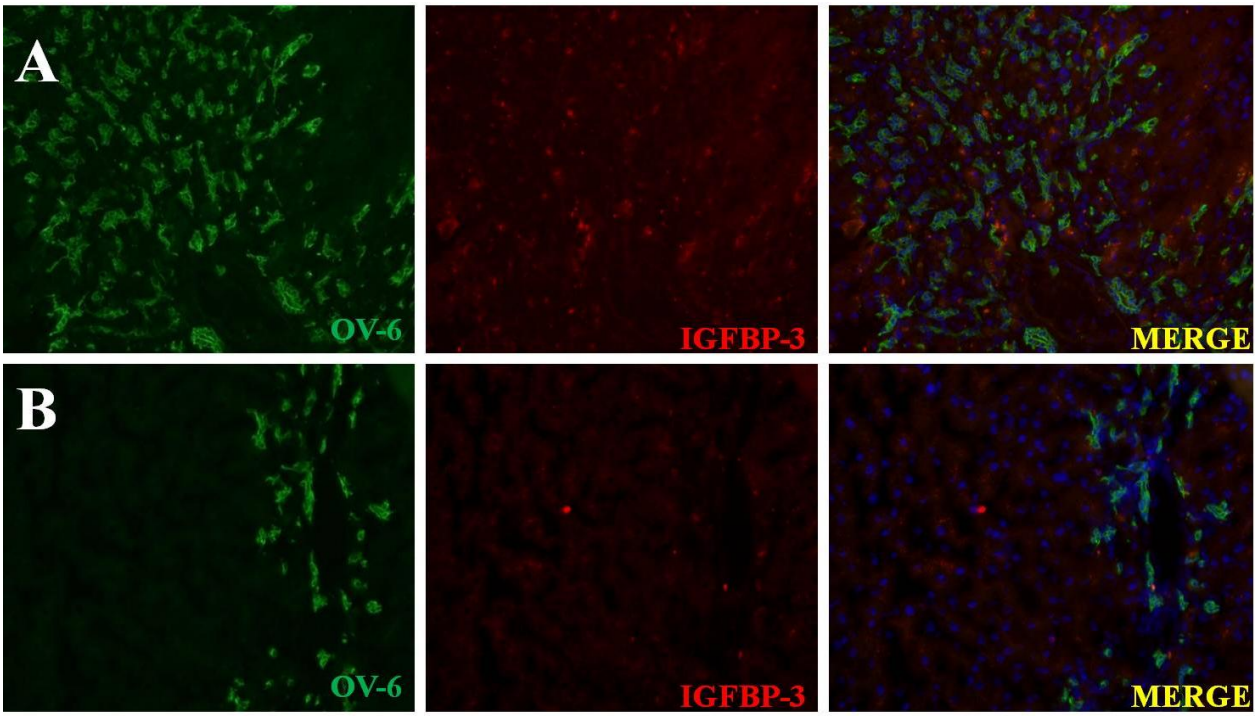

Figure 6-6. Dual immunofluorescent staining of livers at Day 9 post-PHx confirms loss of IGFBP-3 expression and reduction in OV-6 positive oval cells in LPS treated animals. A. Representative dual-IF stain of a Day 9 post-PHx liver section from an untreated animal. Note the large number of OV-6 positive oval cells infiltrating into the liver from the portal triad during peak oval cell proliferation. Also present in the sections are a number of cells that are positive for IGFBP-3 expression. Merge image again confirms that the OV-6 positive oval cells do not express IGFBP-3.
B. Representative dual-IF stain of a Day 9 post-PHx liver section from an LPS treated animal. Note the reduction in OV-6 positive cells in these LPS treated livers. Also, there is a reduction in the amount of IGFBP-3 staining around the portal triad region compared to untreated Day 9 post-PHx livers, further confirming that LPS reduces IGFBP-3 protein expression in the liver. A and B, 20x.

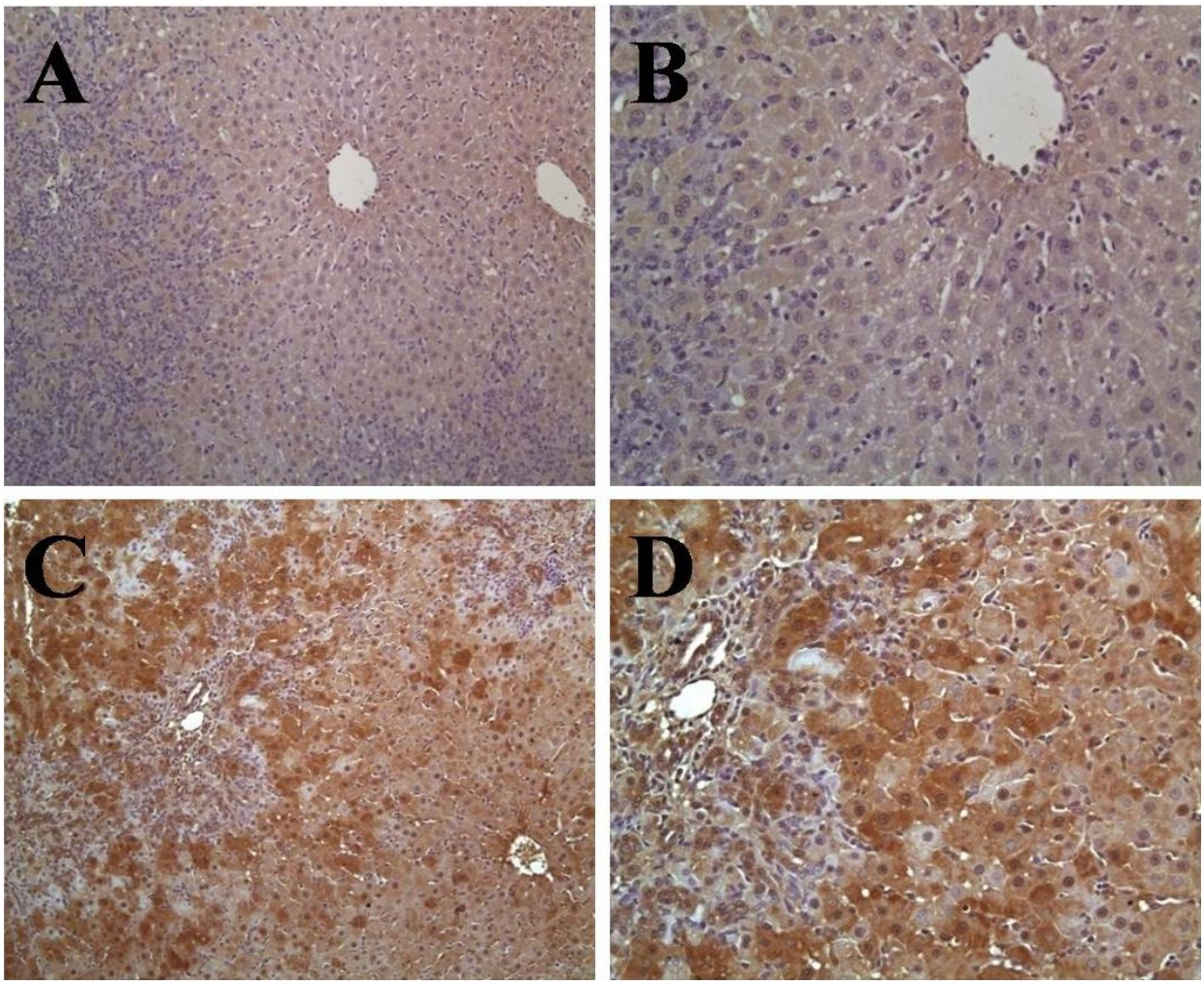

Figure 6-7. LPS treated animals display increased expression of the cytochrome P450 isoform CYP3A. A-B. Representative P450 staining of liver at Day 9 post-PHx alone. C-D. P450 staining of liver taken from LPS treated animals at Day 9 post-PHx. LPS livers display a significant increase in P450 expression compared to animals at Day 9 post-PHx alone. A and C, 10x; B and D, 20x.

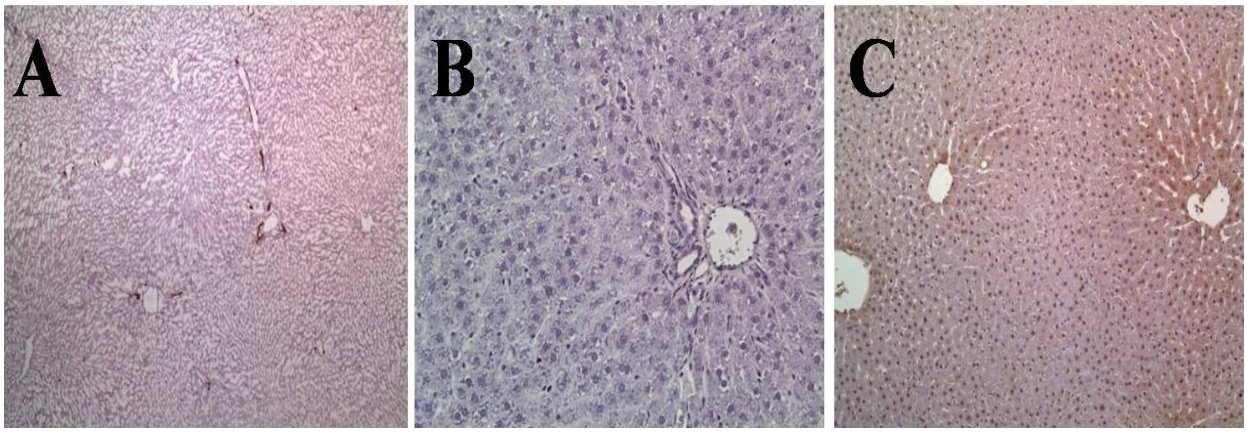

Figure 6-8. Normal rat liver control stains. A. Representative normal liver tissue stained for OV-6. As expected, the only OV-6 positive cells in normal liver are the bile duct epithelial cells. B. Representative Ki67 stain of normal rat liver stained to determine cell proliferative activity. Normal rat liver contains very few cells at any given time point that are actively undergoing replication as evidenced by few, if any Ki67 positive cells. C. P450 stain of normal rat liver showing characteristic expression of cytochrome P450. A-C, 10x.

CHAPTER 7
KNOCKDOWN OF IGFBP-3 ENHANCES OVAL CELL ACTIVATION AND ALTERS OVAL CELL DIFFERENTIATION DURING LIVER REGENERATION

Introduction

Based on the results of our *in vitro* experiments demonstrating that IGFBP-3 at low levels can act as a chemoattractant and inhibit IGF-I induced cell proliferation, we hypothesized that IGFBP-3 may play a role in regulating the activation of oval cells *in vivo*. We therefore set out to inhibit IGFBP-3 expression during the peak of oval cell proliferation by utilizing siRNA technology in our 2AAF/PHx model of oval cell induction. In order to accomplish this, a combination of three different siRNA constructs against IGFBP-3 were utilized to maximize knockdown of IGFBP-3 expression in the liver. In addition to this, we performed a recovery experiment in which animals received injections of exogenous IGFBP-3 protein in addition to siRNA treatment. As with previous experiments, RNA and protein were isolated from livers which were harvested at the peak of oval cell proliferation (Day 9 post-PHx).

Results

Confirmation of IGFBP-3 Knockdown in siRNA Treated Animals

Western blot analysis of pooled liver protein at Day 9 post-PHx confirmed a significant loss of IGFBP-3 protein in animals that received IGFBP-3 siRNA during oval cell-mediated liver regeneration (Figure 7-1, A). Semi-quantitative analysis determined that this difference in protein expression accounts for an approximate 84% decrease in IGFBP-3 protein compared to animals that received 2AAF/PHx alone and an 80% decrease compared to animals that received negative control siRNA (Figure 7-1, B). Additionally, IGFBP-3 expression levels in animals treated with additional IGFBP-3 protein was almost equal to that of levels seen in animals that had been treated with 2AAF/PHx alone or those treated with negative control siRNA at Day 9 post-PHx (Figure 7-1, B).

In addition to Western blot analysis, secreted levels of IGFBP-3 protein were also measured using ELISA techniques. Similar to previous results, secreted IGFBP-3 levels in the serum were again significantly decreased in animals treated with IGFBP-3 siRNA at Day 9 (Figure 7-2). Animals that received IGFBP-3 siRNA in addition to exogenous IGFBP-3 protein displayed significantly increased levels of IGFBP-3 levels in their serum compared to animals treated with IGFBP-3 siRNA alone. However, the levels were not as high as those detected in animals treated with negative control siRNA or at Day 9 post-PHx.

As final confirmation of suppressed protein expression as a result of siRNA treatment, liver sections were stained for the expression of IGFBP-3 protein. At Day 9 post-PHx, IGFBP-3 protein in the liver is highly expressed in cells around the central vein, spreading outward toward the portal triad region (Figure 7-3, A and B). Strong IGFBP-3 staining can also be detected in a few cells which surround the infiltrating oval cells at this time point. In contrast, IGFBP-3 staining of liver from animals treated with IGFBP-3 siRNA alone showed a dramatic reduction in IGFBP-3 protein in the cells surrounding the portal triad region and the cells surrounding the central veins (Figure 7-3, C and D). However, it is interesting to note that livers treated with exogenous IGFBP-3 protein in addition to IGFBP-3 siRNA display elevated levels of IGFBP-3 around the central vein and in a few cells around the portal triad region (Figure 7-3, E and F). This pattern of IGFBP-3 staining is phenotypically similar to IGFBP-3 staining found in Day 9 post-PHx livers (Figure 7-3, A and B) and in those animals treated with negative control siRNA (Figure 7-9, C).

Loss of IGFBP-3 Expression Results in Increased Oval Cell Proliferation and the Formation of Atypical Ductular Structures

Hemotoxylin and eosin staining of liver sections from IGFBP-3 siRNA treated animals at Day 9 post-PHx show a dramatic increase in the number of small ovoid cells present around the

periportal region of the liver compared to sections from animals that received 2AAF/PHx alone (Figure 7-4) or negative control siRNA (Figure 7-9, A). IGFBP-3 siRNA treated livers also had a much higher appearance of cells in this region that were actively undergoing proliferation at Day 9 post-PHx, as demonstrated by an increased number of Ki67 positive cells (Figure 7-4) compared to Day 9 post-PHx alone and animals treated with negative control siRNA at Day 8 post-PHx (Figure 7-4 and Figure 7-9, B). Most noteworthy about IGFBP-3 siRNA treated livers was the appearance of numerous atypical ductular structures around the portal triad regions (Figure 7-5). These structures were not seen in liver sections in animals that received negative control siRNA or in sections from animals that received 2AAF/PHx alone. Proliferative staining of these sections found that the cells within theses duct-like structures are actively undergoing proliferation, as evidence by an increase in Ki67 positive cells within this region (Figure 7-5).

To further confirm the presence of increased oval cell infiltration in IGFBP-3 siRNA treated animals, we performed dual immunofluorescent staining utilizing an IGFBP-3 specific antibody and an antibody against OV-6, a known oval cell and biliary cell marker. IGFBP-3 staining of liver sections confirmed the loss of IGFBP-3 protein expression in siRNA treated livers around the portal triad region of the liver compared to negative control siRNA (Figure 7-8) and Day 9 post-PHx alone (Figure 7-6, A). IGFBP-3 siRNA treated livers showed a marked increase in the appearance of OV-6 positive oval cells around the portal triad at Day 9 compared to 2AAF/PHx alone at Day 9 (Figure 7-6, A and B). Merged images of these stains show that the OV-6 positive oval cells are not expressing IGFBP-3 in the liver during oval cell-mediated regeneration (Figure 7-6, merge). Addition of exogenous IGFBP-3 protein to IGFBP-3 siRNA treated liver demonstrated a marked return in IGFBP-3 protein as evidence by increased

IGFBP-3 positivity in these liver sections, as well as a phenotypically normal OV-6 staining pattern as compared to Day 9 post-PHx liver (Figure 7-6, A and C).

Addition of Exogenous IGFBP-3 Protein Results in Reduced Formation of Atypical Ductular Structures During Oval Cell-Mediated Regeneration

Further histological analysis of the atypical ductular structures present in IGFBP-3 siRNA treated livers revealed that they, like oval cells, are OV-6 positive (Figure 7-7, C and D). The presence of these OV-6 positive ducts could were not detected in liver sections from Day 9 2AAF/PHx alone (Figure 7-7, A and B) or in liver sections from negative control siRNA treated animals (Figure 7-9, D). However, when IGFBP-3 protein was administered to animals in combination with IGFBP-3 siRNA, the appearance of the OV-6 positive atypical ductular structures were greatly reduced (Figure 7-7, E and F). In addition to this, animals treated with exogenous protein also displayed patterns of oval cell infiltration and OV-6 staining that was phenotypically similar in appearance to that seen in Day 9 post-PHx alone liver sections or in liver sections taken from animals at Day 9 post-PHx that received negative control siRNA (Figure 7-9)

Discussion

The results of these experiments demonstrated that administration of IGFBP-3 siRNA in the days leading up to the peak of oval cell proliferation was sufficient enough to produce a significant knockdown of IGFBP-3 protein expression compared to animals at Day 9 post-PHx alone and animals treated with negative control siRNA. Animals treated with IGFBP-3 siRNA displayed a significant decrease in IGFBP-3 protein, both in the liver and serum, as evidenced by Western blot and ELISA analysis.

In addition to this, suppression of IGFBP-3 protein during peak oval cell activation leads to an over-proliferation of oval cells as evidenced by increased Ki67 staining around the portal triad

region in comparison to control animals. In addition to increased oval cell proliferation in these siRNA treated livers, we also noted the unique appearance of numerous atypical ductular structures which were not present in the negative control siRNA treated animals or in animals that received 2AAF/PHx alone. Due to the fact that administration of 2AAF inhibits proliferation of the resident hepatocytes in the regenerating liver, it is believed that these atypical ductular structures were derived from the oval cell population. The hypothesis that these atypical ductular structures are derived from the oval cell population is further supported by the findings that these structures, like the oval cells, are OV-6 positive. This further suggests that IGFBP-3 may play a regulatory role in the ability of these cells to undergo controlled proliferation and may affect their ability to differentiate toward the hepatocyte lineage *in vivo.*

Although reduced expression of IGFBP-3 protein during oval cell-mediated liver regeneration leads to an increased presence of oval cells at Day 9 post-PHx, these cells do not appear to be functioning properly to aid regeneration of the organ. This is evidenced both by their tendency to favor differentiation toward bile ductular structures rather than basophilic hepatocytes and by evidence of reduced liver weights compared to overall body weight at Day 9 post-PHx in the absence of IGFBP-3 (Figure 7-10). Under normal conditions of oval cell-mediated liver regeneration, the average liver weight at Day 9 post-PHx was 6.4 grams, or approximately 3.3% of the animal's total body mass. However, animals treated with siRNA had significantly lower liver weights at Day 9 post-PHx, weighing in at an average of 4.4 grams, or approximately 2.3% of total body mass. The overall reduction in liver weight in siRNA treated animals compared to Day 9post-PHx alone suggests that oval cell function and contribution to liver regeneration was impaired, most likely due to their inability to differentiate toward the hepatocyte lineage as a result of reduced IGFBP-3 expression in the liver. Overall, addition of

exogenous IGFBP-3 protein to siRNA treated animals appeared to have a varied effect on the liver weights of these animals in comparison to total body mass, indicating that oval cell function may still be slightly improved in some of these livers.

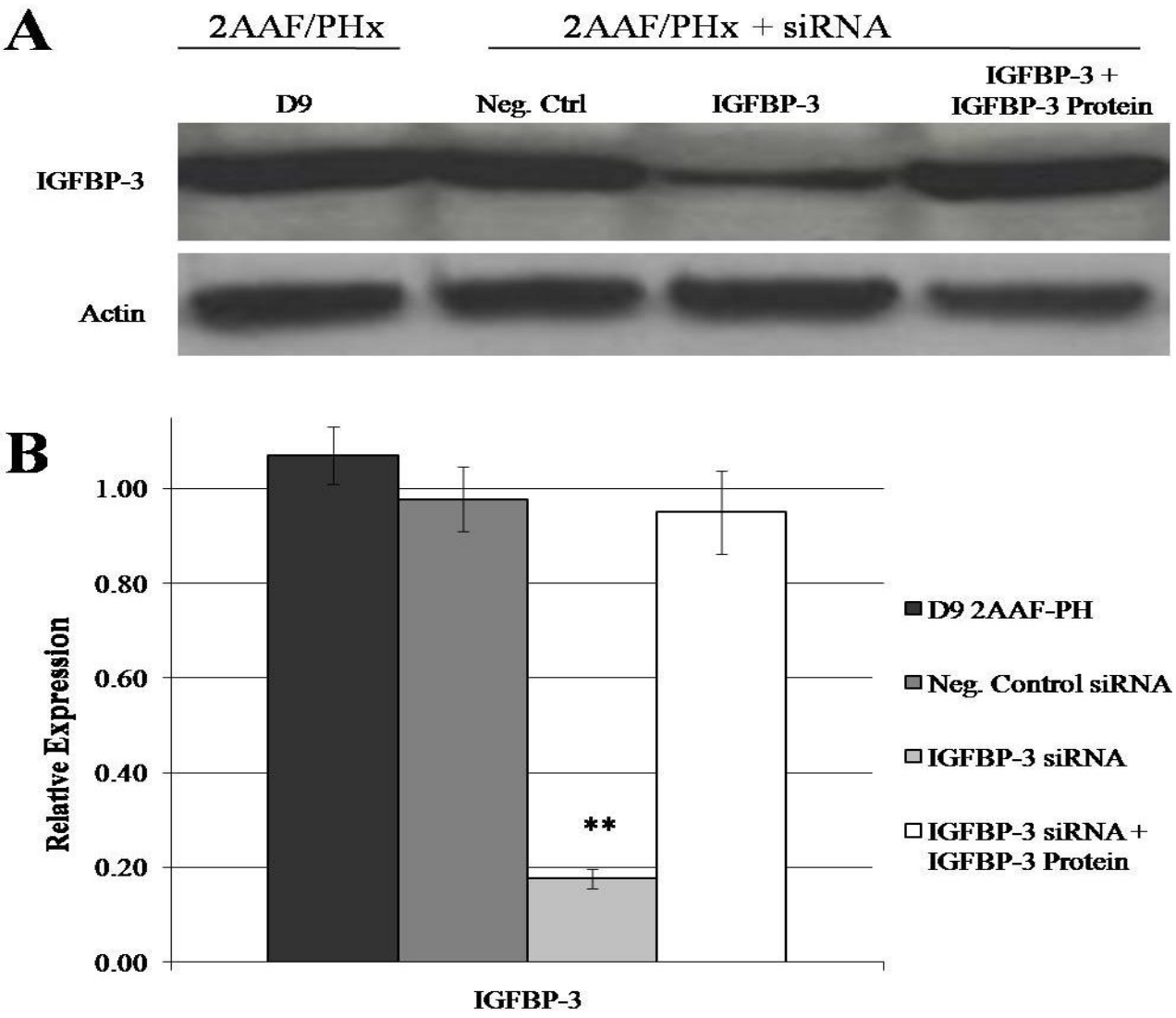

Figure 7-1. Western blot analysis of siRNA treated animals confirms knockdown of IGFBP-3 protein expression in the liver. A. Western blot analysis performed on protein isolated from livers taken at Day 9 post-PHx and probed for IGFBP-3 protein. Note the significant reduction in IGFBP-3 protein levels siRNA treated animals compared to negative control siRNA and 2AAF/PHx treated animals alone at Day 9. Addition of exogenous IGFBP-3 protein resulted in a significant return of protein expression compared to negative control siRNA and untreated livers at Day 9 post-PHx. B. Semi-quantitative analysis of IGFBP-3 protein expression. Data shown were compiled from three independent experiments. Expression was normalized to β-actin and significance calculated by comparison to control animals. **P<0.005.

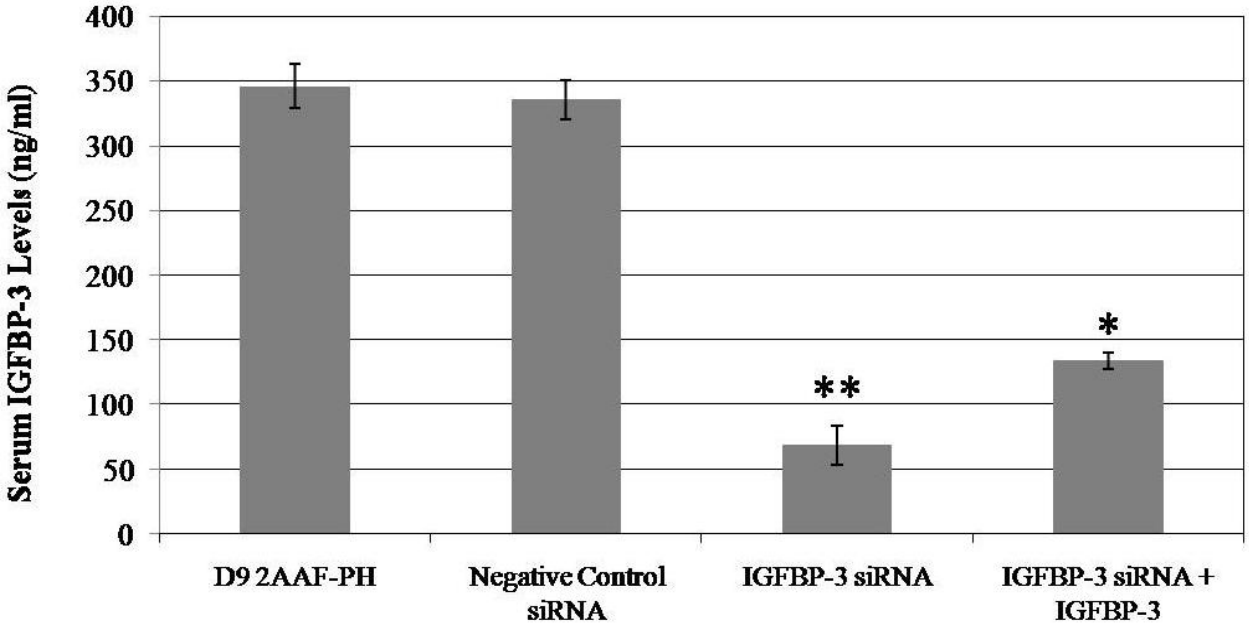

Figure 7-2. IGFBP-3 siRNA treated animals display decreased circulating IGFBP-3 levels in serum. ELISA results from pooled rat serum taken at Day 9 post-PHx. Note the significant reduction in IGFBP-3 secreted protein in animals treated with IGFBP-3 siRNA in comparison to Day 9 post-PHx alone and negative control siRNA. Addition of exogenous IGFBP-3 protein resulted in a slight increase in serum concentrations of IGFBP-3 compared to controls. Data shown were compiled from three independent experiments. * $P < 0.05$, ** $P < 0.005$.

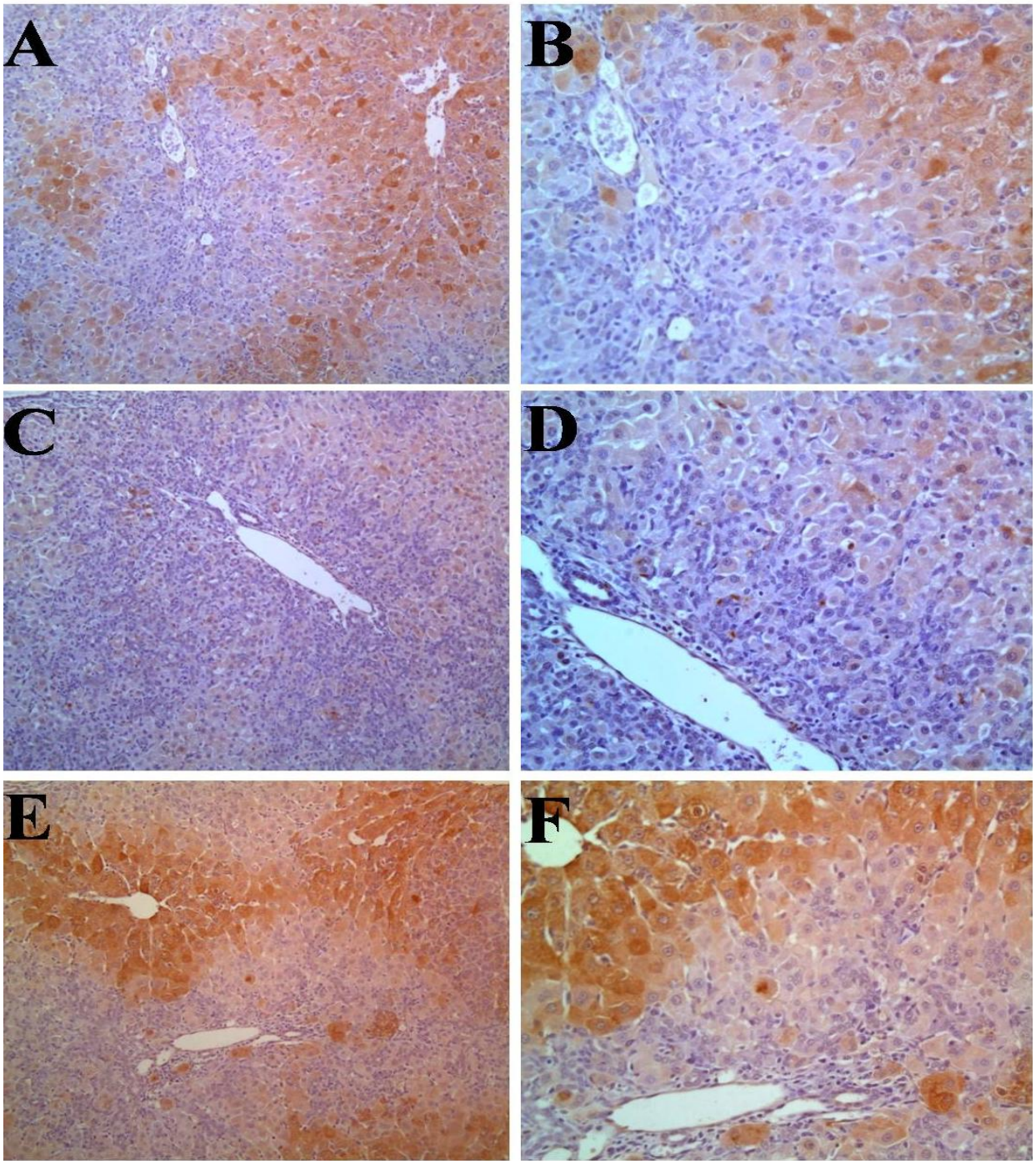

Figure 7-3. IHC analysis of IGFBP-3 siRNA treated animals confirms loss of IGFBP-3 protein in liver. A and B. Day 9 post-PHx alone. C and D. IGFBP-3 siRNA treated liver at Day 9. E and F. IGFBP-3 siRNA plus IGFBP-3 protein treated liver at Day 9 post-PHx.. In IGFBP-3 siRNA treated liver, there is a significant loss of IGFBP-3 expression in the cells surrounding the portal triad region compared to Day 9 post-PHx alone. Note that addition of exogenous IGFBP-3 protein appears to correct for the loss of protein due to siRNA treatment. A, C, E, 10x. B, D, F, 20x.

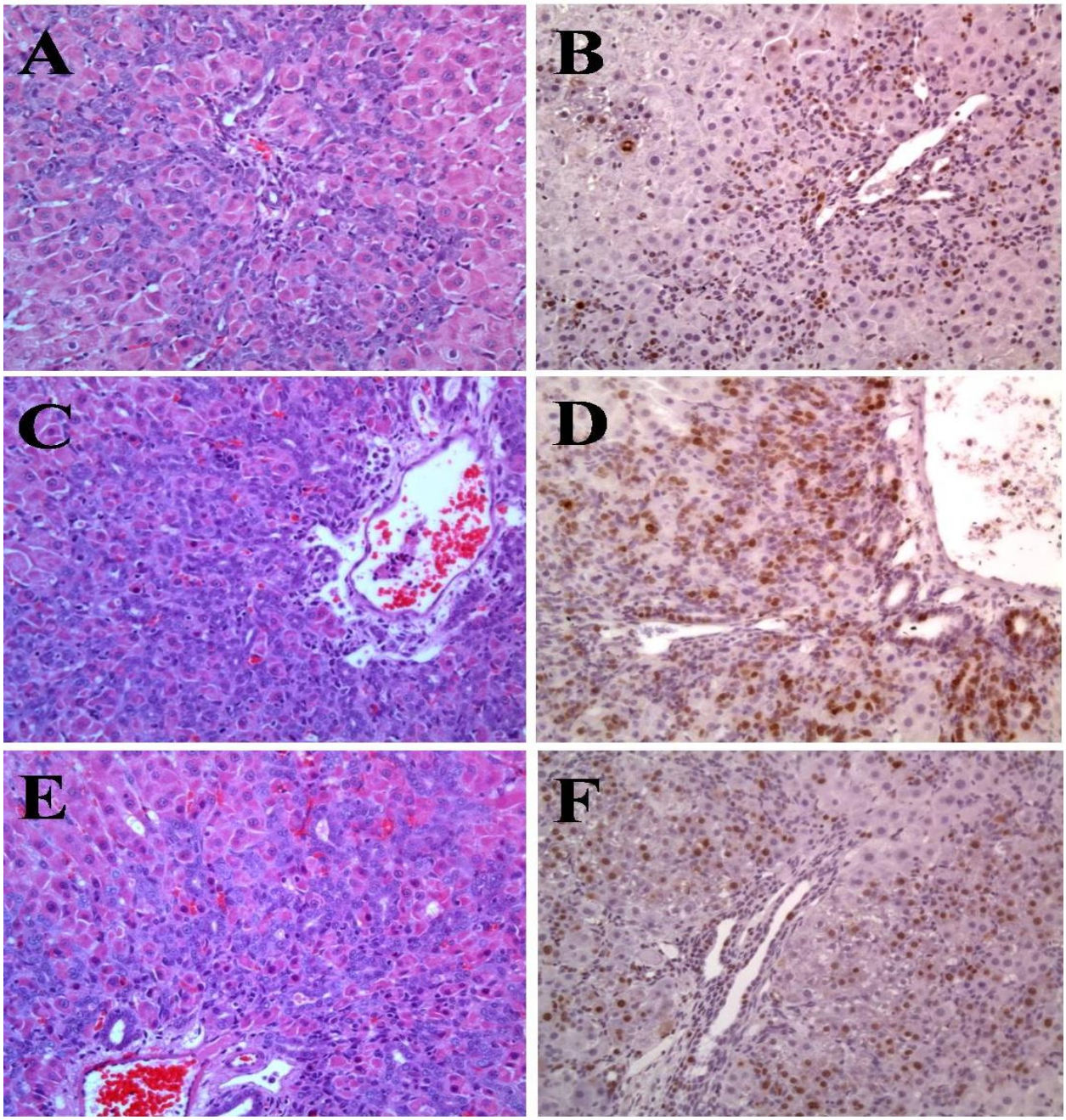

Figure 7-4. Loss of IGFBP-3 expression results in increased oval cell activation. A. H&E stain of liver at Day 9 post-PHx. B. Ki67 stain of liver at Day 9 post-PHx. C. H&E stain of IGFBP-3 siRNA treated liver at Day 9. D. Ki67 stain of IGFBP-3 siRNA treated liver at Day 9. Note the increased appearance of small ovoid cells around the portal triad region of the liver. The number of cells that are actively undergoing proliferation are increased compared to Day 9 post-PHx alone. E. H&E stain of liver treated with IGFBP-3 siRNA and IGFBP-3 protein at Day 9 post-PHx. F. Ki67 stain of liver treated with IGFBP-3 siRNA and IGFBP-3 protein. Note how the sections of liver treated with IGFBP-3 siRNA in combination with IGFBP-3 protein display a phenotypically normal oval cell response for this time point with equal distribution of Ki67 positive cells around the portal triad region of the liver compared to Day 9 post-PHx. A-F, 20x.

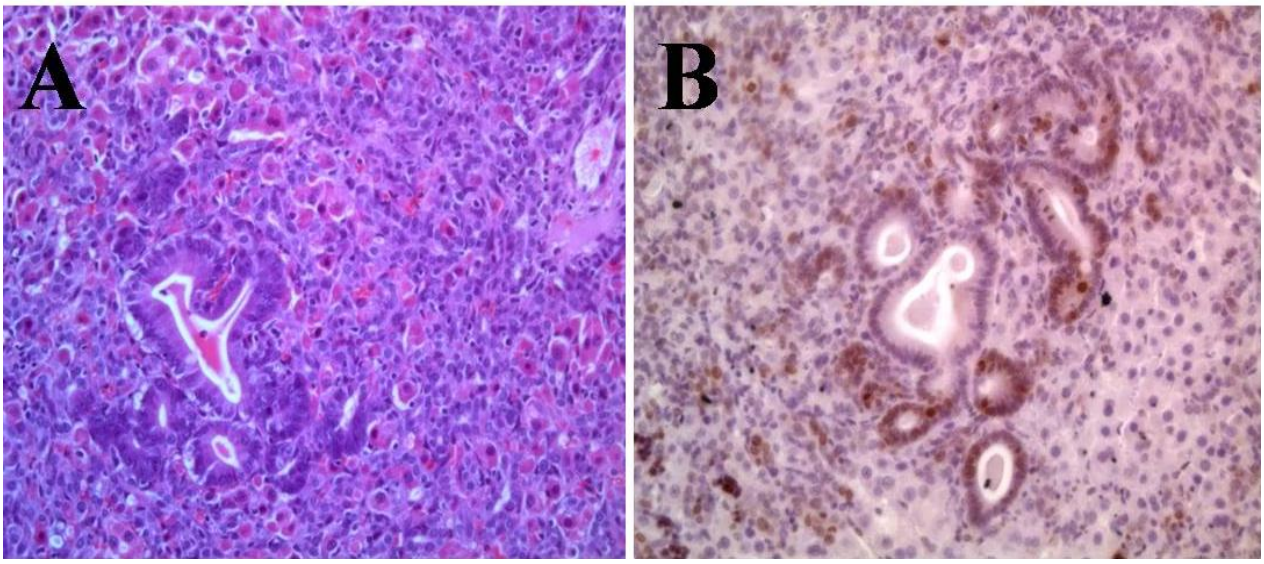

Figure 7-5. Loss of IGFBP-3 during peak days of oval cell proliferation leads to the formation of atypical ductular structures in liver. A. Representative H&E stain of an atypical ductular structure found in IGFBP-3 siRNA treated animals at Day 9 post-PHx. B. Ki67 stain of atypical ductular structure found in liver treated with IGFBP-3 siRNA at Day 9 post-PHx. In animals treated with IGFBP-3 siRNA, we noted the appearance of numerous atypical ductular structures that were not present in Day 9 post-PHx alone or in negative control siRNA treated animals. Note that the cells in these structures are actively undergoing proliferation as evidences by Ki67 positive staining. A and B, 20x.

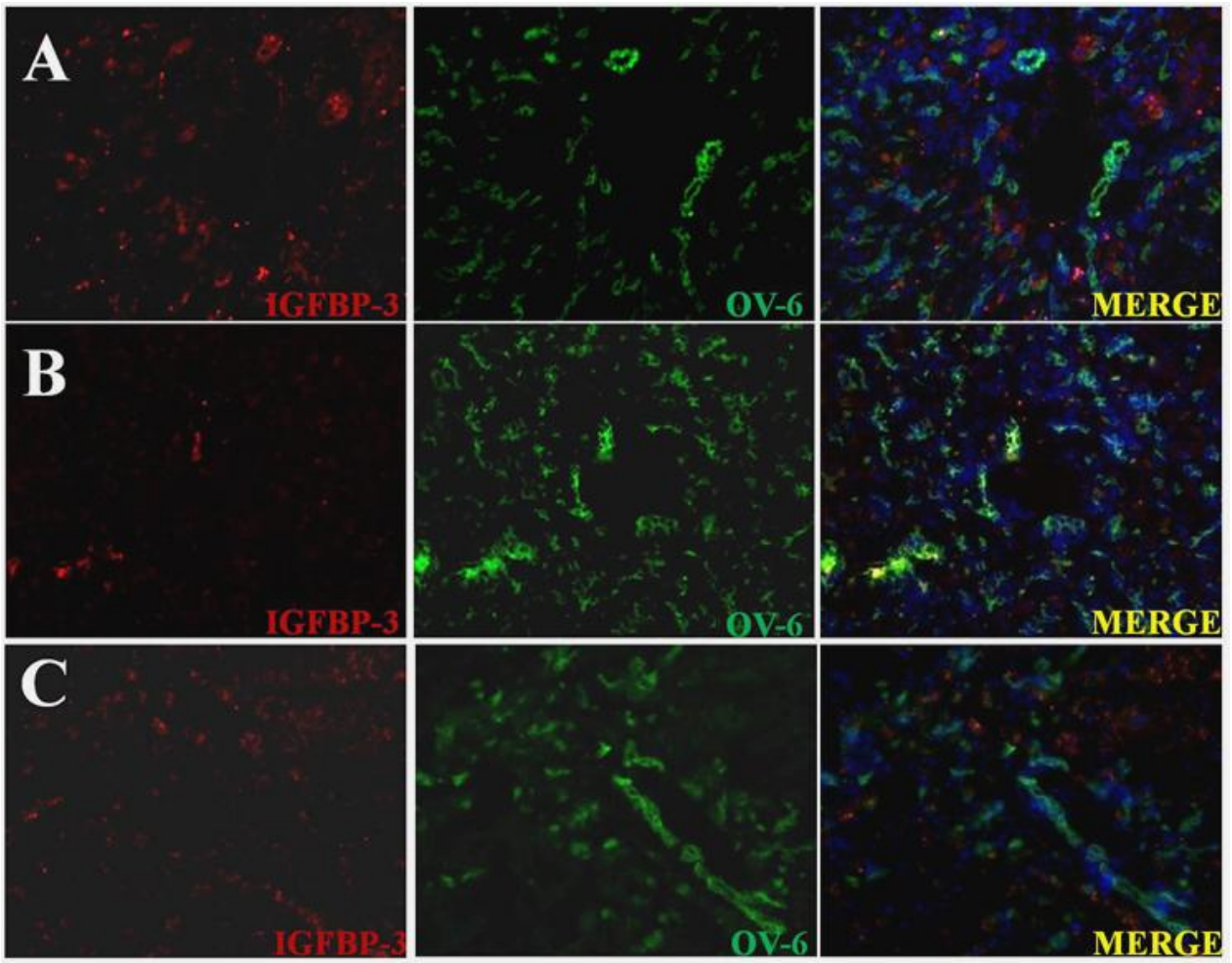

Figure 7-6. Dual IF stain confirms loss of IGFBP-3 expression in siRNA treated animals and increased OV-6 expression at Day 9 post-PHx. A. Dual IF staining of liver at Day 9 post-PHx alone. B. Dual IF staining of liver taken from IGFBP-3 siRNA treated liver at Day 9 post-PHx. C. Dual IF staining of liver taken from animals treated with IGFBP-3 siRNA and IGFBP-3 protein at Day 9 post-PHx. Here, IGFBP-3 is expressed by cells around the portal triad region of the liver at Day 9 post-PHx alone (A, left). Activation of oval cells at Day 9 is confirmed by the presence of OV-6 staining (A, middle). Dual staining demonstrates that the OV-6 positive oval cells do not express IGFBP-3 (A, merge). IGFBP-3 staining confirms loss of protein expression due to IGFBP-3 siRNA treatment (B, left) compared to 2AAF/PHx alone. OV-6 staining shows an increase in the number of positive oval cells around the portal triad region in livers treated with IGFBP-3 siRNA (B, middle). Note that addition of exogenous IGFBP-3 protein results in a return of IGFBP-3 positive expression in the cells around the portal triad region. Also, the OV-6 positive oval cells are arranged in formation similar to that of the OV-6 positive cells present in Day 9 post-PHx alone liver tissue. A-C, 20x

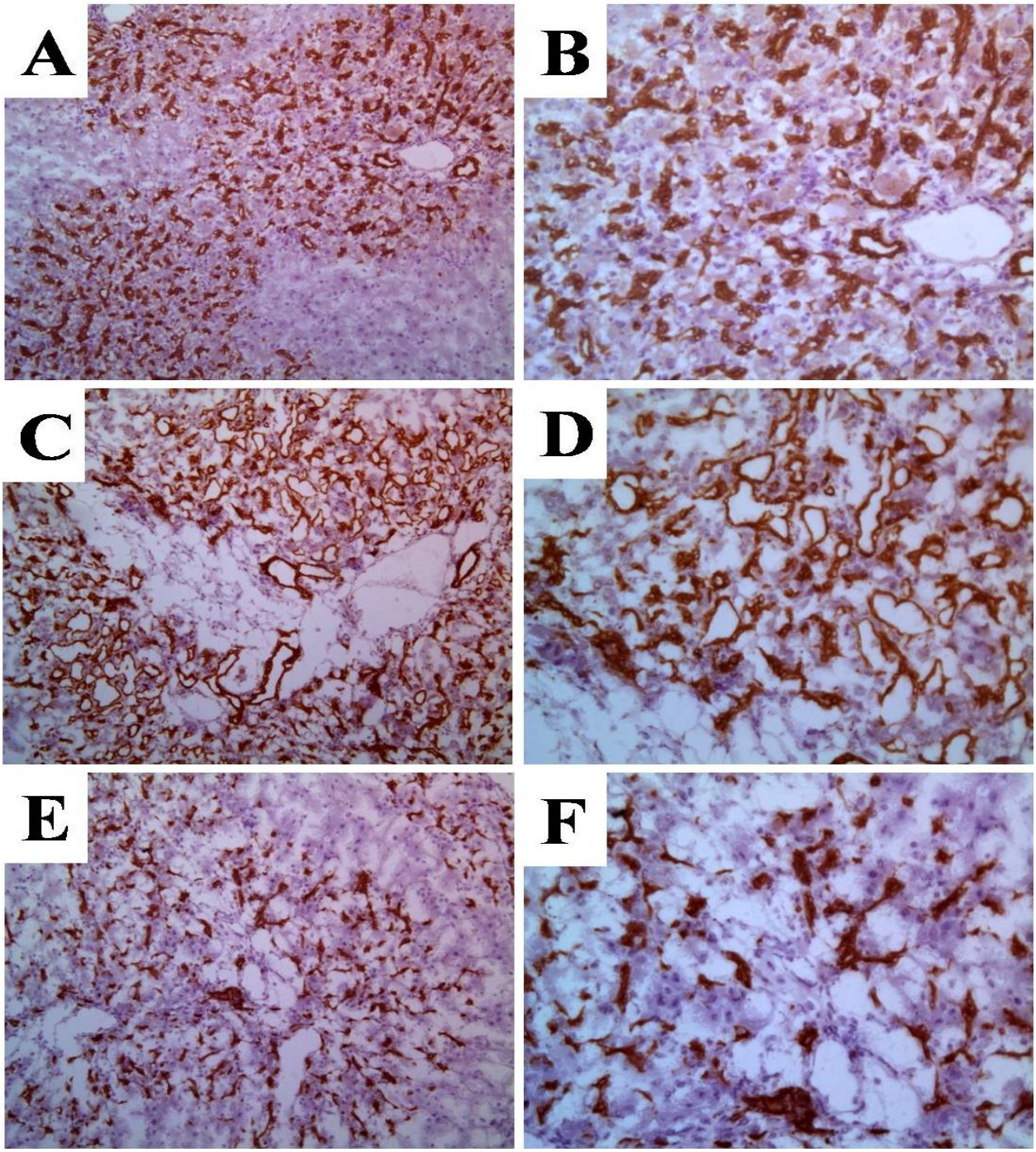

Figure 7-7. Addition of exogenous IGFBP-3 results in reduced formation of atypical ductular structures during peak days of oval cell proliferation. A and B. OV-6 staining of liver at Day 9 post-PHx. C and D. OV-6 stain of IGFBP-3 siRNA treated animals. E and F. OV-6 staining of liver taken from animals that received IGFBP-3 protein in addition to IGFBP-3 siRNA. OV-6 staining of frozen liver sections taken from siRNA animals shows a phenotypical change in arrangement of oval cells at Day 9. The oval cells are arranged in numerous ductular formations. Note the reduction in the number of atypical ductular structures found in these sections. A, C,-E, 10x. B, D, F, 20x.

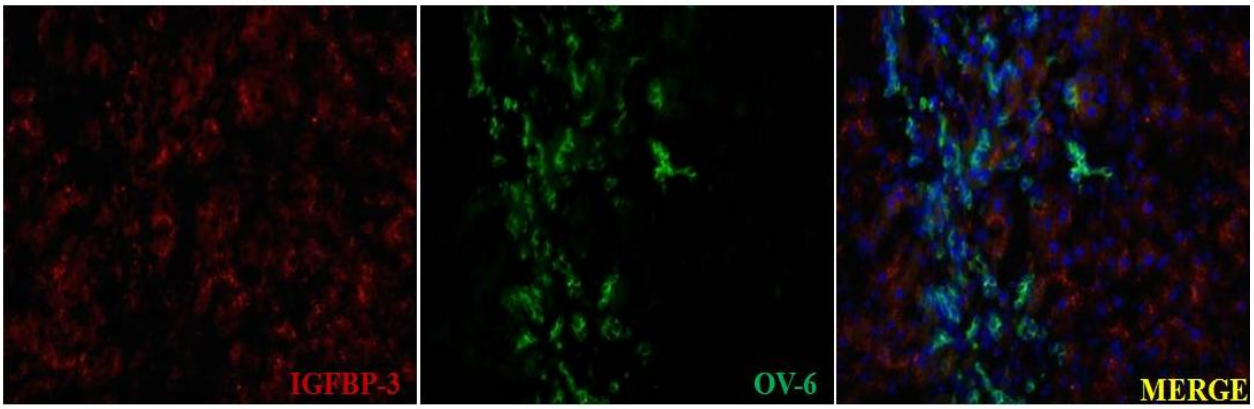

Figure 7-8. Dual IF stain of negative control siRNA treated liver. As with untreated liver at Day 9 post-PHx, negative control siRNA treated liver at Day 9 post-PHx displays elevated IGFBP-3 protein expression around the portal triad region in addition to characteristic OV-6 staining for this time point. All images taken at 20x magnification.

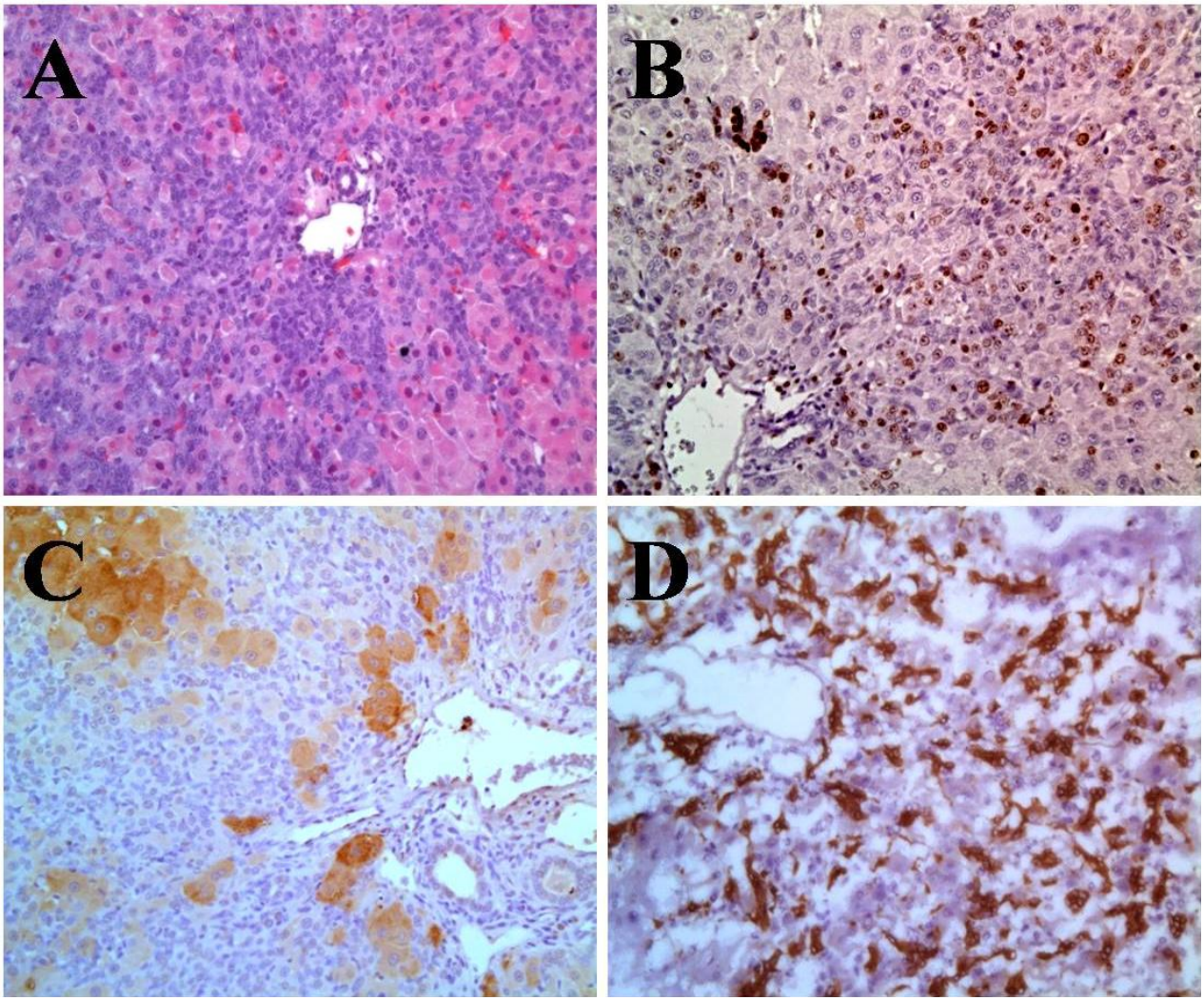

Figure 7-9. Control stains for negative control siRNA treated animals at Day 9 post-PHx..
A. Representative H&E stain. B. Representative Ki67 stain. C. IGFBP-3 stain.
D. OV-6 stain of a negative control siRNA treated liver. Note the phenotypically normal oval cell response at Day 9 post-PHx and positive IGFBP-3 expression around the portal triad region. A-D, 20x.

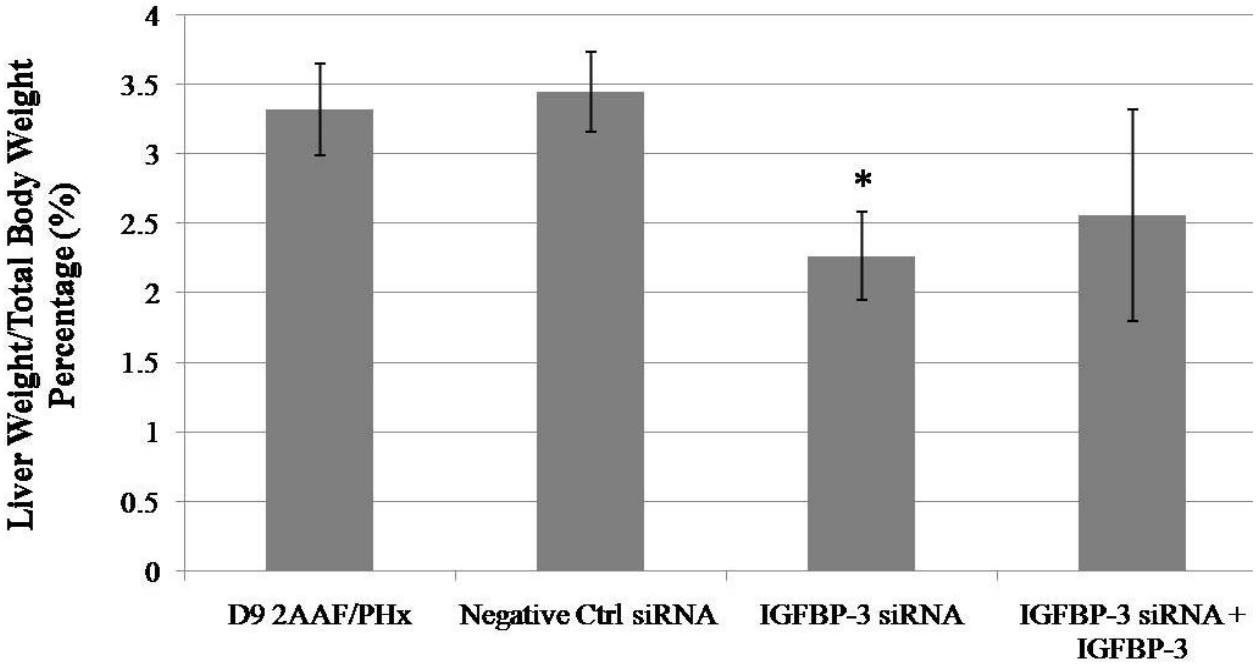

Figure 7-10. Knockdown of IGFBP-3 protein during oval cell-mediated liver regeneration resulted in reduced liver weights in comparison to overall body weight at Day 9 post-PHx. Animals treated with IGFBP-3 siRNA had significantly lower liver weights at Day 9 post-PHx compared to animals at Day 9 post-PHx alone or animals treated with negative control siRNA at Day 9 post-PHx. Addition of exogenous IGFBP-3 protein resulted in varied liver weights at Day 9 post-PHx. Data shown are the averages of three animals per condition. * $P < 0.05$.

CHAPTER 8
KNOCKDOWN OF IGFBP-3 CORRELATES WITH DECREASED EXPRESSION OF TGF-β PATHWAY MEMBERS

Introduction

Activation of the TGF-β pathway has been associated with IGFBP-3 production in a variety of different cell types, including several different types of cancers (111, 140). IGFBP-3 has also been shown to directly regulate cell proliferation through specific interactions with TGF-β receptors, such as TGF-βRV and TGF-βRII, and TGF-β dependent signaling mechanisms, such as Smads 2,3 and 4 (141). Several groups have also demonstrated a connection between the TGF-β pathway and oval cell mediated liver regeneration in which mRNA and protein levels of TGF-β1 were found to be upregulated during peak days of oval cell proliferation (103, 107, 121). We therefore asked whether these IGFBP-3 mediated effects in the liver during oval cell regeneration are dependent on the activation of the TGF-β pathway and if suppression of IGFBP-3 via siRNA is associated with changes in the expression of genes associated with the TGF-β family.

Results

Quantitative real-time-PCR analysis confirmed that IGFBP-3 siRNA treated animals had reduced IGFBP-3 expression, with a more than 9-fold reduction in IGFBP-3 mRNA compared to controls (Figure 8A). Animals treated with additional IGFBP-3 protein showed a 3-fold decrease in IGFBP-3 mRNA. A significant reduction in IGF-I mRNA expression was also detected in animals treated with IGFBP-3 siRNA alone or with additional IGFBP-3 protein (>8-fold and >7-fold down-regulation, respectively). Interestingly, mRNA levels of the proto-oncogene Myc were significantly increased following siRNA treatment (Figure 8-1). This suggests that IGFBP-3 may play a role in regulating cell proliferation in the liver during oval cell activation.

Although no differences in TGF-β1 mRNA expression was detected, we noted a significant fold reduction (>7-fold decrease) in mRNA expression of TGF-βRII in IGFBP-3 siRNA treated animals (Figure 8-2). Addition of exogenous IGFBP-3 protein appeared to correct somewhat for this loss however, TGF-βRII mRNA was still significantly reduced in comparison to the controls at Day 9. In addition, mRNA expression of Smad 2, 3, and 4 were also significantly down regulated in IGFBP-3 siRNA treated animals.

Discussion

In conclusion, qRT-PCR analysis confirms a greater than 9-fold loss of IGFBP-3 mRNA expression in siRNA treated animals at Day 9 post-PHx in comparison to animals at Day 9 post-PHx alone and negative control siRNA treated animals. In these experiments, we also noted a dramatic decrease in IGF-I mRNA when IGFBP-3 expression was suppressed with siRNA. These results further suggest that the effects mediated by IGFBP-3 during the peak of oval cell proliferation may be IGF-I dependent. Another interesting observation in these experiments was a greater than 8-fold increase in mRNA expression of the proto-oncogene, Myc. Upregulation of this proto-oncogene in combination with the increased presence of atypical ductular structures in these livers following siRNA treatment suggests that loss of IGFBP-3 expression may be the beginning stages of cancer progression and preneoplastic changes that are occurring in the liver during the peak of oval cell proliferation.

Although, no changes in TGF-β1 mRNA expression were detected following siRNA treatment, we did note the significant decrease in mRNA expression of TGF-β receptors I and II, as well as downstream transcription factors of the TGF-β pathway including Smads 2, 3 and 4. These results indicate that IGFBP-3 mediated effects in the liver, in addition to possibly being

IGF-dependent, may involve the activation of the TGF-β pathway via the TGF-β receptors I and II, and activation of Smads 2-4.

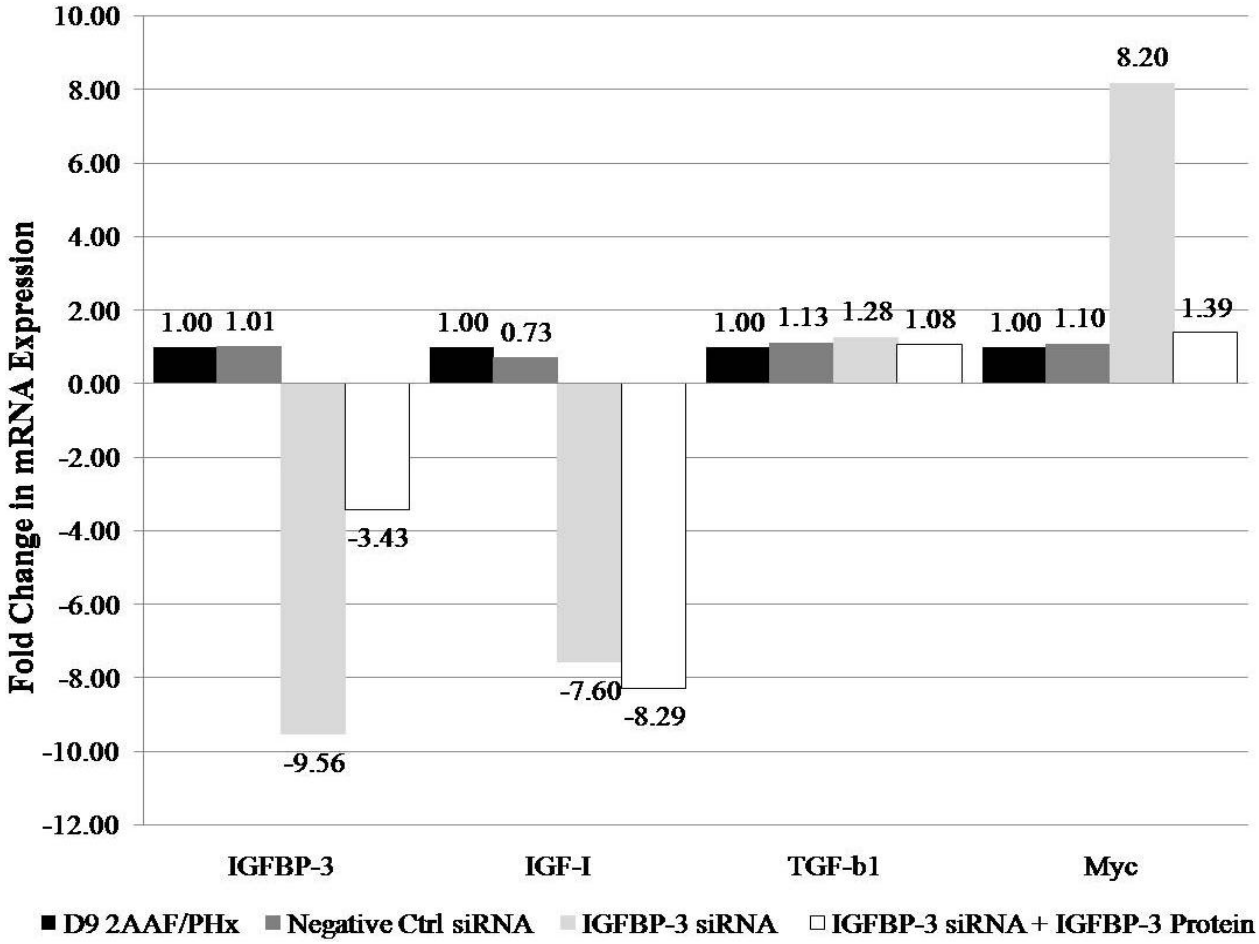

Figure 8-1. Quantitative real-time PCR analysis confirms a significant knockdown of IGFBP-3 mRNA in siRNA treated animals. Analysis of the TGF-β BMP signaling pathway determined that IGFBP-3 and IGF-I mRNA were significantly reduced in comparison to Day 9 post-PHx alone and animals treated with negative control siRNA. In addition to this, the proto-oncogene Myc, was significantly upregulated in IGFBP-3 siRNA treated animals. A fold increase or decrease greater than 2-fold was considered statistically significant. Data shown are based on the results of three independent experiments.

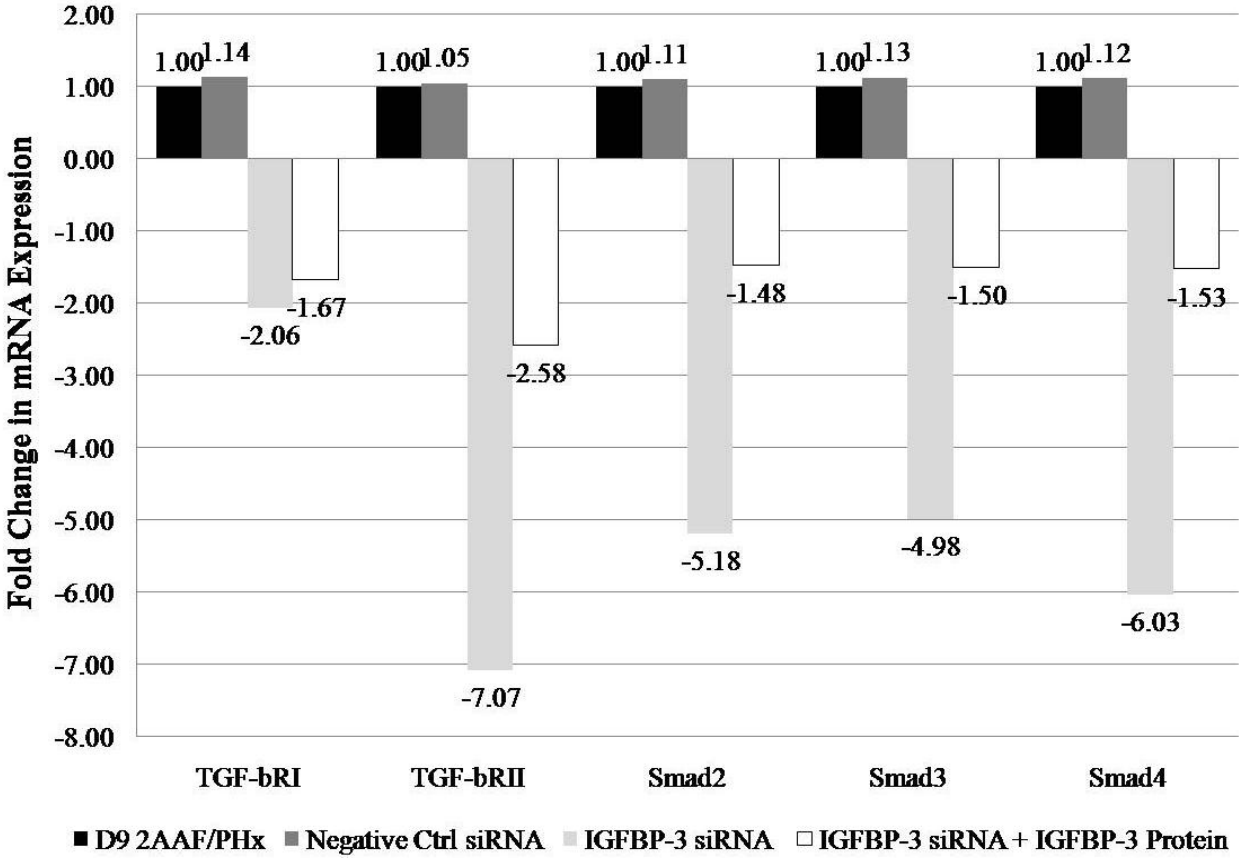

Figure 8-2. IGFBP-3 siRNA results in reduced mRNA expression of several key TGF-β pathway members. Quantitative real-time PCR analysis of RNA from pooled liver samples displays a significant knockdown of TGF-βRI and TGF-βRII mRNA, as well as mRNA from downstream transcription factors Smads 2, 3, and 4 in IGFBP-3 siRNA treated animals at Day 9 post-PHx. Addition of exogenous IGFBP-3 protein resulted in a return in mRNA expression to some of these factors. A fold increase or decrease greater than 2-fold was considered statistically significant. Data shown are based on the results of three independent experiments.

CHAPTER 8
SUMMARY OF RESULTS AND FUTURE DIRECTIONS

Summary

This is the first study to examine the role of IGFBP-3 on oval cell activation both *in vitro* and *in vivo* and is the first report to demonstrate the presence of IGFBP-3 in the liver during this phenomenon. In this study, we demonstrated that IGFBP-3 mRNA and protein are expressed in the rat liver during oval cell-mediated regeneration, and that IGFBP-3 protein is elevated during known days of peak oval cell proliferation in the liver and in the serum. Additionally, *in vitro* studies of Thy-1+ isolated oval cells and the WB-344 cell line determined that exposure to exogenous IGFBP-3 protein at various concentrations enhanced transwell cell migration. These results, taken with IHC results showing the unequal distribution of IGFBP-3 protein in the liver at Day 9 post-PHx, suggest that IGFBP-3 may promote oval cell migration across a concentration gradient. Distribution of IGFBP-3 during the peak of oval cell proliferation suggests that oval cells initiate the regenerative process, where IGFBP-3 concentrations are relatively low, and then migrate toward the central vein, where IGFBP-3 concentrations are much higher.

In addition to promoting oval cell migration, IGFBP-3 inhibited IGF-I induced WB-344 cell proliferation *in vitro*, suggesting that IGFBP-3 may regulate the proliferation of oval cells in an IGF-dependent manner. The notion that IGFBP-3 may regulate oval cell proliferation was further supported by IHC analysis in IGFBP-3 siRNA treated animals which showed that loss of IGFBP-3 protein resulted in an increase in oval cell proliferation as evidenced by increased numbers of OV-6 and Ki67 positive cells at Day 9 post-PHx. Most remarkable and noteworthy about these IGFBP-3 siRNA treated livers were the unique appearance of numerous atypical ductular structures, which were not present in the livers of animals treated with 2AAF/PHx alone

or with negative control siRNA. Further histological analysis of these ductular structures determined that the cells present in these formations were actively undergoing proliferation and were OV-6 positive, indicating that these cells were derived from the oval cell population. These findings further support a role for IGFBP-3 in the regulation of oval cell proliferation, where loss of IGFBP-3 results in an uncontrolled increase in proliferation, possibly leading to a "back-log" of oval cells around the periportal region of the liver. This increase in cell numbers may inhibit the oval cells from receiving the proper differentiation cues from the surrounding liver parenchyma, resulting in the oval cells to differentiate toward the default biliary lineage. It is also possible that IGFBP-3 itself plays a role in oval cell differentiation, where loss of IGFBP-3 inhibits oval cells from differentiating toward the hepatocyte lineage.

Although LPS treatment of animals during oval cell mediated liver regeneration resulted in a significant decrease in oval cell activation, it was unclear whether this result was specifically linked to reduced IGFBP-3 expression in the liver, or if reduced oval cell presence was the results of an side effect from LPS induced toxicity. Although very low amounts of LPS was administered to animals following 2AAF/PHx, it is possible that accumulating levels of LPS over time may have impacted the expression levels of IGF-I, or other IGFBPs, during this time course. In addition, LPS has been shown to activate several signaling pathways in the liver which could have negatively impacted the ability of the oval cells to function normally during the process of liver regeneration.

Previous studies have shown that IGFBP-3 is involved in negatively regulating cell growth and inducing cell apoptosis in a variety of different cells types, including several types of cancer cells (66, 80). Additionally, several antiproliferative agents such as TGF-β, TNF-α, and p53, have been shown to induce IGFBP-3 expression (109-111, 142, 143), further supporting the role

of IGFBP-3 as a negative regulator of cell growth and proliferation. Interestingly, previous studies have also determined that oval cells may contribute to various types of cancers in the liver including hepatocellular carcinoma and cholangiocarcinoma (23, 144).

In our studies, we have shown that loss of IGFBP-3 expression during the peak of oval cell proliferation resulted in an increase in cell proliferation during oval cell-mediated liver regeneration and noted the appearance of numerous atypical ductular structures which may be the result of preneoplastic changes and evidence of early stages of cancer progression occurring within the liver. In addition to increased cell proliferation, several groups have also reported a link between decreased IGFBP-3 levels and increased tumor cell invasiveness, tumor grade, more advanced tumor stage and overall lowered survival rate compared to patients with normal or elevated IGFBP-3 levels (81, 83). Results of these studies suggest that IGFBP-3 may play an important role in regulating cell proliferation and may act as an invasion-metastasis suppressor in certain types of cancer.

Finally, qRT-PCR analysis of IGFBP 3 siRNA treated liver detected decreased mRNA expression levels of several key components of the TGF-β family, including Smads 2, 3 and 4, and TGF-β receptors I and II. Interestingly, TGF-β1 mRNA levels remained unchanged following IGFBP-3 siRNA, indicating that IGFBP-3 effects on the TGF-β pathway are on downstream targets. These results are supported by previous studies which found that IGFBP-3 can directly bind and interact with TGF-β receptors I and II. Results of these experiments indicate a potential role for IGFBP-3 regulation of oval cell proliferation and differentiation *in vivo* and that the regulation of these functions appears to involve activation of the TGF-β pathway.

Future Directions

Although we have shown that IGFBP-3 is produced in the liver during oval cell-mediated liver regeneration, further studies would need to be conducted in order to determine which cell type (or types) in the liver is responsible for the increase in IGFBP-3 protein in liver and serum. We have shown through IHC results of isolated non-parenchymal cells at Day 9 post-PHx that a cell population within the non-parenchymal fraction is producing IGFBP-3. Additionally, these results have also determined that the oval cells themselves are not positive for IGFBP-3 expression. Results of our experiments in which liver sections were stained for IGFBP-3 at Day 9 post-PHx have found that cells, which phenotypically appear to be hepatocytes located around the central vein and portal triad, are positive for IGBFP-3 expression.

Previous studies by other groups have determined that, under normal conditions within the liver, hepatocytes do not express IGFBP-3 protein or IGFBP-3 mRNA (60, 61). Therefore, it would be interesting and novel to determine if hepatocytes begin to express IGFBP-3 mRNA or protein during oval cell-mediated liver regeneration. In order to accomplish this, a dual stain for IGFBP-3 and a hepatocyte marker, such as albumin or HES-6, could be performed to verify that these IGFBP-3 positive cells at Day 9 post-PHx are in fact hepatocytes. Next, hepatocytes, like non-parenchymal cells, can be isolated during the peak of oval cell proliferation via a two-step collagenase digestion and perfusion of the liver. RNA and protein from these isolated hepatocytes could then be examined via RT-PCR, Western blot and/or IHC to determine if hepatocytes during oval cell mediated liver regeneration being transcribing IGFBP-3 mRNA or producing IGFBP-3 protein respectively.

Additionally, we have shown that oval cells are responsive to IGFBP-3 and are induced to migrate in the presence of low levels of IGFBP-3 protein, as demonstrated in the *in vitro* migration assays. Based on the results of our experiments, IGFBP-3 was found to inhibit IGF-I

induced proliferation, and qRT-PCR experiments showed decreased levels of IGF-I mRNA expression following IGBFP-3 siRNA. Therefore, we believe the effects of IGFBP-3 during oval cell-mediated liver regeneration to be IGF-dependent. To further verify that the effects of IGFBP-3 are dependent on IGF-I, it would be important to determine if oval cells express the IGF-I receptor to which IGF-I can bind to. This could be accomplished through IHC analysis and dual IF staining with OV-6. The presence of the IGF-I receptor on the surface of oval cells would be a strong indicator that IGFBP-3 mediated effects are IGF-dependent.

In addition to IGF-dependent effects of IGFBP-3, qRT-PCR analysis demonstrated a decrease in mRNA expression levels of several TGF-β pathway members, including TGF-β receptors I and II, and downstream transcription factors such as Smads 2, 3 and 4, when IGFBP-3 expression was suppressed. This would suggest that IGFBP-3 mediated effects may also involve activation of the TGF-β pathway. However, in order to conclusively demonstrate an interaction between IGFBP-3 and the proteins of TGF-β pathways, additional experiments would need to be conducted to verify if there are changes in the phosphorylation and activation of these proteins when IGFBP-3 expression is decreased. In order to accomplish this, Western blot analysis of total TGF-βR protein or Smad protein can be compared to the amount of phosphorylated proteins that are present in the liver during oval cell mediated liver regeneration. A decrease or loss of phosphorylated protein levels in comparison to total protein levels during oval cell-mediated liver regeneration would indicate that loss of IGFBP-3 expression results in decreased activation of the TGF-β pathway and downstream transcription factors.

Additionally, to further verify an interaction between the TGF-β pathway and IGFBP-3, future studies utilizing a TGF-β inhibitor or neutralizing antibody could be used in various *in vitro* experiments using isolated oval cells or the WB-344 cell line. In our *in vitro* migration

assays, we found that IGFBP-3 protein at low concentration levels could induce oval cell and WB-344 cell migration. However, if cell migration were suppressed in the presence of IGFBP-3 protein at low concentration and a TGF-β receptor inhibitor, it would suggest a possible interaction between IGFBP-3 and the TGF-βRs during of oval cell migration. As previous studies have also shown that IGFBP-3 can interact with TGF-β type V receptor (78, 79), it would be interesting to determine if oval cells or cells that express IGFBP-3 in the liver also expressed this newly identified TGF-β receptor. Unfortunately, although characterized, the TGF-β type V receptor has yet to be cloned, making it difficult to find commercially available antibodies for use in IHC or Western blot experiments.

In addition to these future studies, it would also be interesting to determine the outcome of oval cell mediated liver regeneration using a IGFBP-3 null mouse line in combination with the DDC mouse model of oval cell induction. Previous studies utilizing IGFBP-3 transgenic mice have reported that *Igfbp*3$^{-/-}$ mice displayed similar IGF-I expression levels in comparison to *Igfbp*3$^{+/-}$ and *Igfbp*3$^{+/+}$ litter mates and that no difference in birth weight, litter size, or postnatal growth between these groups could be detected (90, 145). Although the DDC model of oval cell induction in the mouse differs from the 2AAF/PHx model in the rat, the use of an Igfbp3 null mouse line could help to determine how the absence of IGFBP-3 effects oval cell activation throughout the entire process of oval cell-mediated liver regeneration.

LIST OF REFERENCES

1. Desmet, V. (2001) *The Liver: Biology and Pathobiology*, 4th Ed., Lippincott Williams & Wilkins, Philadelphia, PA

2. Jones, A. L. and Schmucker, D. L. (1977) *Gastroenterology* **73,** 833-851

3. McCuskey, R. S. and Reilly, F. D. (1993) *Semin. Liver Dis.* **13,** 1-12

4. Rappaport, A. (1963) Acinas Units and the Pathophysiology of the Liver. In Rouiller, C., Editor. *The Liver. Morphology. Biochemistry. Physiology*, Academic Press, New York, NY

5. Shiojiri, N., Lemire, J. M., and Fausto, N. (1991) *Cancer Res.* **51,** 2611-2620

6. Marceau, N. (1990) *Lab. Invest.* **63,** 4-20

7. Marceau, N., Germain, L., Goyette, R., Noel, M., and Gourdeau, H. (1986) *Biochem. Cell Biol.* **64,** 788-802

8. Dunsford, H. A. and Sell, S. (1989) *Cancer Res.* **49,** 4887-4893

9. Vaneyken, P. and Desmet, V. J. (1993) *Liver* **13,** 113-122

10. Baiocchi, L., LeSage, G., Glaser, S., and Alpini, G. (1999) *J. of Hepatol.* **31,** 179-191

11. Moriwaki, H., Blaner, W. S., Piantedosi, R., and Goodman, D. S. (1988) *J. Lipid Res.* **29,** 1523-1534

12. Oh, K. W., Currin, R. T., and Lemasters, J. J. (2000) *Toxicol. Lett.* **117,** 95-100

13. Gressner, A. M. (1996) *Kidney Int.* **49,** S39-S45

14. Li, D. and Friedman, S. L. (1999) *J. Gastroenterol. Hepatol.* **14,** 618-633

15. Klaassen, C. D. and Watkins, J. B., III (1984) *Pharmacol. Rev.* **36,** 1-67

16. Higgins, G. M. and Anderson, R. M. (1931) *Arch. Pathol.* **12,** 186-202

17. Michalopoulos, G. K. and DeFrances, M. C. (1997) *Science* **276,** 60-66

18. Fausto, N. (2001) Liver Regeneration. In Arais, I., Boyer, J., Chisari, F., Fausto, N., Schachter, D., and Shafritz, D., Editors. *The Liver: Biology and Pathobiology*, Lippincott Williams & Wilkins, Philadelphia, PA

19. Thorgeirsson, S. S. (1996) *FASEB J.* **10,** 1249-1256

20. Sell, S. (2001) *Wound Repair Regen.* **9,** 467-482

21. Shafritz, D. A. and Dabeva, M. D. (2002) *J. Hepatol.* **36,** 552-564

22. Newsome, P. N., Hussain, M. A., and Theise, N. D. (2004) Hepatic Oval Cells: Helping Redefine a Paradigm in Stem Cell Biology. In Schatten, G. P., Editor. *Current Topics in Developmental Biology,* Elsevier Inc., San Diego, CA

23. Farber, E. (1956) *Cancer Res.* **16,** 142-151

24. Fausto, N. and Campbell, J. S. (2003) *Mech. Dev.* **120,** 117-130

25. Petersen, B. E., Bowen, W. C., Patrene, K. D., Mars, W. M., Sullivan, A. K., Murase, N., Boggs, S. S., Greenberger, J. S., and Goff, J. P. (1999) *Science* **284,** 1168-1170

26. Sicklick, J. K., Li, Y. X., Melhem, A., Schmelzer, E., Zdanowicz, M., Huang, J. W., Caballero, M., Fair, J. H., Ludlow, J. W., McClelland, R. E., Reid, L. M., and Diehl, A. M. (2006) *Am. J. Physiol. Gastrointest. Liver Physiol.* **290,** G859-G870

27. Paku, S., Schnur, J., Nagy, P., and Thorgeirsson, S. S. (2001) *Am. J. Pathol.* **158,** 1313-1323

28. Evarts, R. P., Nakatsukasa, H., Marsden, E. R., Hu, Z. Y., and Thorgeirsson, S. S. (1992) *Mol. Carcinog.* **5,** 25-31

29. Fausto, N. (1991) *Dig. Dis. Sci.* **36,** 653-658

30. Hu, Z. Y., Evarts, R. P., Fujio, K., Marsden, E. R., and Thorgeirsson, S. S. (1993) *Am. J. Pathol.* **142,** 1823-1830

31. Nakatsukasa, H., Evarts, R. P., Hsia, C. C., Marsden, E., and Thorgeirsson, S. S. (1991) *Lab. Invest.* **65,** 511-517

32. Lenzi, R., Liu, M. H., Tarsetti, F., Slott, P. A., Alpini, G., Zhai, W. R., Paronetto, F., Lenzen, R., and Tavoloni, N. (1992) *Lab. Invest.* **66,** 390-402

33. Marsden, E. R., Hu, Z. Y., Fujio, K., Nakatsukasa, H., Thorgeirsson, S. S., and Evarts, R. P. (1992) *Lab. Invest.* **67,** 427-433

34. Fausto, N. (2004) *Hepatology* **39,** 1477-1487

35. Bisgaard, H. C., Muller, S., Nagy, P., Rasmussen, L. J., and Thorgeirsson, S. S. (1999) *Am. J. Pathol.* **155,** 1075-1085

36. Alison, M. R., Poulsom, R., Jeffery, R., Dhillon, A. P., Quaglia, A., Jacob, J., Novelli, M., Prentice, G., Williamson, J., and Wright, N. A. (2000) *Nature* **406,** 257

37. Theise, N. D., Nimmakayalu, M., Gardner, R., Illei, P. B., Morgan, G., Teperman, L., Henegariu, O., and Kruse, D. S. (2000) *Hepatology* **32,** 11-16

38. Crosbie, O. M., Reynolds, M., McEntee, G., Traynor, O., Hegarty, J. E., and O'Farrelly, C. (1999) *Hepatology* **29,** 1193-1198

39. Petersen, B. E., Goff, J. P., Greenberger, J. S., and Michalopoulos, G. K. (1998) *Hepatology* **27,** 433-445

40. Fujio, K., Evarts, R. P., Hu, Z. Y., Marsden, E. R., and Thorgeirsson, S. S. (1994) *Lab. Invest.* **70,** 511-516

41. Omori, N., Omori, M., Evarts, R. P., Teramoto, T., Miller, M. J., Hoang, T. N., and Thorgeirsson, S. S. (1997) *Hepatology* **26,** 720-727

42. Dumble, M. L., Croager, E. J., Yeoh, G. C. T., and Quail, E. A. (2002) *Carcinogenesis* **23,** 435-445

43. Lieberman, H. M. and Shafritz, D. (1986) *Prog. Liver Dis.* **8,** 395-415

44. Theise, N. D., Saxena, R., Portmann, B. C., Thung, S. N., Yee, H., Chiriboga, L., Kumar, A., and Crawford, J. M. (1999) *Hepatology* **30,** 1425-1433

45. Wu, P. C., Lai, V. C. H., Fang, J. W. S., Gerber, M. A., Lai, C. L., and Lau, J. Y. N. (1999) *J. Hepatol.* **31,** 965-966

46. Mishra, L., Banker, T., Murray, J., Byers, S., Thenappan, A., He, A. R., Shetty, K., Johnson, L., and Reddy, E. P. (2009) *Hepatology* **49,** 318-329

47. Lund, P. K., Moatsstaats, B. M., Hynes, M. A., Simmons, J. G., Jansen, M., Dercole, A. J., and Vanwyk, J. J. (1986) *J. Biol. Chem.* **261,** 4539-4544

48. Rechler, M. M., Zapf, J., Nissley, S. P., Froesch, E. R., Moses, A. C., Podskalny, J. M., Schilling, E. E., and Humble, R. E. (1980) *Endocrinology* **107,** 1451-1459

49. Russell, W. E., Dercole, A. J., and Underwood, L. E. (1985) *Am. J. Physiol.* **248,** E618-E623

50. Fausto, N. (1994) Insulin. In Arias, I. and Boyer, J., Editors. *The Liver Biology and Pathobiology*, Raven Press, New York, NY

51. Bondy, C. A., Werner, H., Roberts, C. T., and Leroith, D. (1990) *Mol. Endocrinol.* **4,** 1386-1398

52. Baxter, R. C. and Martin, J. L. (1987) *Biochem. Biophys. Res. Commun.* **147,** 408-415

53. Moses, A. C., Nissley, S. P., Cohen, K. L., and Rechler, M. M. (1976) *Nature* **263,** 137-140

54. Firth, S. M. and Baxter, R. C. (2002) *Endocr. Rev.* **23,** 824-854

55. Baxter, R. C., Martin, J. L., and Beniac, V. A. (1989) *J. Biol. Chem.* **264,** 11843-11848

56. Lamphere, L. and Lienhard, G. E. (1992) *Endocrinology* **131,** 2196-2202

57. Cohen, K. L. and Nissley, S. P. (1976) *Acta Endocrinol.* **83,** 243-258

58. Guler, H. P., Zapf, J., Schmid, C., and Froesch, E. R. (1989) *Acta Endocrinol.* **121,** 753-758

59. Villafuerte, B. C., Koop, B. L., Pao, C. I., Gu, L. M., Birdsong, G. G., and Phillips, L. S. (1994) *Endocrinology* **134,** 2044-2050

60. Takenaka, A., Miura, Y., Mori, M., Hirosawa, M., Kato, H., and Noguchi, T. (1991) *Agric. Biol. Chem.* **55,** 1191-1193

61. Arany, E., Afford, S., Strain, A. J., Winwood, P. J., Arthur, M. J. P., and Hill, D. J. (1994) *J. Clin. Endocrinol. Metab.* **79,** 1871-1876

62. Wood, W. I., Cachianes, G., Henzel, W. J., Winslow, G. A., Spencer, S. A., Hellmiss, R., Martin, J. L., and Baxter, R. C. (1988) *Mol. Endocrinol.* **2,** 1176-1185

63. Shimasaki, S., Shimonaka, M., Ui, M., Inouye, S., Shibata, F., and Ling, N. (1990) *J. Biol. Chem.* **265,** 2198-2202

64. Shimonaka, M., Schroeder, R., Shimasaki, S., and Ling, N. (1989) *Biochem. Biophys. Res. Commun.* **165,** 189-195

65. Albiston, A. L. and Herington, A. C. (1990) *Biochem. Biophys. Res. Commun.* **166,** 892-897

66. Rajah, R., Valentinis, B., and Cohen, P. (1997) *J. Biol. Chem.* **272,** 12181-12188

67. Perks, C. M., Bowen, S., Gill, Z. P., Newcomb, P. V., and Holly, J. M. P. (1999) *J. Cell. Biochem.* **75,** 652-664

68. Hong, J., Zhang, G., Dong, F., and Rechler, M. M. (2002) *J. Biol. Chem.* **277,** 10489-10497

69. Buckway, C. K., Wilson, E. M., Ahlsen, M., Bang, P., Oh, Y., and Rosenfeld, R. G. (2001) *J. Clin. Endocrinol. Metab.* **86,** 4943-4950

70. Liu, B. R., Lee, H. Y., Weinzimer, S. A., Powell, D. R., Clifford, J. L., Kurie, J. M., and Cohen, P. (2000) *J. Biol. Chem.* **275,** 33607-33613

71. Jaques, G., Noll, K., Wegmann, B., Witten, S., Kogan, E., Radulescu, R. T., and Havemann, K. (1997) *Endocrinology* **138,** 1767-1770

72. Radulescu, R. T. (1994) *Trends Biochem. Sci.* **19,** 278

73. Li, W. L., Fawcett, J., Widmer, H. R., Fielder, P. J., Rabkin, R., and Keller, G. A. (1997) *Endocrinology* **138,** 1763-1766

74. Firth, S. M., Ganeshprasad, U., and Baxter, R. C. (1998) *J. Biol. Chem.* **273,** 2631-2638

75. Bhattacharyya, N., Pechhold, K., Shahjee, H., Zappala, G., Elbi, C., Raaka, B., Wiench, M., Hong, J., and Rechler, M. M. (2006) *J. Biol. Chem.* **281,** 24588-24601

76. Schedlich, L. J., Le Page, S. L., Firth, S. M., Briggs, L. J., Jans, D. A., and Baxter, R. C. (2000) *J. Biol. Chem.* **275,** 23462-23470

77. Schedlich, L. J., Young, T. F., Firth, S. M., and Baxter, R. C. (1998) *J. Biol. Chem.* **273,** 18347-18352

78. Leal, S. M., Huang, S. S., and Huang, J. S. (1999) *J. Biol. Chem.* **274,** 6711-6717

79. Leal, S. M., Liu, Q. J., Huang, S. S., and Huang, J. S. (1997) *J. Biol. Chem.* **272,** 20572-20576

80. Oh, Y. (1998) *Breast Cancer Res. Treat.* **47,** 283-293

81. Chan, J. M., Stampfer, M. J., Giovannucci, E., Ma, J., and Pollak, M. (2000) *Growth Horm. IGF Res.* **10,** S32-S33

82. Giovannucci, E., Pollak, M., Platz, E. A., Willett, W. C., Stampfer, M. J., Majeed, N., Colditz, G. A., Speizer, F. E., and Hankinson, S. E. (2000) *Growth Horm. IGF Res.* **10,** S30-S31

83. Torng, P. L., Lee, Y. C. G., Huang, C. Y. F., Ye, J. H., Lin, Y. S., Chu, Y. W., Huang, S. C., Cohen, P., Wu, C. W., and Lin, C. T. (2008) *Oncogene* **27,** 2137-2147

84. Gong, Y. W., Cui, L., and Minuk, G. Y. (2000) *Mol. Cell. Biochem.* **207,** 101-104

85. Xi, Y. G., Nakajima, G., Hamil, T., Fodstad, O., Riker, A., and Ju, J. F. (2006) *Mol. Cancer Ther.* **5,** 3078-3084

86. Hintz, R. L., Bock, S., Thorsson, A. V., Bovens, J., Powell, D. R., Jakse, G., and Petrides, P. E. (1991) *J. Urol.* **146,** 1160-1163

87. Theise, N. D., Badve, S., Saxena, R., Henegariu, O., Sell, S., Crawford, J. M., and Krause, D. S. (2000) *Hepatology* **31,** 235-240

88. Lagasse, E., Connors, H., Al Dhalimy, M., Reitsma, M., Dohse, M., Osborne, L., Wang, X., Finegold, M., Weissman, I. L., and Grompe, M. (2000) *Nat. Med.* **6,** 1229-1234

89. Liu, L. Q., Sposato, M., Liu, H. Y., Vaudrain, T., Shi, M. J., Rider, K., Stevens, Z., Visser, J., Deng, H. K., and Kraus, M. (2003) *Oncol. Res.* **13,** 359-371

90. Lofqvist, C., Chen, J., Connor, K. M., Smith, A. C. H., Aderman, C. M., Liu, N., Pintar, J. E., Ludwig, T., Hellstrom, A., and Smith, L. E. H. (2007) *Proc. Natl. Acad. Sci. U. S. A.* **104,** 10589-10594

91. Chang, K. H., Chan-Ling, T., McFarland, E. L., Afzal, A., Pan, H., Baxter, L. C., Shaw, L. C., Caballero, S., Sengupta, N., Calzi, S. L., Sullivan, S. M., and Grant, M. B. (2007) *Proc. Natl. Acad. Sci. U. S. A.* **104,** 10595-10600

92. Ghahary, A., Minuk, G. Y., Luo, J. M., Gauthier, T., and Murphy, L. J. (1992) *Hepatology* **15,** 1125-1131

93. Mohn, K. L., Melby, A. E., Tewari, D. S., Laz, T. M., and Taub, R. (1991) *Mol. Cell. Biol.* **11,** 1393-1401

94. Arai, M., Yokosuka, O., Chiba, T., Imazeki, F., Kato, M., Hashida, J., Ueda, Y., Sugano, S., Hashimoto, K., Saisho, H., Takiguchi, M., and Seki, N. (2003) *J. Biol. Chem.* **278,** 29813-29818

95. Lee, J. Y., Greenbaum, L., Haber, B. A., Nagle, D., Lee, V., Miles, V., Mohn, K. L., Bucan, M., and Taub, R. (1994) *Hepatology* **19,** 656-665

96. Leu, J. I., Crissey, M. A. S., and Taub, R. (2003) *J. Clin. Invest.* **111,** 129-139

97. Demori, I., Balocco, S., Voci, A., and Fugassa, E. (2000) *Am. J. Physiol. Gastrointest. Liver Physiol.* **278,** G384-G389

98. Phillips, I. D., Arany, E., Strain, A. J., Han, V. K. M., and Hill, D. J. (1993) *J. Endocrinol.* **137,** 271-280

99. Caro, J. F., Poulos, J., Ittoop, O., Pories, W. J., Flickinger, E. G., and Sinha, M. K. (1988) *J. Clin. Invest.* **81,** 976-981

100. Alberts, B., Johnson, A., Lewis, J., Raff, M., Roberts, K., and Walter, P. (2004) *Molecular Biology of the Cell*, 4th Ed., Garland Publishing Inc., New York

101. Carr, B. I., Huang, T. H., Itakura, K., Noel, M., and Marceau, N. (1989) *J. Cell. Biochem.* **39,** 477-487

102. Carr, B. I., Hayashi, I., Branum, E. L., and Moses, H. L. (1986) *Cancer Res.* **46,** 2330-2334

103. Braun, L., Mead, J. E., Panzica, M., Mikumo, R., Bell, G. I., and Fausto, N. (1988) *Proc. Natl. Acad. Sci. U. S. A.* **85,** 1539-1543

104. Oberhammer, F. A., Pavelka, M., Sharma, S., Tieffenbacher, R., Purchio, A. F., Bursch, W., and Schultehermann, R. (1992) *Proc. Natl. Acad. Sci. U. S. A.* **89,** 5408-5412

105. Malik, R., Selden, C., and Hodgson, H. (2002) *Semin. Cell Dev. Biol.* **13,** 425-431

106. Taub, R. (2004) *Nat. Rev. Mol. Cell Biol.* **5,** 836-847

107. Thorgeirsson, S. S. (1993) *Am. J. Pathol.* **142,** 1331-1333

108. Nguyen, L. N., Furuya, M. H., Wolfraim, L. A., Nguyen, A. P., Holdren, M. S., Campbell, J. S., Knight, B., Yeoh, G. C. T., Fausto, N., and Parks, W. T. (2007) *Hepatology* **45,** 31-41

109. Martin, J. and Baxter, R. C. (1991) *Endocrinology* **128,** 1425-1433

110. Gucev, Z. S., Oh, Y., Kelley, K. M., and Rosenfeld, R. G. (1996) *Cancer Res.* **56,** 1545-1550

111. Oh, Y., Muller, L., Ng, L., and Rosenfeld, R. G. (1995) *J. Biol. Chem.* **270,** 13589-13592

112. Moses, H. L. (1992) *Mol. Reprod. Dev.* **32,** 179-184

113. Cohen, P., Rajah, R., Rosenbloom, J., and Herrick, D. J. (2000) *Am. J. Physiol. Lung Cell. Mol. Physiol.* **278,** L545-L551

114. Fanayan, S., Firth, S. M., and Baxter, R. C. (2002) *J. Biol. Chem.* **277,** 7255-7261

115. Fanayan, S., Firth, S. M., Butt, A. J., and Baxter, R. C. (2000) *J. Biol. Chem.* **275,** 39146-39151

116. Kuemmerle, J. F. and Bowers, J. G. (2004) *Gastroenterology* **126,** A31

117. Gui, Y. T. and Murphy, L. J. (2003) *Mol. Cell. Biol.* **250,** 189-195

118. Mangasser-Stephan, K. and Gressner, A. M. (1999) *Cell Tissue Res.* **297,** 363-370

119. Dennis, P. A. and Rifkin, D. B. (1991) *Proc. Natl. Acad. Sci. U. S. A.* **88,** 580-584

120. Kovacina, K. S., Steelperkins, G., Purchio, A. F., Lioubin, M., Miyazono, K., Heldin, C. H., and Roth, R. A. (1989) *Biochem. Biophys. Res. Commun.* **160,** 393-403

121. Pi, L. Y., Oh, S. H., Shupe, T., and Petersen, B. E. (2005) *Gastroenterology* **128,** 2077-2088

122. Payet, L. D., Wang, X. H., Baxter, R. C., and Firth, S. M. (2003) *Endocrinology* **144,** 2797-2806

123. Priego, T., Granado, M., Ibanez de Caceres, I., Martin, A. I., Villanua, M. A., and Lopez-Calderon, A. (2003) *J. Endocrinol.* **179,** 107-117

124. Granado, M., Martin, A. I., Priego, T., Villanua, M. A., and Lopez-Calderon, A. (2006) *J. Endocrinol.* **188,** 503-511

125. Pi, L., Ding, X. D., Jorgensen, M., Pan, J. J., Oh, S. H., Pintilie, D., Brown, A., Song, W. Y., and Petersen, B. E. (2008) *Hepatology* **47,** 996-1004

126. Jung, Y. M., Oh, S. H., Zheng, D. H., Shupe, T. D., Witek, R. P., and Petersen, B. E. (2006) *Lab. Invest.* **86,** 477-489

127. Mosmann, T. (1983) *J. Immunol. Methods* **65,** 55-63

128. Scharf, J. G., Dombrowski, F., Novosyadlyy, R., Eisenbach, C., Demori, I., Kubler, B., and Braulke, T. (2004) *Endocrinology* **145,** 3463-3472

129. Sternlicht, M. D. and Werb, Z. (2001) *Annu. Rev. Cell Dev. Biol.* **17,** 463-516

130. Van, T. P., Couchie, D., Martin-Garcia, N., Laperche, Y., Zafrani, E. S., and Mavier, P. (2008) *Matrix Biol.* **27,** 674-681

131. Miyamoto, S., Yano, K., Sugimoto, S., Ishii, G., Hasebe, T., Endoh, Y., Kodama, K., Goya, M., Chiba, T., and Ochiai, A. (2004) *Cancer Res.* **64,** 665-671

132. Belizon, A., Kirman, I., Balik, E., Karten, M., Jain, S., and Whelan, R. L. (2007) *Surg. Endosc.* **21,** 653-658

133. Mira, E., Manes, S., Lacalle, R. A., Marquez, G., and Martinez, C. (1999) *Endocrinology* **140,** 1657-1664

134. Tsao, M. S., Smith, J. D., Nelson, K. G., and Grisham, J. W. (1984) *Exp. Cell Res.* **154,** 38-52

135. Thorgeirsson, S. S. and Grisham, J. W. (2003) *Semin. Liver Dis.* **23,** 303-312

136. Granata, R., Trovato, L., Lupia, E., Sala, G., Settanni, F., Camussi, G., Ghidoni, R., and Ghigo, E. (2007) *J. Throm. Haemost.* **5,** 835-845

137. Leibowitz, B. J. and Cohick, W. S. (2009) *J. Cell. Physiol.* **220,** 182-188

138. Soto, L., Martin, A. I., Millan, S., Vara, E., and Lopez-Calderon, A. (1998) *J. Endocrinol.* **159,** 239-246

139. Priego, T., de Caceres, I. I., Martin, A. I., Villanua, M. A., and Lopez-Calderon, A. (2003) *Mol. Cell. Endocrinol.* **199,** 23-28

140. Kansra, S., Ewton, D. Z., Wang, J. P., and Friedman, E. (2000) *Int. J. Cancer* **87,** 373-378

141. Kuemmerle, J. F., Murthy, K. S., and Bowers, J. G. (2004) *Am. J. Physiol. Gastroint. Liver Physiol.* **287,** G795-G802

142. Buckbinder, L., Talbott, R., Velascomiguel, S., Takenaka, I., Faha, B., Seizinger, B. R., and Kley, N. (1995) *Nature* **377,** 646-649

143. Rozen, F., Zhang, J. C., and Pollak, M. (1998) *Int. J. Oncol.* **13,** 865-869

144. Alison, M. R. (2005) *Stem Cell Rev.* **1,** 253-260

145. Ning, Y., Schuller, A. G. P., Bradshaw, S., Rotwein, P., Ludwig, T., Frystyk, J., and Pintar, J. E. (2006) *Mol. Endocrinol.* **20,** 2173-2186

BIOGRAPHICAL SKETCH

Nicole C. Steiger was born in Woodmere, NY. After graduating from G.W. Hewlett High School in 2001, she attended the State University of New York (SUNY) at Binghamton in Binghamton, NY. In May of 2005, she obtained her Bachelor of Science degree in Cell and Molecular Biology with a minor in Biological Anthropology. Having been an undergraduate research assistant in the laboratory of Dr. Dennis McGee at SUNY Binghamton for three years, she decided to further her education in the field of biomedical research.

In August of 2005, she was accepted into the Interdisciplinary Program (IDP) in Biomedical Sciences at the University of Florida, College of Medicine, to obtain her degree. It was here that she was awarded the prestigious Alumni Fellowship from 2005 to 2009.

On April 3rd, 2009, Nicole married Emery Luther in St. Petersburg Beach, Florida. Finally, in December of 2009, Nicole was awarded a Ph.D. in Medical Sciences with a concentration in Molecular Cell Biology.